Published for SISSA by Springer

Received: February 22, 2021
Accepted: May 24, 2021
Published: June 24, 2021

Search for charged Higgs bosons decaying into a top quark and a bottom quark at $\sqrt{s} = 13$ TeV with the ATLAS detector

The ATLAS collaboration

E-mail: atlas.publications@cern.ch

Abstract: A search for charged Higgs bosons decaying into a top quark and a bottom quark is presented. The data analysed correspond to 139 fb^{-1} of proton-proton collisions at $\sqrt{s} = 13$ TeV, recorded with the ATLAS detector at the LHC. The production of a heavy charged Higgs boson in association with a top quark and a bottom quark, $pp \to tbH^+ \to tbtb$, is explored in the H^+ mass range from 200 to 2000 GeV using final states with jets and one electron or muon. Events are categorised according to the multiplicity of jets and b-tagged jets, and multivariate analysis techniques are used to discriminate between signal and background events. No significant excess above the background-only hypothesis is observed and exclusion limits are derived for the production cross-section times branching ratio of a charged Higgs boson as a function of its mass; they range from 3.6 pb at 200 GeV to 0.036 pb at 2000 GeV at 95% confidence level. The results are interpreted in the hMSSM and M_h^{125} scenarios.

Keywords: Hadron-Hadron scattering (experiments)

ArXiv ePrint: 2102.10076

https://doi.org/10.1007/JHEP06(2021)145

Contents

1 Introduction

The discovery of a Higgs boson with a measured mass of 125 GeV at the Large Hadron Collider (LHC) in 2012 [1–3] raises the question of whether this is the Higgs boson of the Standard Model (SM) or part of an extended scalar sector. Charged Higgs bosons[1] are predicted in several extensions of the SM that add a second doublet [4–7] or triplets [8–12] to the scalar sector. In CP-conserving two-Higgs-doublet models (2HDMs), the properties of the charged Higgs boson depend on its mass, the mixing angle α of the neutral CP-even Higgs bosons, and the ratio of the vacuum expectation values of the two Higgs doublets ($\tan\beta$). This analysis searches for charged Higgs bosons heavier than the top quark and decaying into a top quark and a bottom quark. At the LHC, charged Higgs bosons in this mass range are expected to be produced primarily in association with a top quark and a bottom quark [13], as illustrated in figure 1.

The ATLAS and CMS collaborations have searched for charged Higgs bosons in proton-proton (pp) collisions at $\sqrt{s} = 7, 8$ and 13 TeV with data samples ranging from 2.9 to 36 fb^{-1}, probing the mass range below the top-quark mass in the $\tau\nu$ [14–19], cs [20, 21], and cb [22] decay modes, as well as above the top-quark mass in the $\tau\nu$ and tb decay modes [16, 18, 19, 23–27]. In addition, $H^+ \to WZ$ decays were searched for in the vector-boson-fusion production mode [28, 29]. ATLAS has also set limits on H^+ production in a search for dijet resonances in events with an isolated lepton using the Run 2 dataset [30]. No evidence of charged Higgs bosons was found in any of these searches.

This paper presents an updated search for H^+ production in the $H^+ \to tb$ decay mode with the full Run 2 dataset of pp collisions taken at $\sqrt{s} = 13$ TeV. This decay mode has the

[1] In the following, charged Higgs bosons are denoted H^+, with the charge-conjugate H^- always implied. Similarly, the difference between quarks and antiquarks q and $\bar{q}$ is generally understood from the context, so that e.g. $H^+ \to tb$ means both $H^+ \to t\bar{b}$ and $H^- \to \bar{t}b$.

JHEP06(2021)145

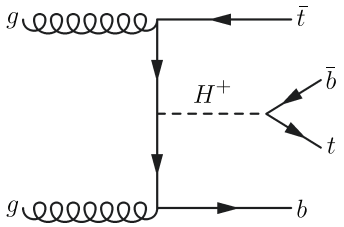

Figure 1. Leading-order Feynman diagram for the production of a heavy charged Higgs boson in association with a top antiquark and a bottom quark, as well as its decay into a top quark and a bottom antiquark.

highest branching ratio for charged Higgs bosons above the top-quark mass [31]. Events with one charged lepton ($\ell = e, \mu$) and jets in the final state are considered, and exclusive regions are defined according to the overall number of jets, and the number of jets tagged as containing a b-hadron. In order to separate signal from SM background, multivariate analysis (MVA) techniques combining jet multiplicities and several kinematic variables are employed in the regions where the signal rate is expected to be largest. Compared to the ATLAS result using 36 fb^{-1}of Run 2 data [25], improved limits on the $pp \to tbH^+$ production cross-section times the $H^+ \to tb$ branching ratio are set by means of a simultaneous fit to the MVA classifier outputs in the different analysis regions, which determines both the contribution from the $H^+ \to tb$ signal and the normalisation of the backgrounds. The improvement is small at low H^+ mass, where the measurement is dominated by systematic uncertainties, but larger than the simple scaling with the square root of the ratio of integrated luminosities at high H^+ mass. The results are interpreted in the framework of the hMSSM [32–35] and various M_h^{125} benchmark scenarios of the Minimal Supersymmetric Standard Model (MSSM) [13, 31, 36–39].

2 Data and simulation samples

The data used in this analysis were recorded with the ATLAS detector at the LHC between 2015 and 2018 from $\sqrt{s} = 13$ TeV pp collisions, and correspond to an integrated luminosity of 139 fb^{-1}. ATLAS [40–42] is a multipurpose detector with a forward-backward symmetric cylindrical geometry and a near 4π coverage in solid angle.[2] It consists of an inner tracking detector (ID) surrounded by a thin superconducting solenoid providing a 2 T axial magnetic field, electromagnetic and hadron calorimeters, and a muon spectrometer (MS). The inner tracking detector covers the pseudorapidity range $|\eta| < 2.5$. It consists of silicon pixel, silicon microstrip, and transition radiation tracking detectors. Lead/liquid-argon (LAr) sampling calorimeters provide electromagnetic (EM) energy measurements with high granularity. A steel/scintillator-tile hadron calorimeter covers the central pseudorapidity range

[2]ATLAS uses a right-handed coordinate system with its origin at the nominal interaction point (IP) in the centre of the detector and the z-axis along the beam pipe. The x-axis points from the IP to the centre of the LHC ring, and the y-axis points upwards. Cylindrical coordinates (r, ϕ) are used in the transverse plane, ϕ being the azimuthal angle around the z-axis. The pseudorapidity is defined in terms of the polar angle θ as $\eta = -\ln\tan(\theta/2)$. Angular distance is measured in units of $\Delta R \equiv \sqrt{(\Delta\eta)^2 + (\Delta\phi)^2}$.

JHEP06(2021)145

($|\eta| < 1.7$). The endcap and forward regions are instrumented with LAr calorimeters for EM and hadronic energy measurements up to $|\eta| = 4.9$. The muon spectrometer surrounds the calorimeters and is based on three large air-core toroidal superconducting magnets with eight coils each. The field integral of the toroids ranges between 2.0 and 6.0 T m across most of the detector. The muon spectrometer includes a system of precision tracking chambers and fast detectors for triggering. Only runs with stable colliding beams and in which all relevant detector components were functional are used.

A two-level trigger system, with the first level implemented in custom hardware and followed by a software-based second level, is used to reduce the trigger rate to around 1 kHz for offline storage [43]. Events in this analysis were recorded using single-lepton triggers. To maximise the event selection efficiency, multiple triggers were used, either with low transverse momentum (p_{T}) thresholds and lepton identification and isolation requirements, or with higher p_{T} thresholds but looser identification criteria and no isolation requirements. Slightly different sets of triggers were used for 2015 and 2016–2018 data due to the increase in the average number of pp interactions per bunch crossing (pile-up). The minimum p_{T} required by the triggers was increased to keep both trigger rate and data storage within their limits. For muons, the lowest p_{T} threshold was 20 (26) GeV in 2015 (2016–2018), while for electrons, triggers with a minimum p_{T} threshold of 24 (26) GeV were used [44]. Simulated events are also required to satisfy the trigger criteria.

Signal and background processes were modelled with Monte Carlo (MC) simulation samples. The $pp \to tbH^+$ process followed by $H^+ \to tb$ decay was modelled with MadGraph5_aMC@NLO [31] at next-to-leading order (NLO) in QCD [45] using a four-flavour scheme (4FS) implementation with the NNPDF2.3NLO [46] parton distribution function (PDF). Parton showers (PS) and hadronisation were modelled by Pythia 8.212 [47] with a set of underlying-event (UE) parameters tuned to ATLAS data and named the A14 tune [48]. Dynamic QCD factorisation and renormalisation scales, μ_{f} and μ_{r}, were set to $\frac{1}{3}\sum_i \sqrt{m(i)^2 + p_{\mathrm{T}}(i)^2}$, where i runs over the final-state particles (H^+, t and b) used in the generation. Only the H^+ decay into tb is considered. For the simulation of the tbH^+ process the narrow-width approximation was used. This assumption has negligible impact on the analysis for the models considered in this paper, as the experimental resolution is much larger than the H^+ natural width [49]. Interference with the SM $t\bar{t}b\bar{b}$ background is neglected. A total of 18 H^+ mass hypotheses are used, with 25 GeV mass steps between a H^+ mass of 200 GeV and 300 GeV, 50 GeV steps between 300 GeV and 400 GeV, 100 GeV steps between 400 GeV and 1000 GeV, and 200 GeV steps from 1000 GeV to 2000 GeV. The step sizes were chosen to match the experimental mass resolution of the H^+ signal.

The production of $t\bar{t}$ + jets events was modelled using the Powheg-Box [50–53] v2 generator in the five-flavour scheme (5FS), which provides matrix elements (ME) at NLO in QCD, with the NNPDF3.0NLO PDF set [54]. The h_{damp} parameter, which controls the transverse momentum of the first additional emission beyond the Born configuration, was set to $1.5m_t$ [55], where m_t is the mass of the top quark. Parton showers and hadronisation were modelled by Pythia 8.230 [56] with the A14 tune for the UE. The scales μ_{f} and μ_{r} were set to the default scale $\sqrt{m_t^2 + p_{\mathrm{T},t}^2}$. The sample was normalised to the Top++ 2.0 [57] theoretical cross-section of 832^{+46}_{-51} pb, calculated at next-to-next-to-leading order (NNLO)

JHEP06(2021)145

in QCD including resummation of next-to-next-to-leading logarithmic (NNLL) soft gluon terms [58–61]. The generation of the $t\bar{t}$ + jets events was performed both inclusively of additional jet flavour, and also with dedicated filtered samples, requiring b- or c-hadrons in addition to those arising from the decays of the top quarks. Events generated with no extra b-hadrons were taken from the unfiltered sample and merged with the $t\bar{t}$ + jets events from the filtered sample, taking the appropriate cross-section and filter efficiencies into account.

Single-top t-channel production was modelled using the Powheg-Box v2 generator at NLO in QCD, generated in the 4FS with the NNPDF3.0NLOnf4 PDF set [54]. The scales μ_{f} and μ_{r} were set to $\sqrt{m_b^2 + p_{\mathrm{T},b}^2}$ following the recommendation in ref. [62]. Single-top tW and s-channel production was modelled using the Powheg-Box v2 generator at NLO in QCD, generated in the 5FS with the NNPDF3.0NLO PDF set. The scales μ_{f} and μ_{r} were set to the default scale, which is equal to the top-quark mass. For tW associated production, the diagram removal scheme [63] was employed to handle the interference with $t\bar{t}$ production [55]. All single-top events were showered with Pythia 8.230.

Production of vector bosons with additional jets was simulated with the Sherpa 2.2.1 generator [64]. Matrix elements with NLO accuracy for up to two partons, and with leading-order (LO) accuracy for up to four partons, were calculated with the Comix [65] and OpenLoops [66, 67] libraries. The default Sherpa PS algorithm [68] based on Catani-Seymour dipole factorisation and the cluster hadronisation model [69] was used. It employs the dedicated set of tuned parameters developed by the Sherpa authors for this version, based on the NNPDF3.0NNLO PDF set. The NLO ME of a given jet multiplicity were matched to the PS using a colour-exact variant of the MC@NLO algorithm [70]. Different jet multiplicities were then merged into an inclusive sample using an improved CKKW matching procedure [71, 72], which is extended to NLO accuracy using the MEPS@NLO prescription [73]. The merging cut was set to 20 GeV.

The production of $t\bar{t}V$ events, i.e. $t\bar{t}W$ or $t\bar{t}Z$, was modelled using the MadGraph5_aMC@NLO 2.3.3 generator, which provides ME at NLO in QCD with the NNPDF3.0NLO PDF set. The scales μ_{f} and μ_{r} were set to the default scale $\frac{1}{2}\sum_i \sqrt{m_i^2 + p_{\mathrm{T}i}^2}$, where the sum runs over all the particles generated in the ME calculation. The events were showered with Pythia 8.210. Additional $t\bar{t}V$ samples were produced with the Sherpa 2.2.0 [64] generator at LO accuracy, using the MEPS@LO prescription with up to one additional parton for the $t\bar{t}Z$ sample and two additional partons for $t\bar{t}W$. A dynamic scale μ_{r} is used, defined similarly to that of the nominal MadGraph5_aMC@NLO samples. The CKKW matching scale of the additional emissions was set to 30 GeV. The default Sherpa 2.2.0 PS was used along with the NNPDF3.0NNLO PDF set. The production of $t\bar{t}H$ events was modelled in the 5FS using the Powheg-Box [74] generator at NLO with the NNPDF3.0NLO PDF set. The h_{damp} parameter was set to $\frac{3}{4}(2m_t + m_H) = 352.5$ GeV, and the events are showered with Pythia 8.230.

Diboson (VV) samples were simulated with the Sherpa 2.2 generator. Multiple ME calculations were matched and merged with the Sherpa PS using the MEPS@NLO prescription. For semileptonically and fully leptonically decaying diboson samples, as well as loop-induced diboson samples, the virtual QCD correction for ME at NLO accuracy were provided by the OpenLoops library. For electroweak $VVjj$ production, the calculation was

JHEP06(2021)145

Physics process	ME generator	PS generator	Normalisation	PDF set	Simulation
tbH^+	MG5_aMC 2.6.2	Pythia 8.212	NLO	NNPDF2.3NLO	Fast
$t\bar{t}$ + jets	Powheg-Box v2	Pythia 8.230	NNLO+NNLL	NNPDF3.0NLO	Fast
Single-top t-chan	Powheg-Box v2	Pythia 8.230	aNNLO	NNPDF3.0NLOnf4	Full
Single-top tW	Powheg-Box v2	Pythia 8.230	aNNLO	NNPDF3.0NLO	Full
Single-top s-chan	Powheg-Box v2	Pythia 8.230	aNNLO	NNPDF3.0NLO	Full
V + jets	Sherpa 2.2.1	Sherpa 2.2.1	NNLO	NNPDF3.0NNLO	Full
$t\bar{t}V$	MG5_aMC 2.3.3	Pythia 8.210	NLO	NNPDF3.0NLO	Full
$t\bar{t}H$	Powheg-Box v2	Pythia 8.230	NLO	NNPDF3.0NLO	Full
Diboson	Sherpa 2.2	Sherpa 2.2	NLO	NNPDF3.0NNLO	Full
$tHjb$	MG5_aMC 2.6.0	Pythia 8.230	NLO	NNPDF3.0NLOnf4	Full
tHW	MG5_aMC 2.6.2	Pythia 8.235	NLO	NNPDF3.0NLO	Full
tZq	MG5_aMC 2.3.3	Pythia 8.212	NLO	CTEQ6L1LO	Full
tZW	MG5_aMC 2.3.3	Pythia 8.212	NLO	NNPDF3.0NLO	Full
Four top quarks	MG5_aMC 2.3.3	Pythia 8.230	NLO	NNPDF3.1NLO	Fast

Table 1. Nominal simulated signal and background event samples. The ME generator, PS generator and calculation accuracy of the cross-section in QCD used for normalisation (aNNLO stands for approximate NNLO in QCD) are shown together with the applied PDF set. Either Sherpa 2.2.1 or Sherpa 2.2.2 was used for different diboson contributions. The rightmost column shows whether fast or full simulation was used to produce the samples.

performed in the G_μ-scheme [75], ensuring an optimal description of pure electroweak interactions at the electroweak scale. All samples were generated using the NNPDF3.0NNLO PDF set, along with the dedicated set of tuned PS parameters developed by the Sherpa authors.

Other minor backgrounds ($tHjb$, tHW, tZq, tZW and four top quarks) were also simulated and accounted for, even though they contribute less than 1% in any analysis region. All samples and their basic generation parameters are summarised in table 1.

Most of the samples mentioned above were produced using the full ATLAS detector simulation [76] based on Geant4 [77], and the rest were produced using fast simulation [78], where the complete Geant4 simulation of the calorimeter response is replaced by a detailed parameterisation of the shower shapes, as shown in table 1. For the observables used in this analysis, the two simulations were found to give compatible results. Additional pile-up interactions, simulated with Pythia 8.186 using the A3 set of tuned parameters [55], were overlaid onto the simulated hard-scatter event. All simulation samples were reweighted such that the distribution of the number of pile-up interactions matches that of the data. In all samples the top-quark mass was set to 172.5 GeV, and the decays of b- and c-hadrons were performed by EvtGen v1.2.0 [79], except in samples simulated by the Sherpa event generator.

3 Object reconstruction and event selection

Charged leptons and jets, including those compatible with the hadronisation of b-quarks, are the main reconstructed objects used in this analysis. Electrons are reconstructed from

JHEP06(2021)145

energy clusters in the electromagnetic calorimeter associated with tracks reconstructed in the ID [80], and are required to have $|\eta| < 2.47$. Candidates in the calorimeter transition region ($1.37 < |\eta| < 1.52$) are excluded. Electrons must satisfy the *tight* identification criterion described in ref. [81], based on shower-shape and track-matching variables. Muons are reconstructed from either track segments or full tracks in the MS which are matched to tracks in the ID. Tracks are then re-fit using information from both detector systems. Muons must satisfy the *medium* identification criterion [82]. Muons are required to have $|\eta| < 2.5$. To reduce the contribution of leptons from hadronic decays (non-prompt leptons), both the electrons and muons must satisfy isolation criteria. These criteria include both track and calorimeter information, and have an efficiency of 90% for leptons with a p_{T} greater than 25 GeV, rising to 99% above 60 GeV, as measured in $Z \to ee$ and $Z \to \mu\mu$ data samples [80, 82]. Finally, the lepton tracks must point to the primary vertex of the event,[3] the longitudinal impact parameter must satisfy $|z_0| < 0.5$ mm and the transverse impact parameter significance must satisfy $|d_0|/\sigma_{d_0} < 5\,(3)$ for electrons (muons).

Jets are reconstructed from three-dimensional topological energy clusters [83] in the calorimeter using the anti-k_t jet algorithm [84] with a radius parameter of 0.4. Each topological cluster is calibrated to the electromagnetic scale response prior to jet reconstruction. The reconstructed jets are then calibrated with a series of simulation-based corrections and in situ techniques based on 13 TeV data [85]. After energy calibration, jets are required to have $p_{\mathrm{T}} > 25$ GeV and $|\eta| < 2.5$. Quality criteria are imposed to identify jets arising from non-collision sources or detector noise, and any event containing such a jet is removed [86]. Finally, to reduce the effect of pile-up, jets with $p_{\mathrm{T}} < 120$ GeV and $|\eta| < 2.4$ are matched to tracks with $p_{\mathrm{T}} > 0.5$ GeV, thus ensuring they originate from the primary vertex. This algorithm is known as the jet vertex tagger (JVT) [87]. To identify jets containing b-hadrons, referred to as b-jets in the following, the MV2c10 tagger algorithm [88], which combines impact parameter information with the explicit identification of secondary and tertiary vertices within the jet into a multivariate discriminant, is used. Jets are b-tagged by requiring the discriminant output to be above a threshold, providing a specific b-jet efficiency in simulated $t\bar{t}$ events. A criterion with an efficiency of 70% is used to determine the b-jet multiplicity in this analysis. For this working point and for the same $t\bar{t}$ sample, the c-jet and light-flavour-quark or gluon jet (light-jets) rejection factors are 8.9 and 300, respectively [89].

To avoid counting a single detector signal as more than one lepton or jet, an overlap removal procedure is applied. First, the closest jet within $\Delta R_y = \sqrt{(\Delta y)^2 + (\Delta\phi)^2} = 0.2$ of a selected electron is removed.[4] If the nearest jet surviving that selection is within $\Delta R_y = 0.4$ of the electron, the electron is discarded. Muons are removed if they are separated from the nearest jet by $\Delta R_y < 0.4$, which reduces the background from semileptonic decays of heavy-flavour hadrons. However, if this jet has fewer than three associated tracks, the

[3] Events are required to have at least one reconstructed vertex with three or more associated tracks which have $p_{\mathrm{T}} > 400$ MeV. The primary vertex is chosen as the vertex candidate with the largest sum of the squared transverse momenta of associated tracks.

[4] The rapidity is defined as $y = \frac{1}{2} \ln \frac{E+p_z}{E-p_z}$, where E is the energy and p_z is the momentum component along the beam pipe.

JHEP06(2021)145

muon is kept and the jet is removed instead; this avoids an inefficiency for high-energy muons undergoing significant energy loss in the calorimeter.

The missing transverse momentum (of size $E_{\mathrm{T}}^{\mathrm{miss}}$) in the event is computed as the negative vector sum of the p_{T} of all the selected electrons, muons and jets described above, with a correction for soft energy not associated with any of the hard objects. This additional 'soft term' is calculated from ID tracks matched to the primary vertex to make it resilient to pile-up contamination [90]. The missing transverse momentum is not used in the event selection, but included in the multivariate discriminant used in the analysis.

Events are required to have exactly one electron or muon, with $p_{\mathrm{T}} > 27\,\mathrm{GeV}$, within $\Delta R < 0.15$ of a lepton of the same flavour reconstructed by the trigger algorithm, and at least five jets, at least three of which must be b-tagged. The total event acceptance for the H^+ signal samples ranges from 2% (at 200 GeV) to 8.5% (at 1000 GeV). Above 1000 GeV, the acceptance decreases due to the boosted topology of the events, which fail the requirement on jet multiplicity. At 2000 GeV, the acceptance is 6%. The selected events are categorised into four separate regions according to the number of reconstructed jets (j) and b-jets (b) in the event, in order to improve the sensitivity of the fit and constrain some of the systematic uncertainties. The analysis regions are 5j3b, 5j≥4b, ≥6j3b and ≥6j≥4b, where XjYb means that X jets are found in the event, and among them Y are b-tagged. In addition, the ≥5j2b region is used to derive data-based corrections, which are implemented to improve the level of agreement between simulation and data.

4 Background modelling

With the isolation criteria applied both at the trigger and analysis level, as well as the purity-enhancing identification criteria used for electrons and muons (section 3), the background due to non-prompt leptons is expected to be negligible. To confirm this assumption, the ratio $(N_{\mathrm{Data}} - N_{\mathrm{MC}}^{\mathrm{total}})/N_{\mathrm{MC}}^{\mathrm{total}}$ was checked and found to not decrease when moving from a loose to a tight isolation selection. Such behaviour shows that the non-prompt-lepton background, which is not present in the simulation, provides a negligible contribution to the data, as expected given that non-prompt leptons are unlikely to be isolated in data. If data and the MC predictions differed due to a mismodelling of the other backgrounds, tighter isolation requirements would remove events in data and MC simulation alike. All backgrounds in this analysis are estimated using the simulation samples described in section 2.

To define the background categories in the likelihood fit (section 7), the $t\bar{t}$ + jets background is categorised according to the flavour of the jets in the event. Generator-level particle jets are reconstructed from stable particles (mean lifetime $\tau > 3 \times 10^{-11}$ s) using the anti-k_t algorithm with a radius parameter $R = 0.4$, and are required to have $p_{\mathrm{T}} > 15\,\mathrm{GeV}$ and $|\eta| < 2.5$. The flavour of a jet is determined by counting the number of b- or c-hadrons within $\Delta R = 0.4$ of the jet axis. Jets matched to one or more b-hadrons, of which at least one must have p_{T} above 5 GeV, are labelled as b-jets; c-jets are defined analogously, only considering jets not already defined as b-jets. Events that have at least one b-jet, not including heavy-flavour jets from top-quark or W-boson decays, are labelled

JHEP06(2021)145

as $t\bar{t}$ + ≥1b; those with no b-jets but at least one c-jet are labelled as $t\bar{t}$ + ≥1c. Finally, events not containing any heavy-flavour jets, aside from those from top-quark or W-boson decays, are labelled as $t\bar{t}$ + light.

After the event selection, $t\bar{t}$ + jets constitutes the main background. It is observed that the simulation of $t\bar{t}$ + jets does not properly model high jet multiplicities nor the hardness of additional jet emissions, and data-based corrections are applied to the simulation [91, 92]. Given that the additional jets in the $t\bar{t}$ + jets sample are simulated in the parton shower, the mentioned mismodelling is expected to be independent of whether the additional jets are b-tagged or not. Therefore, data and MC predictions are compared and reweighting factors are derived in a sample with at least five jets and exactly two b-tagged jets, and then applied in the 3b and ≥4b regions. The level of agreement between data and simulation in these regions improves to the point where the remaining differences are well within the model's systematic uncertainty. The reweighting factors are expressed as:

$$R(x) = \frac{N_{\text{Data}}(x) - N_{\text{MC}}^{\text{non-}t\bar{t}}(x)}{N_{\text{MC}}^{t\bar{t}}(x)},$$

where x is the variable mismodelled by the simulation. In this context, $t\bar{t}$ + light, $t\bar{t}$ + ≥1b and $t\bar{t}$ + ≥1c, as well as Wt single-top contributions, are included in the $t\bar{t}$ sample. For the range of H^+ masses considered in this analysis and assuming the observed upper limits on the cross-section times branching ratio published in ref. [25], signal events contribute less than 1% to the ≥5j2b region and are neglected. Weights are calculated from the number of jets distribution (R(nJets)) first and subsequently applied to the $H_{\text{T}}^{\text{all}}$ distributions[5] to derive the reweighting factors in the 5j2b, 6j2b, 7j2b and ≥8j2b regions ($R(H_{\text{T}}^{\text{all}})$). Thus, events are weighted by the product R(nJets) × $R(H_{\text{T}}^{\text{all}})$ depending on their jet multiplicity and $H_{\text{T}}^{\text{all}}$ value. Figure 2 shows R(nJets) in the ≥5j2b region and $R(H_{\text{T}}^{\text{all}})$ in the 5j2b, 6j2b, 7j2b and ≥8j2b regions. Among various functions tried, a hyperbola plus a sigmoid functional form was found to be the best fit to the $H_{\text{T}}^{\text{all}}$ weight distributions.

After the reweighting, agreement between simulation and data in the analysis regions improves, as can be seen, for example, in figure 3, which shows the leading jet's p_{T} distribution before the fit, both before and after applying the reweighting. The final $t\bar{t}$ + ≥1b and $t\bar{t}$ + ≥1c normalisation factors and their uncertainties, which account for the remaining mismodelling observed after applying the reweighting, are not applied. These normalisations are extracted from the fit to data, as described in section 7.

5 Analysis strategy

To enhance the separation between signal and background, a neural network algorithm (NN) is used. Its architecture is sequential with two fully connected layers of 64 nodes, and is implemented with the Python deep learning library, Keras [93]. The activation function used is the commonly employed 'rectified linear unit' and the loss function is the 'binary cross-entropy'. Batch normalisation [94] is performed to speed up the learning process,

[5] $H_{\text{T}}^{\text{all}}$ is defined as the scalar sum of the transverse momenta of all jets and the lepton in the event.

JHEP06(2021)145

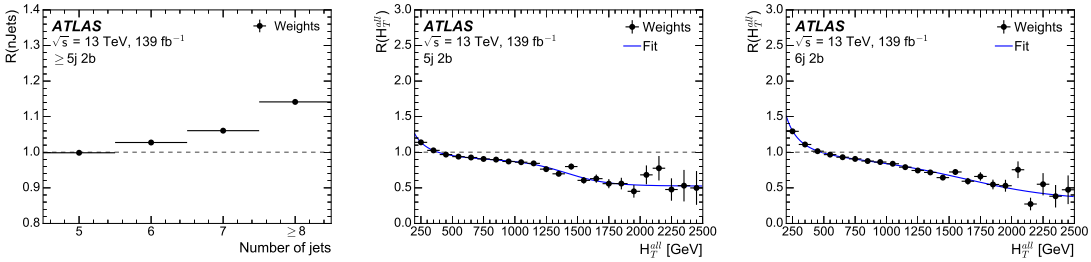

(a) ≥5j2b. **(b)** 5j2b. **(c)** 6j2b.

(d) 7j2b. **(e)** ≥8j2b.

Figure 2. Reweighting factors (weights) obtained from the comparison between data and simulation of the number of jets (a) and $H_{\mathrm{T}}^{\mathrm{all}}$ for various jet multiplicity selections (b) to (e). The errors in the data points include the statistical uncertainties in data and MC predictions.

dropout [95] is applied at a 10% rate, and the Adam algorithm [96] is used to optimise the parameters.

All signal samples are used in the training against all background samples, which are weighted according to their cross-sections. The training is performed separately in each analysis region, but the separate trainings include all H^+ mass samples, and use the value of the H^+ mass as a parameter [97]. For signal events the parameter corresponds to the mass of the H^+ sample they belong to, while for background events a random value of the H^+ mass, taken from the distribution of signal masses, is assigned to each event. A total of 15 variables are used in the NN:

- kinematic discriminant D defined in the text,
- scalar sum of the p_{T} of all jets,
- centrality calculated using all jets and leptons,
- p_{T} of the leading jet,
- p_{T} of fifth leading jet,
- invariant mass of the b-jet pair with minimum ΔR,
- invariant mass of the b-jet pair with maximum p_{T},
- largest invariant mass of a b-jet pair,

JHEP06(2021)145

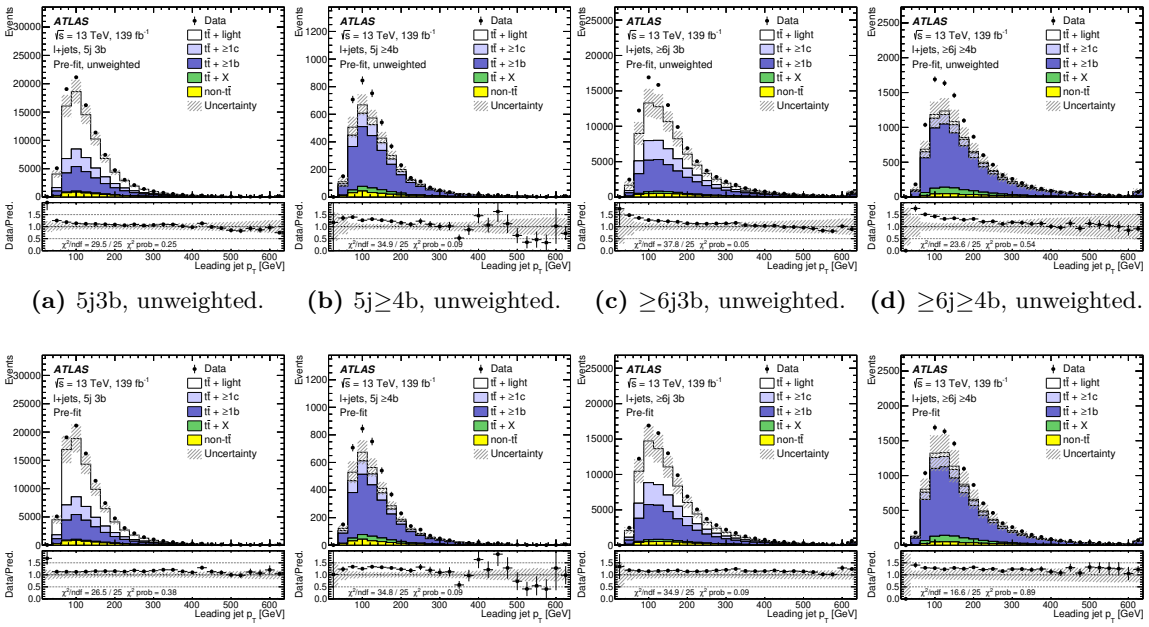

(a) 5j3b, unweighted. **(b)** 5j≥4b, unweighted. **(c)** ≥6j3b, unweighted. **(d)** ≥6j≥4b, unweighted.

(e) 5j3b, reweighted. **(f)** 5j≥4b, reweighted. **(g)** ≥6j3b, reweighted. **(h)** ≥6j≥4b, reweighted.

Figure 3. Comparison of the predicted leading jet p_{T} and data before the fit in the four analysis regions before (top) and after (bottom) the reweighting was applied. The uncertainty bands include both the statistical and systematic uncertainties. Since the normalisations of the $t\bar{t}$ + ≥1b and $t\bar{t}$ + ≥1c backgrounds are allowed to vary in the fit, no cross-section uncertainties associated with these processes are included. The lower panels display the ratio of the data to the total prediction. The hatched bands show the uncertainties before the fit to the data, which are dominated by systematic uncertainties. The χ^2/ndf and the χ^2 probability are also shown. Statistical uncertainties on MC predictions and data are uncorrelated across bins, while systematic uncertainties on the predictions are correlated.

- invariant mass of the jet triplet with maximum p_{T},
- invariant mass of the untagged jet-pair with minimum ΔR (not in 5j≥4b),
- average ΔR between all b-jet pairs in the event,
- ΔR between the lepton and the pair of b-jets with smallest ΔR,
- second Fox-Wolfram moment calculated using all jets and leptons [98],
- number of jets (only in ≥6j3b and ≥6j≥4b regions), and
- number of b-jets (only in 5j≥4b and ≥6j≥4b regions).

The variables are chosen to provide the best discrimination against the $t\bar{t}$ + ≥1b background. Among them, the kinematic discriminant, scalar sum of the p_{T} of all jets, centrality, and leading jet p_{T} provide the most discrimination. The centrality is computed as the scalar sum of the p_{T} of all jets and leptons in the event divided by the sum of their

JHEP06(2021)145

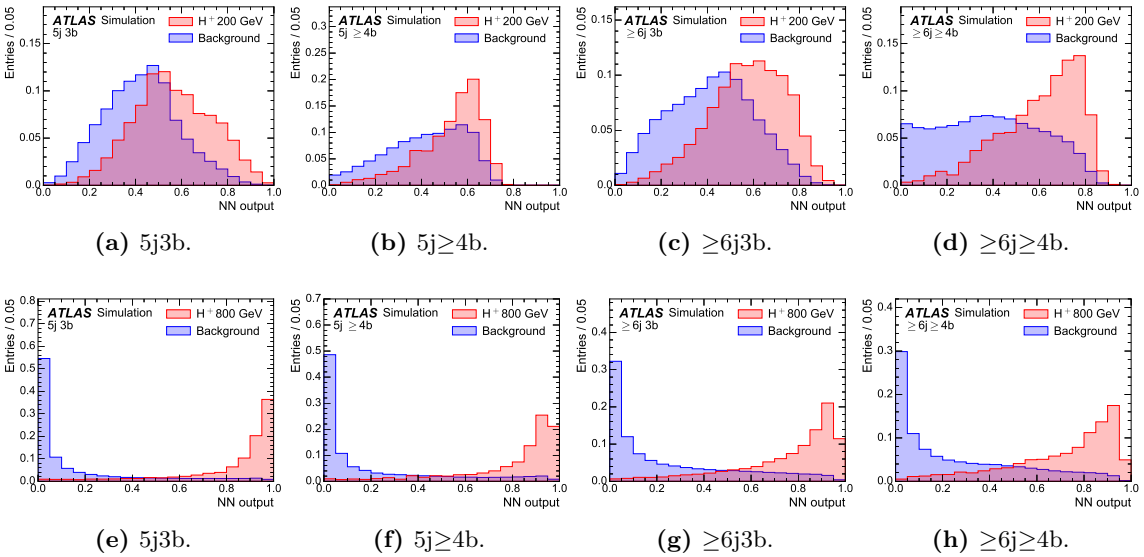

(a) 5j3b. **(b)** 5j≥4b. **(c)** ≥6j3b. **(d)** ≥6j≥4b.

(e) 5j3b. **(f)** 5j≥4b. **(g)** ≥6j3b. **(h)** ≥6j≥4b.

Figure 4. Expected distributions of the NN output for H^+ masses of 200 GeV (top) and 800 GeV (bottom) for SM backgrounds and H^+ signal in the four analysis regions. All distributions are normalised to unity.

energies. The kinematic discriminant is a variable reflecting the probability that an event is compatible with the $H^+ \to tb$ hypothesis rather than the $t\bar{t}$ hypothesis, and is defined as $D = P_{H^+(\mathbf{x})}/(P_{H^+(\mathbf{x})} + P_{t\bar{t}(\mathbf{x})})$, where $P_{H^+(\mathbf{x})}$ and $P_{t\bar{t}(\mathbf{x})}$ are probability density functions for $\mathbf{x}$ under the signal hypothesis and background ($t\bar{t}$) hypothesis, respectively. The event variable $\mathbf{x}$ indicates the set of the missing transverse momentum and the four-momenta of the reconstructed lepton and the jets [25].

Figure 4 shows the predicted NN output distributions in the four analysis regions for selected H^+ signal samples and the SM background. These distributions are used in a fit to extract the amount of H^+ signal in data. The separation of the H^+ signal from the background is most difficult for low H^+ masses because the two processes have very similar kinematics and topology. The kinematic discriminant has large separating power at low H^+ masses, whereas at higher masses, where the topologies of the H^+ signal and the background are no longer alike, other variables, such as the scalar sum of the p_{T} of all jets, provide the largest separation.

6 Systematic uncertainties

Various sources of experimental and theoretical uncertainties are considered in this analysis. They may affect the overall normalisation of the processes, the shapes of the NN output distributions, or both. All the experimental uncertainties considered, with the exception of that in the luminosity, affect both normalisation and shape in all the simulated samples. Uncertainties related to the modelling of the signal and background affect both normalisation and shape, with the exception of cross-section uncertainties, which only affect the normalisation of the sample considered. Nonetheless, the normalisation uncertainties modify the relative fractions of the different samples, leading to a shape variation in the

JHEP06(2021)145

final NN output distributions. A single independent nuisance parameter (NP) is assigned to each source of systematic uncertainty in the statistical analysis. Some of the systematic uncertainties, in particular most of the experimental uncertainties, are decomposed into several independent sources. Each individual source has a correlated effect across all analysis regions and signal and background samples.

The uncertainty of the integrated luminosity for the full Run-2 dataset is 1.7% [99], obtained using the LUCID-2 detector [100] for the primary luminosity measurements. A variation in the pile-up reweighting of the simulated events described in section 2 is included to cover the uncertainty in the ratio of the predicted and measured inelastic cross-sections in a given fiducial volume [101].

Uncertainties associated with charged leptons arise from the trigger selection, the lepton reconstruction, identification and isolation criteria, as well as the lepton momentum scale and resolution. The reconstruction, identification and isolation efficiency of electrons and muons, as well as the efficiency of the trigger used to record the events, differ slightly between data and simulation, which is compensated for by dedicated correction factors (CFs). Efficiency CFs are measured using tag-and-probe techniques in $Z \to \ell^+\ell^-$ data and simulated samples [82, 102], and are applied to the simulation to correct for the differences. The effect of these CFs, as well as of their uncertainties, are propagated as corrections to the MC event weight. Additional sources of uncertainty originate from the corrections applied to adjust the lepton momentum scale and resolution in the simulation to match those in data. The impact of these uncertainties on $\sigma(pp \to tbH^+) \times \mathcal{B}(H^+ \to tb)$ is smaller than 1%.

Uncertainties associated with jets arise from the efficiency of pile-up rejection by the JVT, from the jet energy scale (JES) and resolution (JER), and from b-tagging. Correction factors are applied to correct for differences between data and MC simulation for JVT efficiencies. These CFs are estimated using $Z(\to \mu^+\mu^-)$ + jets with tag-and-probe techniques similar to those in ref. [87]. The JES and its uncertainty are derived by combining information from test-beam data, collision data and simulation [85]. Additional uncertainties are considered, related to jet flavour, quark/gluon fraction, pile-up corrections, η dependence, high-p_{T} jets, and differences between full and fast simulation. The JER uncertainty is obtained by combining dijet balance measurements in data and simulation [103]. The b-tagging efficiencies in simulated samples are corrected to match efficiencies in data. Correction factors are derived as a function of p_{T} for b-, c- and light-jets separately in dedicated calibration analyses. For b-jet efficiencies, $t\bar{t}$ events in the di-lepton topology are used, exploiting the very pure sample of b-jets arising from the decays of the top quarks [89]. For c-jet mistag rates, $t\bar{t}$ events in single-lepton topology are used, exploiting the c-jets from the hadronically decaying W bosons, using techniques similar to those in ref. [104]. For light-jet mistag rates, the so-called negative-tag method similar to that in ref. [105] is used, but using Z+jets events instead of di-jet events.

All the uncertainties described above on energy scales or resolutions of the reconstructed objects are propagated to the missing transverse momentum. Additional uncertainties in the scale and resolution of the soft term are considered, which account for the disagreement between data and simulation of the p_{T} balance between the hard and the

JHEP06(2021)145

soft components. A total of three independent sources are added: an offset along the hard component p_{T} axis, and the smearing resolution along and perpendicular to this axis [106, 107]. Since the missing transverse momentum is not used in selection but only in the event reconstruction, the associated uncertainties have an impact smaller than 1%.

The uncertainty in the H^+ signal due to different scale choices is estimated by varying μ_{f} and μ_{r} up and down by a factor of two. The uncertainties from the modelling of the PDF are evaluated replacing the nominal NNPDF2.3NLO PDF set by a symmetrised Hessian set, PDF4LHC15_nlo_30, following the PDF4LHC recommendations for LHC Run 2 [108].

The modelling of the $t\bar{t}$ + jets background is one of the largest sources of uncertainty in the analysis, and several different components are considered. The 6% uncertainty for the inclusive $t\bar{t}$ production cross-section predicted at NNLO+NNLL includes effects from varying μ_{f} and μ_{r}, the PDF, α_{S}, and the top-quark mass [109]. This uncertainty is applied to $t\bar{t}$ + light only, since the normalisation of $t\bar{t}$ + $\geq$1b and $t\bar{t}$ + $\geq$1c are allowed to vary freely in the fit. Besides normalisation, the $t\bar{t}$ + light, $t\bar{t}$ + $\geq$1b and $t\bar{t}$ + $\geq$1c processes are affected by different types of uncertainties: the uncertainties associated with additional Feynman diagrams for the $t\bar{t}$ + light are constrained from relatively precise measurements in data [110]; $t\bar{t}$ + $\geq$1b and $t\bar{t}$ + $\geq$1c can have similar or different Feynman diagrams depending on the flavour scheme used for the PDF, and the different masses of the b- and the c-quarks contribute to additional differences between these two processes. For these reasons, all uncertainties in the $t\bar{t}$ + jets background modelling are assigned independent NP for $t\bar{t}$ + light, $t\bar{t}$ + $\geq$1b and $t\bar{t}$ + $\geq$1c. Systematic uncertainties in the acceptance and shapes are extracted by comparing the nominal prediction with alternative MC samples or settings. Such comparisons would significantly change the fractions of $t\bar{t}$ + $\geq$1b and $t\bar{t}$ + $\geq$1c. However, since the normalisation of these sub-processes in the analysis regions is determined in the fit, these alternative predictions are reweighted in such a way that they keep the same fractions of $t\bar{t}$ + $\geq$1b and $t\bar{t}$ + $\geq$1c as the nominal sample in the phase-space selected by the analysis.

The uncertainty due to initial state radiation (ISR) is estimated by using the *Var3cUp* (*Var3cDown*) variant from the A14 tune [48], corresponding to $\alpha_{\mathrm{S}}^{\mathrm{ISR}} = 0.140$ (0.115) instead of the nominal $\alpha_{\mathrm{S}}^{\mathrm{ISR}} = 0.127$. Uncertainties related to μ_{f} and μ_{r} are estimated by scaling each one up and down by a factor of two. For the final state radiation (FSR), the amount of radiation is increased (decreased) in the PS corresponding to $\alpha_{\mathrm{S}}^{\mathrm{FSR}} = 0.142$ (0.115) instead of the nominal $\alpha_{\mathrm{S}}^{\mathrm{FSR}} = 0.127$. The nominal PowhegBox+Pythia sample is compared with the PowhegBox+Herwig sample to assess the effect of the PS and hadronisation models, and to the MadGraph5_aMC@NLO sample to assess the effect of the NLO matching technique. The nominal PowhegBox+Pythia 5FS prediction for the dominant $t\bar{t}$ + $\geq$1b background, in which all the additional partons are produced by the PS, is compared with an alternative PowhegBox+Pythia 4FS sample, in which the $b\bar{b}$ pair is generated in addition to the $t\bar{t}$ pair at the ME level. An uncertainty resulting from the comparison of the shapes of the two models is included. Finally, the weights derived in section 4 to improve the agreement of the simulation with data are varied within their statistical uncertainties, in a correlated way among the three $t\bar{t}$ + jets components. All the sources of systematic uncertainty for the $t\bar{t}$ + jets modelling are summarised in table 2.

JHEP06(2021)145

Uncertainty source	Description		Components
$t\bar{t}$ cross-section	Up or down by 6%		$t\bar{t}$ + light
$t\bar{t}$ reweighting	Statistical uncertainties of fitted function (six) parameters		All $t\bar{t}$ and Wt
$t\bar{t}$ + $\geq$1b modelling	4FS vs. 5FS		$t\bar{t}$ + $\geq$1b
$t\bar{t}$ + $\geq$1b normalisation	Free-floating		$t\bar{t}$ + $\geq$1b
$t\bar{t}$ + $\geq$1c normalisation	Free-floating		$t\bar{t}$ + $\geq$1c
NLO matching	MadGraph5_aMC@NLO+Pythia	vs. PowhegBox+Pythia	All $t\bar{t}$
PS & hadronisation	PowhegBox+Herwig	vs. PowhegBox+Pythia	All $t\bar{t}$
ISR	Varying $\alpha_{\mathrm{S}}^{\mathrm{ISR}}$	in PowhegBox+Pythia	All $t\bar{t}$
μ_{f}	Scaling by 0.5 (2.0)	in PowhegBox+Pythia	All $t\bar{t}$
μ_{r}	Scaling by 0.5 (2.0)	in PowhegBox+Pythia	All $t\bar{t}$
FSR	Varying $\alpha_{\mathrm{S}}^{\mathrm{FSR}}$	in PowhegBox+Pythia	All $t\bar{t}$

Table 2. Summary of the sources of systematic uncertainty for $t\bar{t}$ + jets modelling. The systematic uncertainties listed in the second section of the table are evaluated in such a way as to have no impact on the normalisation of the three, $t\bar{t}$ + $\geq$1b, $t\bar{t}$ + $\geq$1c and $t\bar{t}$ + light, components in the phase-space selected in the analysis. The last column of the table indicates the $t\bar{t}$ + jets components to which the systematic uncertainty is assigned. All systematic uncertainty sources, except those associated to the $t\bar{t}$ reweighting, are treated as uncorrelated across the three components.

A 5% uncertainty is considered for the cross-sections of the three single-top production modes [111–115]. Uncertainties associated with the PS and hadronisation model, and with the NLO matching scheme are evaluated by comparing, for each process, the nominal PowhegBox+Pythia sample with a sample produced using PowhegBox+Herwig [116] and MadGraph5_aMC@NLO+Pythia, respectively. As mentioned in section 4, the Wt single-top mode is included in the reweighting procedure, and thus the same uncertainties used for $t\bar{t}$ are applied here. The uncertainty associated to the interference between Wt and $t\bar{t}$ production at NLO [63] is assessed by comparing the nominal PowhegBox+Pythia sample produced using the "diagram removal" scheme with an alternative sample produced with the same generator but using the "diagram subtraction" scheme [62, 63].

The predicted SM $t\bar{t}H$ signal cross-section uncertainty is $^{+5.8\%}_{-9.2\%}$ (QCD scale) $\pm$3.6% (PDF + α_{S}) [13, 117–121]. Uncertainties of the Higgs boson branching ratios amount to 2.2% for the $b\bar{b}$ decay mode [13]. For the ISR and FSR, the amount of radiation is varied following the same procedure as for $t\bar{t}$. The nominal PowhegBox+Pythia sample is compared with the PowhegBox+Herwig sample to assess the uncertainty due to PS and hadronisation, and to the MadGraph5_aMC@NLO sample for the uncertainty due to the NLO matching.

The uncertainty of the $t\bar{t}V$ NLO cross-section prediction is 15%, split into PDF and scale uncertainties as for $t\bar{t}H$ [13, 122]. An additional $t\bar{t}V$ modelling uncertainty, related to the choice of PS and hadronisation model and matching scheme, is assessed by comparing the nominal MadGraph5_aMC@NLO+Pythia samples with alternative samples generated with Sherpa.

An overall 50% normalisation uncertainty is considered for the four-top-quarks background, covering effects from varying μ_{f}, μ_{r}, PDF and α_{S} [45, 123]. The small background

JHEP06(2021)145

tZq is assigned a 7.9% and a 0.9% uncertainty accounting for μ_f and μ_r scales and PDF variations, respectively. Finally, a single 50% uncertainty is used for tZW [45].

An uncertainty of 40% is assumed for the W+jets normalisation, with an additional 30% for W + heavy-flavour jets, taken as uncorrelated between events with two and more than two heavy-flavour jets. These uncertainties are based on variations of the μ_f and μ_r scales and of the matching parameters in the Sherpa samples. An uncertainty of 35% is applied to the Z+jets normalisation, uncorrelated across jet bins, to account for both the variations of the scales and matching parameters in the Sherpa samples and the uncertainty in the extraction from data of the correction factor for the heavy-flavour component [54, 124]. Finally, a 50% normalisation uncertainty in the diboson background is assumed, which includes uncertainties in the inclusive cross-section and additional jet production [125].

7 Results

A binned maximum-likelihood fit to the data is performed simultaneously on the NN output distributions in the four analysis regions, and each mass hypothesis is tested separately. A profile-likelihood-ratio test and the CL_S method [126–128] are used to quantify the level of agreement with the background-only hypothesis or background-plus-signal hypothesis and to determine exclusion limits. The parameter of interest is the product of the production cross-section $\sigma(pp \to tbH^+)$ and the branching ratio $\mathcal{B}(H^+ \to tb)$. In addition, two unconstrained factors, for which no prior knowledge is assumed, are used to normalise the $t\bar{t}$ + $\geq$1b and $t\bar{t}$ + $\geq$1c backgrounds. These normalisation factors range from 1.2 to 1.6 (0.2 to 1.8) with a typical uncertainty of 0.2 (0.6) for the $t\bar{t}$ + $\geq$1b ($t\bar{t}$ + $\geq$1c) background, depending on the H^+ mass hypothesis used in the fit. The fitted $t\bar{t}$ + heavy-flavour jets backgrounds in the different fits are consistent within two standard deviations. All systematic uncertainties are implemented as nuisance parameters with log-normal constraint terms. There are about 170 nuisance parameters considered in the fit, the number varying slightly across the range of mass hypotheses. A summary of the systematic uncertainties with similar sources grouped together is given in table 3. Depending on the particular H^+ mass hypothesis, the total systematic uncertainty is dominated by the uncertainties in the modelling of the $t\bar{t}$ background, in particular $t\bar{t}$ + $\geq$1b and $t\bar{t}$ + $\geq$1c, jet flavour-tagging uncertainties, and jet energy scale and resolution.

Table 4 shows the event yields after the background-plus-signal fit under the 200 GeV and 800 GeV H^+ mass hypotheses. The corresponding post-fit distributions of the NN output in each analysis region are shown in figure 5 for the 200 GeV and 800 GeV H^+ mass hypotheses. After the fit, good agreement between the data and simulation is found in the input variables to the NN. No significant excess above the expected SM background is observed in all regions and mass intervals and upper limits on the cross-section times branching ratio are derived as function of the H^+ mass.

The 95% confidence level (CL) upper limits on $\sigma(pp \to tbH^+) \times \mathcal{B}(H^+ \to tb)$ obtained using the CL_S method are presented in figure 6. Uncertainties in the predicted H^+ cross-

JHEP06(2021)145

Uncertainty source	$\Delta\mu(H^+_{200})$ [pb]	$\Delta\mu(H^+_{800})$ [pb]
$t\bar{t}$ + ≥1b modelling	1.01	0.025
Jet energy scale and resolution	0.35	0.009
$t\bar{t}$ + ≥1c modelling	0.32	0.006
Jet flavour tagging	0.20	0.025
Reweighting	0.22	0.007
$t\bar{t}$ + light modelling	0.33	0.009
Other background modelling	0.19	0.011
MC statistics	0.11	0.008
JVT, pile-up modelling	<0.01	0.001
Luminosity	<0.01	0.002
Lepton ID, isolation, trigger, $E_{\mathrm{T}}^{\mathrm{miss}}$	<0.01	<0.001
H^+ modelling	0.05	0.002
Total systematic uncertainty	1.35	0.049
$t\bar{t}$ + ≥1b normalisation	0.23	0.007
$t\bar{t}$ + ≥1c normalisation	0.045	0.015
Total statistical uncertainty	0.43	0.025
Total uncertainty	1.42	0.055

Table 3. Summary of the statistical and systematic uncertainties on $\mu = \sigma(pp \to tbH^+) \times \mathcal{B}(H^+ \to tb)$ shown for a H^+ signal with a mass of 200 and 800 GeV, extracted from the fit to the data. A value of $\mu = 1$ pb is assumed for all H^+ mass hypotheses. Due to correlations between the different sources of uncertainty, the total systematic uncertainty can be different from the sum in quadrature of the individual sources. The normalisation factors for both $t\bar{t}$ + ≥1b and $t\bar{t}$ + ≥1c are included in the statistical component.

sections or branching ratios are not included. The observed (expected) limits range from $\sigma \times \mathcal{B} = 3.6\,(2.6)$ pb at $m_{H^+} = 200$ GeV to $\sigma \times \mathcal{B} = 0.036\,(0.019)$ pb at $m_{H^+} = 2$ TeV.

Figure 7 shows 95% CL exclusion limits set on $\tan\beta$ as a function of m_{H^+} for various benchmark scenarios in the MSSM. It is the first time that they are shown for all M_h^{125} available scenarios using the $H^+ \to tb$ channel. In the hMSSM framework, effective couplings of the lighter Higgs boson to the top quark, bottom quark and vector bosons are derived from fits to LHC data on the production and decay rates of the observed Higgs boson, including the limits from the search for heavier neutral and charged Higgs boson states. The M_h^{125}, $M_h^{125}(\tilde{\chi})$, $M_h^{125}(\tilde{\tau})$, M_h^{125}(alignment) and $M_{h_1}^{125}$(CPV) scenarios also feature a scalar particle with mass and couplings compatible with those of the observed Higgs boson, and force a significant portion of their parameter space to be compatible with the limits from searches for supersymmetric particles. In the M_h^{125} scenario, all supersymmetric particles are relatively heavy and the decays of the MSSM Higgs bosons are essentially unaffected, whereas the $M_h^{125}(\tilde{\chi})$ and $M_h^{125}(\tilde{\tau})$ models include either light charginos and

JHEP06(2021)145

m_{H^+}= 200 GeV hypothesis				
	5j, 3b	5j, ≥ 4b	≥ 6j, 3b	≥ 6j, ≥ 4b
$t\bar{t}$ + light	45000 ± 4000	310 ± 110	32000 ± 4000	340 ± 140
$t\bar{t}$ + ≥1b	29600 ± 2900	2940 ± 220	40200 ± 3300	8000 ± 500
$t\bar{t}$ + ≥1c	14000 ± 4000	440 ± 140	19000 ± 6000	1010 ± 290
$t\bar{t}$ + W	110 ± 15	3.2 ± 0.6	236 ± 35	16.2 ± 2.7
$t\bar{t}$ + Z	300 ± 40	51 ± 6	670 ± 90	174 ± 23
Single-top Wt-channel	2300 ± 600	80 ± 50	1900 ± 800	150 ± 90
Single-top t-channel	740 ± 300	51 ± 20	500 ± 400	60 ± 50
Other top-quark sources	128 ± 16	17.5 ± 3.2	180 ± 70	58 ± 24
VV & V + jets	1600 ± 600	65 ± 23	1600 ± 600	120 ± 40
$t\bar{t}H$	530 ± 60	127 ± 19	1140 ± 120	430 ± 60
H^+	600 ± 900	70 ± 90	700 ± 1000	160 ± 230
Total	95700 ± 2900	4150 ± 140	98400 ± 2900	10500 ± 400
Data	95852	4109	98929	10552
m_{H^+}= 800 GeV hypothesis				
	5j, 3b	5j, ≥ 4b	≥ 6j, 3b	≥ 6j, ≥ 4b
$t\bar{t}$ + light	46000 ± 4000	330 ± 120	33000 ± 4000	500 ± 200
$t\bar{t}$ + ≥1b	29600 ± 3100	2920 ± 210	41000 ± 4000	8100 ± 400
$t\bar{t}$ + ≥1c	14000 ± 6000	440 ± 190	17000 ± 7000	870 ± 330
$t\bar{t}$ + W	108 ± 15	3.3 ± 0.6	233 ± 35	16.0 ± 2.7
$t\bar{t}$ + Z	300 ± 40	50 ± 7	660 ± 90	171 ± 23
Single-top Wt-channel	2000 ± 500	56 ± 33	1400 ± 500	100 ± 60
Single-top t-channel	740 ± 300	53 ± 21	600 ± 500	70 ± 50
Other top-quark sources	130 ± 16	17.7 ± 3.2	190 ± 70	61 ± 24
VV & V + jets	1900 ± 700	73 ± 25	1700 ± 600	130 ± 50
$t\bar{t}H$	520 ± 60	125 ± 19	1130 ± 120	420 ± 60
H^+	30 ± 80	4 ± 10	70 ± 180	20 ± 50
Total	94700 ± 2800	4070 ± 140	97800 ± 2800	10400 ± 400
Data	95852	4109	98929	10552

Table 4. Event yields of the H^+ signal and SM background processes in the four analysis regions after the fit to the data under the H^+ mass (m_{H^+}) hypotheses of 200 GeV (top) and 800 GeV (bottom). The quoted uncertainties take into account correlations and constraints of the nuisance parameters and include both the statistical and systematic uncertainties. The signal yield uncertainty includes the uncertainty of the $\sigma(pp \to tbH^+) \times \mathcal{B}(H^+ \to tb)$ values fitted under the 200 or 800 GeV H^+ mass hypotheses. Negative correlations among $t\bar{t}$ + light, $t\bar{t}$ + ≥1b and $t\bar{t}$ + ≥1c modelling uncertainties can cause the uncertainty on the total yields to be smaller than on individual components.

JHEP06(2021)145

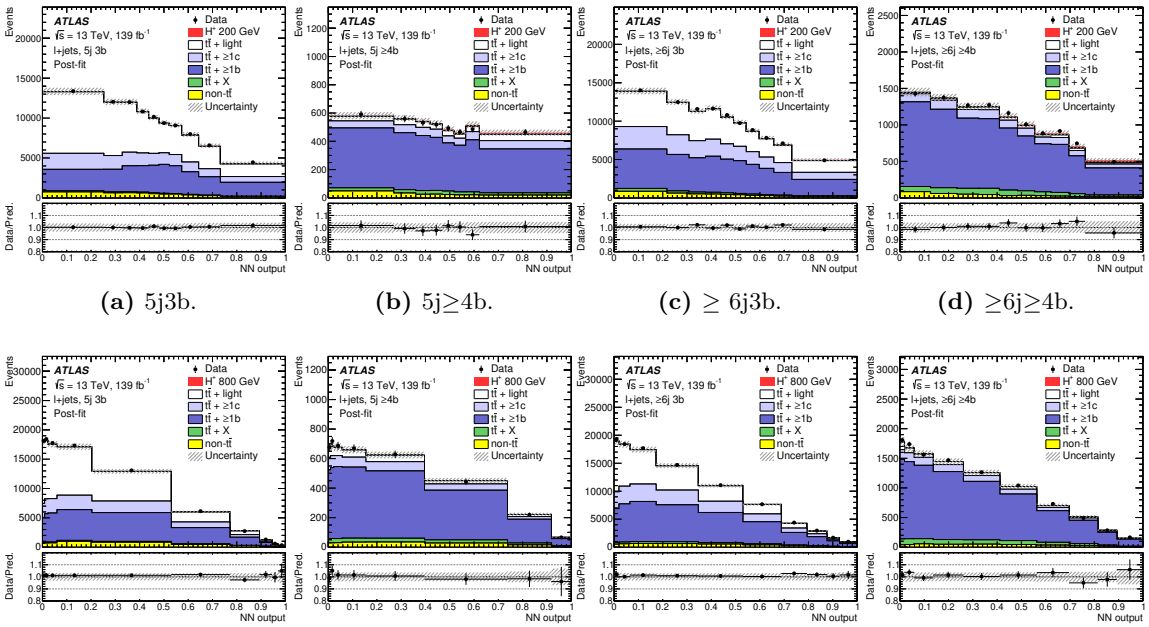

Figure 5. Distributions of the NN output after the fit for the 200 GeV (top) and 800 GeV (bottom) H^+ mass hypotheses in the four analysis regions. The lower panels display the ratio of the data to the total prediction. The hatched bands show the uncertainties after the fit.

neutralinos ($M_h^{125}(\tilde{\chi})$) or light staus ($M_h^{125}(\tilde{\tau})$). In both cases a charged Higgs boson of sufficiently high mass is allowed to decay into the supersymmetric particles. Finally, the value of $\tan\beta$ in both the M_h^{125}(alignment) scenario, characterised by one of the two neutral CP-even scalars having couplings like those of the SM Higgs boson, and the $M_{h_1}^{125}$(CPV) scenario, which includes CP violation in the Higgs sector, is already constrained to be in the range 1–20 by previous searches at the LHC [36]. Uncertainties in the predicted H^+ cross-sections or branching ratios are not included in the limits. For all scenarios except the hMSSM, Higgs boson masses and mixing (and effective Yukawa couplings) have been calculated with the code FeynHiggs [129–135]. Whereas in the hMSSM the branching ratios are computed solely with HDECAY [136, 137], all other scenarios combine the most precise results of FeynHiggs, HDECAY and PROPHECY4f [138, 139].

In the context of these scenarios, $\tan\beta$ values below 1 are observed to be excluded at 95% CL for H^+ masses between 200 and ∼790 GeV. High values of $\tan\beta$ between 34 and 60 are excluded in a similar mass range in the hMSSM and $M_h^{125}(\tilde{\chi})$ models. The most stringent limit, $\tan\beta < 2.1$ excluded at 95% CL, is set for the H^+ mass hypothesis of 225 GeV in the hMSSM and for the 250 GeV H^+ mass hypothesis in the M_h^{125}, $M_h^{125}(\tilde{\chi})$, $M_h^{125}(\tilde{\tau})$, M_h^{125}(alignment) and $M_{h_1}^{125}$(CPV) models. The low $\tan\beta$ and high H^+ mass parameter space was not excluded by any other analysis before, while the high $\tan\beta$ was already excluded by the $H^+ \to \tau\nu$ search. Compared to previous results of the same search channel, this analysis excludes a broader region of large $\tan\beta$. Additionally, an extended region of low $\tan\beta$ and low and high H^+ masses is also excluded.

JHEP06(2021)145

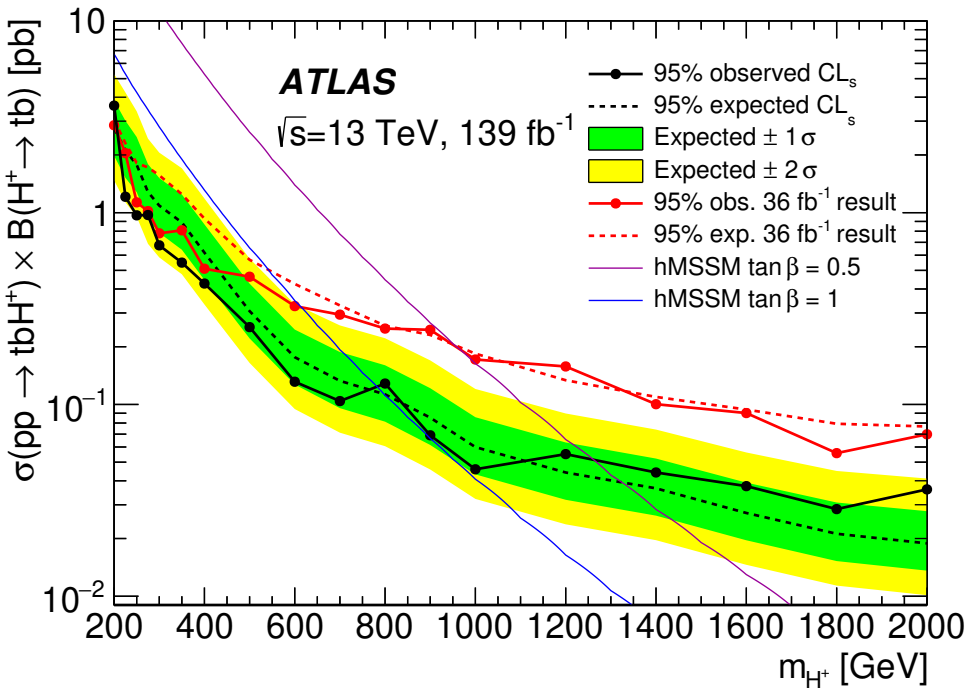

Figure 6. Observed and expected upper limits for the production of $H^+ \to tb$ in association with a top quark and a bottom quark. The bands surrounding the expected limit show the 68% and 95% confidence intervals. The red lines show the observed and expected 95% CL exclusion limits obtained with the 36 fb^{-1} data sample [25]. Theory predictions are shown for two representative values of $\tan\beta$ in the hMSSM benchmark scenario. Uncertainties in the predicted H^+ cross-sections or branching ratios are not considered.

8 Conclusion

A search for charged Higgs bosons is presented using a data sample corresponding to an integrated luminosity of 139 fb^{-1} from proton-proton collisions at $\sqrt{s} = 13$ TeV, recorded with the ATLAS detector at the LHC. The search for $pp \to tbH^+$ is performed in the H^+ mass range 200–2000 GeV. A neural network that combines jet multiplicities and several kinematic variables is built in the regions where the signal rate is expected to be largest. The neural network output depends on the H^+ mass, and a fit to the data is performed simultaneously on the neural network output distributions in the analysis regions, separately for each signal mass hypothesis.

No significant excess above the expected Standard Model background is found and observed (expected) upper limits at 95% confidence level are set on the $\sigma(pp \to tbH^+)$ production cross-section times the branching ratio $\mathcal{B}(H^+ \to tb)$, which range from $\sigma \times \mathcal{B} = 3.6\,(2.6)$ pb at $m_{H^+} = 200$ GeV to $\sigma \times \mathcal{B} = 0.036\,(0.019)$ pb at $m_{H^+} = 2$ TeV. Compared to the previous ATLAS search for tbH^+ production followed by $H^+ \to tb$ decays with 36 fb^{-1}, the observed $\sigma \times \mathcal{B}$ limits improved by 5% to 70%, depending on the H^+ mass, apart from the lowest one. In the low H^+ mass region the measurement is dominated by systematic uncertainties, while in the high H^+ mass region the use of tighter lepton

JHEP06(2021)145

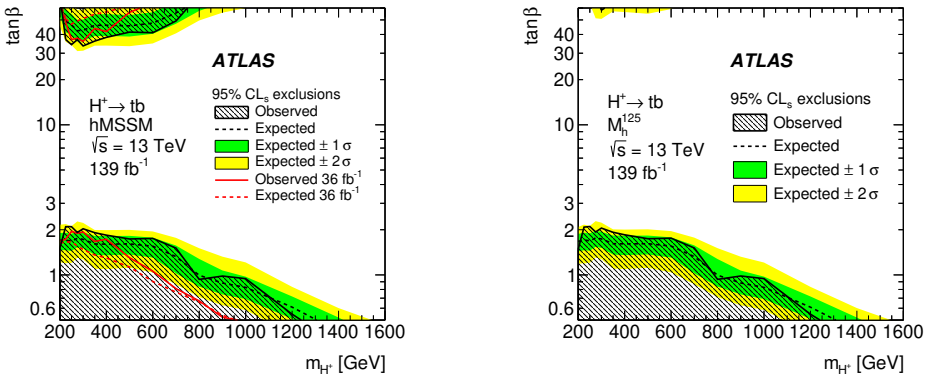

(a)

(b)

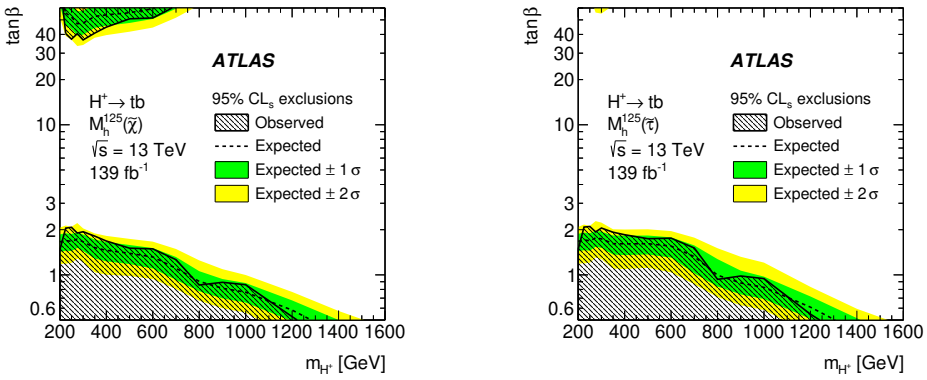

(c)

(d)

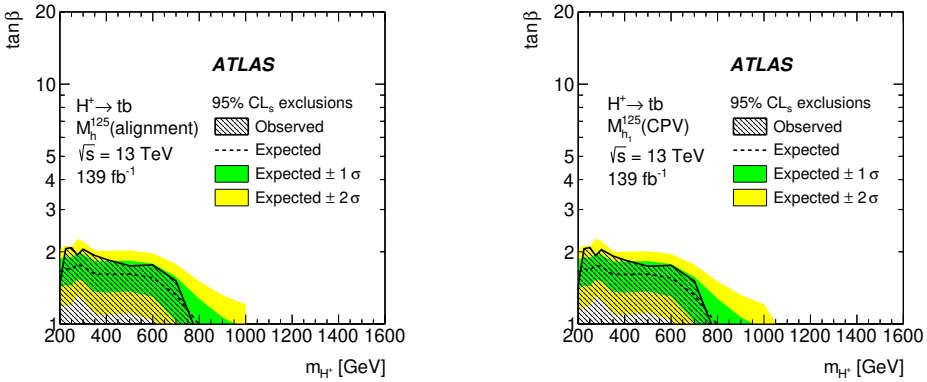

(e)

(f)

Figure 7. Observed and expected limits on $\tan\beta$ as a function of m_{H^+} in various scenarios: (a) hMSSM, (b) M_h^{125}, (c) $M_h^{125}(\tilde{\chi})$, (d) $M_h^{125}(\tilde{\tau})$, (e) M_h^{125}(alignment) and (f) $M_{h_1}^{125}$(CPV). Limits are shown for $\tan\beta$ values in the range of 0.5–60 or 1–20 depending on the availability of model predictions. The bands surrounding the expected limits show the 68% and 95% confidence intervals. Uncertainties in the predicted H^+ cross-sections or branching ratios are not considered.

JHEP06(2021)145

triggers and refined b-tagging techniques, along with the H^+ mass-independent training of the neural network, leads to an improvement beyond the simple scaling with the square root of the ratio of integrated luminosities.

In the context of the hMSSM and several M_h^{125} scenarios, some values of $\tan\beta$, in the range 0.5–2.1, are excluded for H^+ masses between 200 and 1200 GeV. For H^+ masses between ∼200 and ∼750 GeV, values of $\tan\beta > 34$ are also excluded. Compared to previous results of the same search channel, this analysis excludes a broader region of large $\tan\beta$. Additionally, an extended region of low $\tan\beta$ and low and high H^+ masses is also excluded.

Acknowledgments

We thank CERN for the very successful operation of the LHC, as well as the support staff from our institutions without whom ATLAS could not be operated efficiently.

We acknowledge the support of ANPCyT, Argentina; YerPhI, Armenia; ARC, Australia; BMWFW and FWF, Austria; ANAS, Azerbaijan; SSTC, Belarus; CNPq and FAPESP, Brazil; NSERC, NRC and CFI, Canada; CERN; ANID, Chile; CAS, MOST and NSFC, China; COLCIENCIAS, Colombia; MSMT CR, MPO CR and VSC CR, Czech Republic; DNRF and DNSRC, Denmark; IN2P3-CNRS and CEA-DRF/IRFU, France; SRNSFG, Georgia; BMBF, HGF and MPG, Germany; GSRT, Greece; RGC and Hong Kong SAR, China; ISF and Benoziyo Center, Israel; INFN, Italy; MEXT and JSPS, Japan; CNRST, Morocco; NWO, Netherlands; RCN, Norway; MNiSW and NCN, Poland; FCT, Portugal; MNE/IFA, Romania; JINR; MES of Russia and NRC KI, Russian Federation; MESTD, Serbia; MSSR, Slovakia; ARRS and MIZŠ, Slovenia; DST/NRF, South Africa; MICINN, Spain; SRC and Wallenberg Foundation, Sweden; SERI, SNSF and Cantons of Bern and Geneva, Switzerland; MOST, Taiwan; TAEK, Turkey; STFC, U.K.; DOE and NSF, U.S.A.. In addition, individual groups and members have received support from BCKDF, CANARIE, Compute Canada, CRC and IVADO, Canada; Beijing Municipal Science & Technology Commission, China; COST, ERC, ERDF, Horizon 2020 and Marie Skłodowska-Curie Actions, European Union; Investissements d'Avenir Labex, Investissements d'Avenir Idex and ANR, France; DFG and AvH Foundation, Germany; Herakleitos, Thales and Aristeia programmes co-financed by EU-ESF and the Greek NSRF, Greece; BSF-NSF and GIF, Israel; La Caixa Banking Foundation, CERCA Programme Generalitat de Catalunya and PROMETEO and GenT Programmes Generalitat Valenciana, Spain; Göran Gustafssons Stiftelse, Sweden; The Royal Society and Leverhulme Trust, U.K..

The crucial computing support from all WLCG partners is acknowledged gratefully, in particular from CERN, the ATLAS Tier-1 facilities at TRIUMF (Canada), NDGF (Denmark, Norway, Sweden), CC-IN2P3 (France), KIT/GridKA (Germany), INFN-CNAF (Italy), NL-T1 (Netherlands), PIC (Spain), ASGC (Taiwan), RAL (U.K.) and BNL (U.S.A.), the Tier-2 facilities worldwide and large non-WLCG resource providers. Major contributors of computing resources are listed in ref. [140].

JHEP06(2021)145

References

[1] ATLAS collaboration, *Observation of a new particle in the search for the Standard Model Higgs boson with the ATLAS detector at the LHC*, *Phys. Lett. B* **716** (2012) 1 [arXiv:1207.7214] [INSPIRE].

[2] CMS collaboration, *Observation of a New Boson at a Mass of* 125 *GeV with the CMS Experiment at the LHC*, *Phys. Lett. B* **716** (2012) 30 [arXiv:1207.7235] [INSPIRE].

[3] ATLAS and CMS collaborations, *Combined Measurement of the Higgs Boson Mass in pp Collisions at* $\sqrt{s} = 7$ *and* 8 *TeV with the ATLAS and CMS Experiments*, *Phys. Rev. Lett.* **114** (2015) 191803 [arXiv:1503.07589] [INSPIRE].

[4] T.D. Lee, *A Theory of Spontaneous T Violation*, *Phys. Rev. D* **8** (1973) 1226 [INSPIRE].

[5] G.C. Branco, P.M. Ferreira, L. Lavoura, M.N. Rebelo, M. Sher and J.P. Silva, *Theory and phenomenology of two-Higgs-doublet models*, *Phys. Rept.* **516** (2012) 1 [arXiv:1106.0034] [INSPIRE].

[6] K. Inoue, A. Kakuto, H. Komatsu and S. Takeshita, *Aspects of Grand Unified Models with Softly Broken Supersymmetry*, *Prog. Theor. Phys.* **68** (1982) 927 [*Erratum ibid.* **70** (1983) 330] [INSPIRE].

[7] J.F. Gunion and H.E. Haber, *The CP conserving two Higgs doublet model: The Approach to the decoupling limit*, *Phys. Rev. D* **67** (2003) 075019 [hep-ph/0207010] [INSPIRE].

[8] T.P. Cheng and L.-F. Li, *Neutrino Masses, Mixings and Oscillations in* SU(2) × U(1) *Models of Electroweak Interactions*, *Phys. Rev. D* **22** (1980) 2860 [INSPIRE].

[9] J. Schechter and J.W.F. Valle, *Neutrino Masses in* SU(2) × U(1) *Theories*, *Phys. Rev. D* **22** (1980) 2227 [INSPIRE].

[10] G. Lazarides, Q. Shafi and C. Wetterich, *Proton Lifetime and Fermion Masses in an* SO(10) *Model*, *Nucl. Phys. B* **181** (1981) 287 [INSPIRE].

[11] R.N. Mohapatra and G. Senjanović, *Neutrino Masses and Mixings in Gauge Models with Spontaneous Parity Violation*, *Phys. Rev. D* **23** (1981) 165 [INSPIRE].

[12] M. Magg and C. Wetterich, *Neutrino Mass Problem and Gauge Hierarchy*, *Phys. Lett. B* **94** (1980) 61 [INSPIRE].

[13] LHC Higgs Cross Section Working Group, *Handbook of LHC Higgs Cross Sections: 4. Deciphering the Nature of the Higgs Sector*, arXiv:1610.07922 [INSPIRE].

[14] ATLAS collaboration, *Search for charged Higgs bosons decaying via* $H^+ \to \tau\nu$ *in top quark pair events using pp collision data at* $\sqrt{s} = 7$ *TeV with the ATLAS detector*, *JHEP* **06** (2012) 039 [arXiv:1204.2760] [INSPIRE].

[15] ATLAS collaboration, *Search for charged Higgs bosons through the violation of lepton universality in* $t\bar{t}$ *events using pp collision data at* $\sqrt{s} = 7$ *TeV with the ATLAS experiment*, *JHEP* **03** (2013) 076 [arXiv:1212.3572] [INSPIRE].

[16] ATLAS collaboration, *Search for charged Higgs bosons decaying via* $H^\pm \to \tau^\pm\nu$ *in fully hadronic final states using pp collision data at* $\sqrt{s} = 8$ *TeV with the ATLAS detector*, *JHEP* **03** (2015) 088 [arXiv:1412.6663] [INSPIRE].

[17] CMS collaboration, *Search for a light charged Higgs boson in top quark decays in pp collisions at* $\sqrt{s} = 7$ *TeV*, *JHEP* **07** (2012) 143 [arXiv:1205.5736] [INSPIRE].

[18] CMS collaboration, *Search for a charged Higgs boson in pp collisions at* $\sqrt{s} = 8$ *TeV*, *JHEP* **11** (2015) 018 [arXiv:1508.07774] [INSPIRE].

JHEP06(2021)145

[19] ATLAS collaboration, *Search for charged Higgs bosons decaying via $H^{\pm} \to \tau^{\pm}\nu_{\tau}$ in the τ + jets and τ + lepton final states with 36 fb^{-1} of pp collision data recorded at $\sqrt{s} = 13$ TeV with the ATLAS experiment*, *JHEP* **09** (2018) 139 [arXiv:1807.07915] [INSPIRE].

[20] ATLAS collaboration, *Search for a light charged Higgs boson in the decay channel $H^{+} \to c\bar{s}$ in $t\bar{t}$ events using pp collisions at $\sqrt{s} = 7$ TeV with the ATLAS detector*, *Eur. Phys. J. C* **73** (2013) 2465 [arXiv:1302.3694] [INSPIRE].

[21] CMS collaboration, *Search for a light charged Higgs boson decaying to $c\bar{s}$ in pp collisions at $\sqrt{s} = 8$ TeV*, *JHEP* **12** (2015) 178 [arXiv:1510.04252] [INSPIRE].

[22] CMS collaboration, *Search for a charged Higgs boson decaying to charm and bottom quarks in proton-proton collisions at $\sqrt{s} = 8$ TeV*, *JHEP* **11** (2018) 115 [arXiv:1808.06575] [INSPIRE].

[23] ATLAS collaboration, *Search for charged Higgs bosons in the $H^{\pm} \to tb$ decay channel in pp collisions at $\sqrt{s} = 8$ TeV using the ATLAS detector*, *JHEP* **03** (2016) 127 [arXiv:1512.03704] [INSPIRE].

[24] ATLAS collaboration, *Search for charged Higgs bosons produced in association with a top quark and decaying via $H^{\pm} \to \tau\nu$ using pp collision data recorded at $\sqrt{s} = 13$ TeV by the ATLAS detector*, *Phys. Lett. B* **759** (2016) 555 [arXiv:1603.09203] [INSPIRE].

[25] ATLAS collaboration, *Search for charged Higgs bosons decaying into top and bottom quarks at $\sqrt{s} = 13$ TeV with the ATLAS detector*, *JHEP* **11** (2018) 085 [arXiv:1808.03599] [INSPIRE].

[26] CMS collaboration, *Search for a charged Higgs boson decaying into top and bottom quarks in events with electrons or muons in proton-proton collisions at $\sqrt{s} = 13$ TeV*, *JHEP* **01** (2020) 096 [arXiv:1908.09206] [INSPIRE].

[27] CMS collaboration, *Search for charged Higgs bosons decaying into a top and a bottom quark in the all-jet final state of pp collisions at $\sqrt{s} = 13$ TeV*, *JHEP* **07** (2020) 126 [arXiv:2001.07763] [INSPIRE].

[28] ATLAS collaboration, *Search for a Charged Higgs Boson Produced in the Vector-Boson Fusion Mode with Decay $H^{\pm} \to W^{\pm}Z$ using pp Collisions at $\sqrt{s} = 8$ TeV with the ATLAS Experiment*, *Phys. Rev. Lett.* **114** (2015) 231801 [arXiv:1503.04233] [INSPIRE].

[29] CMS collaboration, *Search for Charged Higgs Bosons Produced via Vector Boson Fusion and Decaying into a Pair of W and Z Bosons Using pp Collisions at $\sqrt{s} = 13$ TeV*, *Phys. Rev. Lett.* **119** (2017) 141802 [arXiv:1705.02942] [INSPIRE].

[30] ATLAS collaboration, *Search for dijet resonances in events with an isolated charged lepton using $\sqrt{s} = 13$ TeV proton-proton collision data collected by the ATLAS detector*, *JHEP* **06** (2020) 151 [arXiv:2002.11325] [INSPIRE].

[31] C. Degrande, M. Ubiali, M. Wiesemann and M. Zaro, *Heavy charged Higgs boson production at the LHC*, *JHEP* **10** (2015) 145 [arXiv:1507.02549] [INSPIRE].

[32] A. Djouadi and J. Quevillon, *The MSSM Higgs sector at a high $M_{\rm SUSY}$: reopening the low $\tan\beta$ regime and heavy Higgs searches*, *JHEP* **10** (2013) 028 [arXiv:1304.1787] [INSPIRE].

[33] L. Maiani, A.D. Polosa and V. Riquer, *Bounds to the Higgs Sector Masses in Minimal Supersymmetry from LHC Data*, *Phys. Lett. B* **724** (2013) 274 [arXiv:1305.2172] [INSPIRE].

[34] A. Djouadi, L. Maiani, G. Moreau, A.D. Polosa, J. Quevillon and V. Riquer, *The post-Higgs MSSM scenario: Habemus MSSM?*, *Eur. Phys. J. C* **73** (2013) 2650 [arXiv:1307.5205] [INSPIRE].

JHEP06(2021)145

[35] A. Djouadi, L. Maiani, A.D. Polosa, J. Quevillon and V. Riquer, *Fully covering the MSSM Higgs sector at the LHC*, *JHEP* **06** (2015) 168 [arXiv:1502.05653] [INSPIRE].

[36] E. Bagnaschi et al., *MSSM Higgs Boson Searches at the LHC: Benchmark Scenarios for Run 2 and Beyond*, *Eur. Phys. J. C* **79** (2019) 617 [arXiv:1808.07542] [INSPIRE].

[37] M. Flechl, R. Klees, M. Krämer, M. Spira and M. Ubiali, *Improved cross-section predictions for heavy charged Higgs boson production at the LHC*, *Phys. Rev. D* **91** (2015) 075015 [arXiv:1409.5615] [INSPIRE].

[38] S. Dittmaier, M. Krämer, M. Spira and M. Walser, *Charged-Higgs-boson production at the LHC: NLO supersymmetric QCD corrections*, *Phys. Rev. D* **83** (2011) 055005 [arXiv:0906.2648] [INSPIRE].

[39] E.L. Berger, T. Han, J. Jiang and T. Plehn, *Associated production of a top quark and a charged Higgs boson*, *Phys. Rev. D* **71** (2005) 115012 [hep-ph/0312286] [INSPIRE].

[40] ATLAS collaboration, *The ATLAS Experiment at the CERN Large Hadron Collider*, 2008 *JINST* **3** S08003 [INSPIRE].

[41] ATLAS collaboration, *ATLAS Insertable B-Layer Technical Design Report*, ATLAS-TDR-19 [CERN-LHCC-2010-01] (2010).

[42] B. Abbott et al. *Production and Integration of the ATLAS Insertable B-Layer*, 2018 *JINST* **13** T05008 [arXiv:1803.00844] [INSPIRE].

[43] ATLAS collaboration, *Performance of the ATLAS Trigger System in 2015*, *Eur. Phys. J. C* **77** (2017) 317 [arXiv:1611.09661] [INSPIRE].

[44] ATLAS collaboration, *Performance of electron and photon triggers in ATLAS during LHC Run 2*, *Eur. Phys. J. C* **80** (2020) 47 [arXiv:1909.00761] [INSPIRE].

[45] J. Alwall et al., *The automated computation of tree-level and next-to-leading order differential cross sections, and their matching to parton shower simulations*, *JHEP* **07** (2014) 079 [arXiv:1405.0301] [INSPIRE].

[46] R.D. Ball et al., *Parton distributions with LHC data*, *Nucl. Phys. B* **867** (2013) 244 [arXiv:1207.1303] [INSPIRE].

[47] T. Sjöstrand, S. Mrenna and P.Z. Skands, *A Brief Introduction to PYTHIA 8.1*, *Comput. Phys. Commun.* **178** (2008) 852 [arXiv:0710.3820] [INSPIRE].

[48] ATLAS collaboration, *ATLAS PYTHIA 8 tunes to 7 TeV data*, ATL-PHYS-PUB-2014-021 (2014).

[49] A. Arhrib, R. Benbrik, H. Harouiz, S. Moretti and A. Rouchad, *A Guidebook to Hunting Charged Higgs Bosons at the LHC*, *Front. Phys.* **8** (2020) 1 [arXiv:1810.09106] [INSPIRE].

[50] P. Nason, *A New method for combining NLO QCD with shower Monte Carlo algorithms*, *JHEP* **11** (2004) 040 [hep-ph/0409146] [INSPIRE].

[51] S. Frixione, P. Nason and C. Oleari, *Matching NLO QCD computations with Parton Shower simulations: the POWHEG method*, *JHEP* **11** (2007) 070 [arXiv:0709.2092] [INSPIRE].

[52] S. Alioli, P. Nason, C. Oleari and E. Re, *A general framework for implementing NLO calculations in shower Monte Carlo programs: the POWHEG BOX*, *JHEP* **06** (2010) 043 [arXiv:1002.2581] [INSPIRE].

[53] J.M. Campbell, R.K. Ellis, P. Nason and E. Re, *Top-Pair Production and Decay at NLO Matched with Parton Showers*, *JHEP* **04** (2015) 114 [arXiv:1412.1828] [INSPIRE].

[54] NNPDF collaboration, *Parton distributions for the LHC Run II*, *JHEP* **04** (2015) 040 [arXiv:1410.8849] [INSPIRE].

JHEP06(2021)145

[55] ATLAS collaboration, *Studies on top-quark Monte Carlo modelling for Top2016*, ATL-PHYS-PUB-2016-020 (2016).

[56] T. Sjöstrand et al., *An introduction to PYTHIA 8.2*, *Comput. Phys. Commun.* **191** (2015) 159 [arXiv:1410.3012] [INSPIRE].

[57] M. Czakon and A. Mitov, *Top++: A Program for the Calculation of the Top-Pair Cross-Section at Hadron Colliders*, *Comput. Phys. Commun.* **185** (2014) 2930 [arXiv:1112.5675] [INSPIRE].

[58] M. Cacciari, M. Czakon, M. Mangano, A. Mitov and P. Nason, *Top-pair production at hadron colliders with next-to-next-to-leading logarithmic soft-gluon resummation*, *Phys. Lett. B* **710** (2012) 612 [arXiv:1111.5869] [INSPIRE].

[59] P. Bärnreuther, M. Czakon and A. Mitov, *Percent Level Precision Physics at the Tevatron: First Genuine NNLO QCD Corrections to $q\bar{q} \to t\bar{t} + X$*, *Phys. Rev. Lett.* **109** (2012) 132001 [arXiv:1204.5201] [INSPIRE].

[60] M. Czakon and A. Mitov, *NNLO corrections to top-pair production at hadron colliders: the all-fermionic scattering channels*, *JHEP* **12** (2012) 054 [arXiv:1207.0236] [INSPIRE].

[61] M. Czakon, P. Fiedler and A. Mitov, *Total Top-Quark Pair-Production Cross Section at Hadron Colliders Through $\mathcal{O}(\alpha_S^4)$*, *Phys. Rev. Lett.* **110** (2013) 252004 [arXiv:1303.6254] [INSPIRE].

[62] R. Frederix, E. Re and P. Torrielli, *Single-top t-channel hadroproduction in the four-flavour scheme with POWHEG and aMC@NLO*, *JHEP* **09** (2012) 130 [arXiv:1207.5391] [INSPIRE].

[63] S. Frixione, E. Laenen, P. Motylinski, C.D. White and B.R. Webber, *Single-top hadroproduction in association with a W boson*, *JHEP* **07** (2008) 029 [arXiv:0805.3067] [INSPIRE].

[64] E. Bothmann et al., *Event Generation with Sherpa 2.2*, *SciPost Phys.* **7** (2019) 034 [arXiv:1905.09127] [INSPIRE].

[65] T. Gleisberg and S. Höche, *Comix, a new matrix element generator*, *JHEP* **12** (2008) 039 [arXiv:0808.3674] [INSPIRE].

[66] F. Cascioli, P. Maierhöfer and S. Pozzorini, *Scattering Amplitudes with Open Loops*, *Phys. Rev. Lett.* **108** (2012) 111601 [arXiv:1111.5206] [INSPIRE].

[67] A. Denner, S. Dittmaier and L. Hofer, *Collier: a fortran-based Complex One-Loop LIbrary in Extended Regularizations*, *Comput. Phys. Commun.* **212** (2017) 220 [arXiv:1604.06792] [INSPIRE].

[68] S. Schumann and F. Krauss, *A Parton shower algorithm based on Catani-Seymour dipole factorisation*, *JHEP* **03** (2008) 038 [arXiv:0709.1027] [INSPIRE].

[69] J.-C. Winter, F. Krauss and G. Soff, *A Modified cluster hadronization model*, *Eur. Phys. J. C* **36** (2004) 381 [hep-ph/0311085] [INSPIRE].

[70] S. Höche, F. Krauss, M. Schönherr and F. Siegert, *A critical appraisal of NLO + PS matching methods*, *JHEP* **09** (2012) 049 [arXiv:1111.1220] [INSPIRE].

[71] S. Catani, F. Krauss, R. Kuhn and B.R. Webber, *QCD matrix elements + parton showers*, *JHEP* **11** (2001) 063 [hep-ph/0109231] [INSPIRE].

[72] S. Hëche, F. Krauss, S. Schumann and F. Siegert, *QCD matrix elements and truncated showers*, *JHEP* **05** (2009) 053 [arXiv:0903.1219] [INSPIRE].

JHEP06(2021)145

[73] S. Hëche, F. Krauss, M. Schönherr and F. Siegert, *QCD matrix elements + parton showers: The NLO case*, *JHEP* **04** (2013) 027 [arXiv:1207.5030] [INSPIRE].

[74] H.B. Hartanto, B. Jäger, L. Reina and D. Wackeroth, *Higgs boson production in association with top quarks in the POWHEG BOX*, *Phys. Rev. D* **91** (2015) 094003 [arXiv:1501.04498] [INSPIRE].

[75] A. Denner, S. Dittmaier, M. Roth and M.M. Weber, *Electroweak radiative corrections to $e^+e^- \to \nu\bar{\nu}H$*, *Nucl. Phys. B* **660** (2003) 289 [hep-ph/0302198] [INSPIRE].

[76] ATLAS collaboration, *The ATLAS Simulation Infrastructure*, *Eur. Phys. J. C* **70** (2010) 823 [arXiv:1005.4568] [INSPIRE].

[77] S. Agostinelli et al., *GEANT4 — a simulation toolkit*, *Nucl. Instrum. Meth. A* **506** (2003) 250 [INSPIRE].

[78] ATLAS collaboration, *The simulation principle and performance of the ATLAS fast calorimeter simulation FastCaloSim*, ATL-PHYS-PUB-2010-013 (2010).

[79] D.J. Lange, *The EvtGen particle decay simulation package*, *Nucl. Instrum. Meth. A* **462** (2001) 152 [INSPIRE].

[80] ATLAS collaboration, *Electron and photon performance measurements with the ATLAS detector using the 2015–2017 LHC proton-proton collision data*, 2019 *JINST* **14** P12006 [arXiv:1908.00005] [INSPIRE].

[81] ATLAS collaboration, *Electron efficiency measurements with the ATLAS detector using the 2015 LHC proton-proton collision data*, ATLAS-CONF-2016-024 (2016).

[82] ATLAS collaboration, *Muon reconstruction performance of the ATLAS detector in proton-proton collision data at $\sqrt{s} = 13$ TeV*, *Eur. Phys. J. C* **76** (2016) 292 [arXiv:1603.05598] [INSPIRE].

[83] ATLAS collaboration, *Topological cell clustering in the ATLAS calorimeters and its performance in LHC Run 1*, *Eur. Phys. J. C* **77** (2017) 490 [arXiv:1603.02934] [INSPIRE].

[84] M. Cacciari, G.P. Salam and G. Soyez, *The anti-k_t jet clustering algorithm*, *JHEP* **04** (2008) 063 [arXiv:0802.1189] [INSPIRE].

[85] ATLAS collaboration, *Jet energy scale measurements and their systematic uncertainties in proton-proton collisions at $\sqrt{s} = 13$ TeV with the ATLAS detector*, *Phys. Rev. D* **96** (2017) 072002 [arXiv:1703.09665] [INSPIRE].

[86] ATLAS collaboration, *Selection of jets produced in 13 TeV proton-proton collisions with the ATLAS detector*, ATLAS-CONF-2015-029 (2015).

[87] ATLAS collaboration, *Performance of pile-up mitigation techniques for jets in pp collisions at $\sqrt{s} = 8$ TeV using the ATLAS detector*, *Eur. Phys. J. C* **76** (2016) 581 [arXiv:1510.03823] [INSPIRE].

[88] ATLAS collaboration, *Measurements of b-jet tagging efficiency with the ATLAS detector using $t\bar{t}$ events at $\sqrt{s} = 13$ TeV*, *JHEP* **08** (2018) 089 [arXiv:1805.01845] [INSPIRE].

[89] ATLAS collaboration, *ATLAS b-jet identification performance and efficiency measurement with $t\bar{t}$ events in pp collisions at $\sqrt{s} = 13$ TeV*, *Eur. Phys. J. C* **79** (2019) 970 [arXiv:1907.05120] [INSPIRE].

[90] ATLAS collaboration, *Performance of missing transverse momentum reconstruction for the ATLAS detector in the first proton-proton collisions at at $\sqrt{s} = 13$ TeV*, ATL-PHYS-PUB-2015-027 (2015).

JHEP06(2021)145

[91] ATLAS collaboration, *Improvements in $t\bar{t}$ modelling using NLO+PS Monte Carlo generators for Run2*, ATL-PHYS-PUB-2018-009 (2018).

[92] ATLAS collaboration, *Measurements of top-quark pair single- and double-differential cross-sections in the all-hadronic channel in pp collisions at $\sqrt{s} = 13$ TeV using the ATLAS detector*, *JHEP* **01** (2021) 033 [arXiv:2006.09274] [INSPIRE].

[93] F. Chollet et al., *Keras*, (2015) https://keras.io.

[94] S. Ioffe and C. Szegedy, *Batch Normalization: Accelerating Deep Network Training by Reducing Internal Covariate Shift*, arXiv:1502.03167 [INSPIRE].

[95] G.E. Hinton, N. Srivastava, A. Krizhevsky, I. Sutskever and R.R. Salakhutdinov, *Improving neural networks by preventing co-adaptation of feature detectors*, arXiv:1207.0580.

[96] D.P. Kingma and J. Ba, *Adam: A Method for Stochastic Optimization*, arXiv:1412.6980 [INSPIRE].

[97] P. Baldi, K. Cranmer, T. Faucett, P. Sadowski and D. Whiteson, *Parameterized neural networks for high-energy physics*, *Eur. Phys. J. C* **76** (2016) 235 [arXiv:1601.07913] [INSPIRE].

[98] G.C. Fox and S. Wolfram, *Event Shapes in e^+e^- Annihilation*, *Nucl. Phys. B* **149** (1979) 413 [*Erratum ibid.* **157** (1979) 543] [INSPIRE].

[99] ATLAS collaboration, *Luminosity determination in pp collisions at $\sqrt{s} = 13$ TeV using the ATLAS detector at the LHC*, ATLAS-CONF-2019-021 (2019).

[100] G. Avoni et al., *The new LUCID-2 detector for luminosity measurement and monitoring in ATLAS*, 2018 *JINST* **13** P07017 [INSPIRE].

[101] ATLAS collaboration, *Measurement of the Inelastic Proton-Proton Cross Section at $\sqrt{s} = 13$ TeV with the ATLAS Detector at the LHC*, *Phys. Rev. Lett.* **117** (2016) 182002 [arXiv:1606.02625] [INSPIRE].

[102] ATLAS collaboration, *Electron reconstruction and identification in the ATLAS experiment using the 2015 and 2016 LHC proton-proton collision data at $\sqrt{s} = 13$ TeV*, *Eur. Phys. J. C* **79** (2019) 639 [arXiv:1902.04655] [INSPIRE].

[103] ATLAS collaboration, *Jet energy scale and resolution measured in proton-proton collisions at $\sqrt{s} = 13$ TeV with the ATLAS detector*, arXiv:2007.02645 [INSPIRE].

[104] ATLAS collaboration, *Measurement of b-tagging Efficiency of c-jets in $t\bar{t}$ Events Using a Likelihood Approach with the ATLAS Detector*, ATLAS-CONF-2018-001 (2018).

[105] ATLAS collaboration, *Calibration of light-flavour b-jet mistagging rates using ATLAS proton-proton collision data at $\sqrt{s} = 13$ TeV*, ATLAS-CONF-2018-006 (2018).

[106] ATLAS collaboration, *Performance of missing transverse momentum reconstruction with the ATLAS detector using proton-proton collisions at $\sqrt{s} = 13$ TeV*, *Eur. Phys. J. C* **78** (2018) 903 [arXiv:1802.08168] [INSPIRE].

[107] ATLAS collaboration, *E_T^{miss} performance in the ATLAS detector using 2015–2016 LHC pp collisions*, ATLAS-CONF-2018-023 (2018).

[108] J. Butterworth et al., *PDF4LHC recommendations for LHC Run II*, *J. Phys. G* **43** (2016) 023001 [arXiv:1510.03865] [INSPIRE].

[109] LHCTopWG, *ATLAS-CMS recommended predictions for top-quark-pair cross sections*, (2021) https://twiki.cern.ch/twiki/bin/view/LHCPhysics/TtbarNNLO.

JHEP06(2021)145

[110] ATLAS collaboration, *Measurements of differential cross sections of top quark pair production in association with jets in pp collisions at $\sqrt{s} = 13$ TeV using the ATLAS detector*, *JHEP* **10** (2018) 159 [arXiv:1802.06572] [INSPIRE].

[111] LHCTopWG, *ATLAS-CMS recommended predictions for single-top cross sections*, (2017) https://twiki.cern.ch/twiki/bin/view/LHCPhysics/SingleTopRefXsec.

[112] A.D. Martin, W.J. Stirling, R.S. Thorne and G. Watt, *Parton distributions for the LHC*, *Eur. Phys. J. C* **63** (2009) 189 [arXiv:0901.0002] [INSPIRE].

[113] A.D. Martin, W.J. Stirling, R.S. Thorne and G. Watt, *Uncertainties on α_S in global PDF analyses and implications for predicted hadronic cross sections*, *Eur. Phys. J. C* **64** (2009) 653 [arXiv:0905.3531] [INSPIRE].

[114] M. Aliev, H. Lacker, U. Langenfeld, S. Moch, P. Uwer and M. Wiedermann, *HATHOR: HAdronic Top and Heavy quarks crOss section calculatoR*, *Comput. Phys. Commun.* **182** (2011) 1034 [arXiv:1007.1327] [INSPIRE].

[115] P. Kant et al., *HatHor for single top-quark production: Updated predictions and uncertainty estimates for single top-quark production in hadronic collisions*, *Comput. Phys. Commun.* **191** (2015) 74 [arXiv:1406.4403] [INSPIRE].

[116] J. Bellm et al., *HERWIG 7.0/HERWIG++ 3.0 release note*, *Eur. Phys. J. C* **76** (2016) 196 [arXiv:1512.01178] [INSPIRE].

[117] R. Raitio and W.W. Wada, *Higgs Boson Production at Large Transverse Momentum in QCD*, *Phys. Rev. D* **19** (1979) 941 [INSPIRE].

[118] W. Beenakker, S. Dittmaier, M. Krämer, B. Plumper, M. Spira and P.M. Zerwas, *NLO QCD corrections to $t\bar{t}H$ production in hadron collisions*, *Nucl. Phys. B* **653** (2003) 151 [hep-ph/0211352] [INSPIRE].

[119] S. Dawson, C. Jackson, L.H. Orr, L. Reina and D. Wackeroth, *Associated Higgs production with top quarks at the large hadron collider: NLO QCD corrections*, *Phys. Rev. D* **68** (2003) 034022 [hep-ph/0305087] [INSPIRE].

[120] Y. Zhang, W.-G. Ma, R.-Y. Zhang, C. Chen and L. Guo, *QCD NLO and EW NLO corrections to $t\bar{t}H$ production with top quark decays at hadron collider*, *Phys. Lett. B* **738** (2014) 1 [arXiv:1407.1110] [INSPIRE].

[121] S. Frixione, V. Hirschi, D. Pagani, H.-S. Shao and M. Zaro, *Electroweak and QCD corrections to top-pair hadroproduction in association with heavy bosons*, *JHEP* **06** (2015) 184 [arXiv:1504.03446] [INSPIRE].

[122] J.M. Campbell and R.K. Ellis, *$t\bar{t}W^{+-}$ production and decay at NLO*, *JHEP* **07** (2012) 052 [arXiv:1204.5678] [INSPIRE].

[123] R. Frederix, D. Pagani and M. Zaro, *Large NLO corrections in $t\bar{t}W^{\pm}$ and $t\bar{t}t\bar{t}$ hadroproduction from supposedly subleading EW contributions*, *JHEP* **02** (2018) 031 [arXiv:1711.02116] [INSPIRE].

[124] E. Bothmann, M. Schönherr and S. Schumann, *Reweighting QCD matrix-element and parton-shower calculations*, *Eur. Phys. J. C* **76** (2016) 590 [arXiv:1606.08753] [INSPIRE].

[125] ATLAS collaboration, *Multi-Boson Simulation for 13 TeV ATLAS Analyses*, ATL-PHYS-PUB-2016-002 (2016).

[126] G. Cowan, K. Cranmer, E. Gross and O. Vitells, *Asymptotic formulae for likelihood-based tests of new physics*, *Eur. Phys. J. C* **71** (2011) 1554 [*Erratum ibid.* **73** (2013) 2501] [arXiv:1007.1727] [INSPIRE].

JHEP06(2021)145

[127] A.L. Read, *Presentation of search results: The CL_s technique*, *J. Phys. G* **28** (2002) 2693 [INSPIRE].

[128] T. Junk, *Confidence level computation for combining searches with small statistics*, *Nucl. Instrum. Meth. A* **434** (1999) 435 [hep-ex/9902006] [INSPIRE].

[129] S. Heinemeyer, W. Hollik and G. Weiglein, *FeynHiggs: A Program for the calculation of the masses of the neutral CP even Higgs bosons in the MSSM*, *Comput. Phys. Commun.* **124** (2000) 76 [hep-ph/9812320] [INSPIRE].

[130] S. Heinemeyer, W. Hollik and G. Weiglein, *The Masses of the neutral CP-even Higgs bosons in the MSSM: Accurate analysis at the two loop level*, *Eur. Phys. J. C* **9** (1999) 343 [hep-ph/9812472] [INSPIRE].

[131] G. Degrassi, S. Heinemeyer, W. Hollik, P. Slavich and G. Weiglein, *Towards high precision predictions for the MSSM Higgs sector*, *Eur. Phys. J. C* **28** (2003) 133 [hep-ph/0212020] [INSPIRE].

[132] M. Frank, T. Hahn, S. Heinemeyer, W. Hollik, H. Rzehak and G. Weiglein, *The Higgs Boson Masses and Mixings of the Complex MSSM in the Feynman-Diagrammatic Approach*, *JHEP* **02** (2007) 047 [hep-ph/0611326] [INSPIRE].

[133] T. Hahn, S. Heinemeyer, W. Hollik, H. Rzehak and G. Weiglein, *High-Precision Predictions for the Light CP-Even Higgs Boson Mass of the Minimal Supersymmetric Standard Model*, *Phys. Rev. Lett.* **112** (2014) 141801 [arXiv:1312.4937] [INSPIRE].

[134] H. Bahl and W. Hollik, *Precise prediction for the light MSSM Higgs boson mass combining effective field theory and fixed-order calculations*, *Eur. Phys. J. C* **76** (2016) 499 [arXiv:1608.01880] [INSPIRE].

[135] H. Bahl, S. Heinemeyer, W. Hollik and G. Weiglein, *Reconciling EFT and hybrid calculations of the light MSSM Higgs-boson mass*, *Eur. Phys. J. C* **78** (2018) 57 [arXiv:1706.00346] [INSPIRE].

[136] A. Djouadi, J. Kalinowski and M. Spira, *HDECAY: A Program for Higgs boson decays in the standard model and its supersymmetric extension*, *Comput. Phys. Commun.* **108** (1998) 56 [hep-ph/9704448] [INSPIRE].

[137] A. Djouadi, J. Kalinowski, M. Muehlleitner and M. Spira, *HDECAY: Twenty$_{++}$ years after*, *Comput. Phys. Commun.* **238** (2019) 214 [arXiv:1801.09506] [INSPIRE].

[138] A. Bredenstein, A. Denner, S. Dittmaier and M.M. Weber, *Precise predictions for the Higgs-boson decay $H \to WW/ZZ \to 4$ leptons*, *Phys. Rev. D* **74** (2006) 013004 [hep-ph/0604011] [INSPIRE].

[139] A. Bredenstein, A. Denner, S. Dittmaier and M.M. Weber, *Radiative corrections to the semileptonic and hadronic Higgs-boson decays $H \to WW/ZZ \to 4$ fermions*, *JHEP* **02** (2007) 080 [hep-ph/0611234] [INSPIRE].

[140] ATLAS collaboration, *ATLAS Computing Acknowledgements*, ATL-SOFT-PUB-2020-001 (2020).

JHEP06(2021)145

The ATLAS collaboration

G. Aad[102], B. Abbott[128], D.C. Abbott[103], A. Abed Abud[36], K. Abeling[53], D.K. Abhayasinghe[94], S.H. Abidi[167], O.S. AbouZeid[40], N.L. Abraham[156], H. Abramowicz[161], H. Abreu[160], Y. Abulaiti[6], B.S. Acharya[67a,67b,o], B. Achkar[53], L. Adam[100], C. Adam Bourdarios[5], L. Adamczyk[84a], L. Adamek[167], J. Adelman[121], A. Adiguzel[12c,ad], S. Adorni[54], T. Adye[143], A.A. Affolder[145], Y. Afik[160], C. Agapopoulou[65], M.N. Agaras[38], A. Aggarwal[119], C. Agheorghiesei[27c], J.A. Aguilar-Saavedra[139f,139a,ac], A. Ahmad[36], F. Ahmadov[80], W.S. Ahmed[104], X. Ai[18], G. Aielli[74a,74b], S. Akatsuka[86], M. Akbiyik[100], T.P.A. Åkesson[97], E. Akilli[54], A.V. Akimov[111], K. Al Khoury[65], G.L. Alberghi[23b,23a], J. Albert[176], M.J. Alconada Verzini[161], S. Alderweireldt[36], M. Aleksa[36], I.N. Aleksandrov[80], C. Alexa[27b], T. Alexopoulos[10], A. Alfonsi[120], F. Alfonsi[23b,23a], M. Alhroob[128], B. Ali[141], S. Ali[158], M. Aliev[166], G. Alimonti[69a], C. Allaire[36], B.M.M. Allbrooke[156], B.W. Allen[131], P.P. Allport[21], A. Aloisio[70a,70b], F. Alonso[89], C. Alpigiani[148], E. Alunno Camelia[74a,74b], M. Alvarez Estevez[99], M.G. Alviggi[70a,70b], Y. Amaral Coutinho[81b], A. Ambler[104], L. Ambroz[134], C. Amelung[36], D. Amidei[106], S.P. Amor Dos Santos[139a], S. Amoroso[46], C.S. Amrouche[54], F. An[79], C. Anastopoulos[149], N. Andari[144], T. Andeen[11], J.K. Anders[20], S.Y. Andrean[45a,45b], A. Andreazza[69a,69b], V. Andrei[61a], C.R. Anelli[176], S. Angelidakis[9], A. Angerami[39], A.V. Anisenkov[122b,122a], A. Annovi[72a], C. Antel[54], M.T. Anthony[149], E. Antipov[129], M. Antonelli[51], D.J.A. Antrim[18], F. Anulli[73a], M. Aoki[82], J.A. Aparisi Pozo[174], M.A. Aparo[156], L. Aperio Bella[46], N. Aranzabal[36], V. Araujo Ferraz[81a], R. Araujo Pereira[81b], C. Arcangeletti[51], A.T.H. Arce[49], J-F. Arguin[110], S. Argyropoulos[52], J.-H. Arling[46], A.J. Armbruster[36], A. Armstrong[171], O. Arnaez[167], H. Arnold[120], Z.P. Arrubarrena Tame[114], G. Artoni[134], H. Asada[117], K. Asai[126], S. Asai[163], T. Asawatavonvanich[165], N. Asbah[59], E.M. Asimakopoulou[172], L. Asquith[156], J. Assahsah[35e], K. Assamagan[29], R. Astalos[28a], R.J. Atkin[33a], M. Atkinson[173], N.B. Atlay[19], H. Atmani[65], P.A. Atmasiddha[106], K. Augsten[141], V.A. Austrup[182], G. Avolio[36], M.K. Ayoub[15a], G. Azuelos[110,ak], D. Babal[28a], H. Bachacou[144], K. Bachas[162], F. Backman[45a,45b], P. Bagnaia[73a,73b], M. Bahmani[85], H. Bahrasemani[152], A.J. Bailey[174], V.R. Bailey[173], J.T. Baines[143], C. Bakalis[10], O.K. Baker[183], P.J. Bakker[120], E. Bakos[16], D. Bakshi Gupta[8], S. Balaji[157], R. Balasubramanian[120], E.M. Baldin[122b,122a], P. Balek[180], F. Balli[144], W.K. Balunas[134], J. Balz[100], E. Banas[85], M. Bandieramonte[138], A. Bandyopadhyay[19], Sw. Banerjee[181,j], L. Barak[161], W.M. Barbe[38], E.L. Barberio[105], D. Barberis[55b,55a], M. Barbero[102], G. Barbour[95], T. Barillari[115], M-S. Barisits[36], J. Barkeloo[131], T. Barklow[153], R. Barnea[160], B.M. Barnett[143], R.M. Barnett[18], Z. Barnovska-Blenessy[60a], A. Baroncelli[60a], G. Barone[29], A.J. Barr[134], L. Barranco Navarro[45a,45b], F. Barreiro[99], J. Barreiro Guimarães da Costa[15a], U. Barron[161], S. Barsov[137], F. Bartels[61a], R. Bartoldus[153], G. Bartolini[102], A.E. Barton[90], P. Bartos[28a], A. Basalaev[46], A. Basan[100], A. Bassalat[65,ah], M.J. Basso[167], R.L. Bates[57], S. Batlamous[35f], J.R. Batley[32], B. Batool[151], M. Battaglia[145], M. Bauce[73a,73b], F. Bauer[144,*], P. Bauer[24], H.S. Bawa[31], A. Bayirli[12c], J.B. Beacham[49], T. Beau[135], P.H. Beauchemin[170], F. Becherer[52], P. Bechtle[24], H.C. Beck[53], H.P. Beck[20,q], K. Becker[178], C. Becot[46], A. Beddall[12d], A.J. Beddall[12a], V.A. Bednyakov[80], M. Bedognetti[120], C.P. Bee[155], T.A. Beermann[182], M. Begalli[81b], M. Begel[29], A. Behera[155], J.K. Behr[46], F. Beisiegel[24], M. Belfkir[5], A.S. Bell[95], G. Bella[161], L. Bellagamba[23b], A. Bellerive[34], P. Bellos[9], K. Beloborodov[122b,122a], K. Belotskiy[112], N.L. Belyaev[112], D. Benchekroun[35a], N. Benekos[10], Y. Benhammou[161], D.P. Benjamin[6], M. Benoit[29], J.R. Bensinger[26], S. Bentvelsen[120], L. Beresford[134], M. Beretta[51], D. Berge[19], E. Bergeaas Kuutmann[172], N. Berger[5], B. Bergmann[141], L.J. Bergsten[26], J. Beringer[18], S. Berlendis[7], G. Bernardi[135], C. Bernius[153], F.U. Bernlochner[24], T. Berry[94], P. Berta[100], A. Berthold[48], I.A. Bertram[90],

JHEP06(2021)145

O. Bessidskaia Bylund[182], N. Besson[144], S. Bethke[115], A. Betti[42], A.J. Bevan[93], J. Beyer[115], S. Bhatta[155], D.S. Bhattacharya[177], P. Bhattarai[26], V.S. Bhopatkar[6], R. Bi[138], R.M. Bianchi[138], O. Biebel[114], D. Biedermann[19], R. Bielski[36], K. Bierwagen[100], N.V. Biesuz[72a,72b], M. Biglietti[75a], T.R.V. Billoud[141], M. Bindi[53], A. Bingul[12d], C. Bini[73a,73b], S. Biondi[23b,23a], C.J. Birch-sykes[101], M. Birman[180], T. Bisanz[36], J.P. Biswal[3], D. Biswas[181,j], A. Bitadze[101], C. Bittrich[48], K. Bjørke[133], T. Blazek[28a], I. Bloch[46], C. Blocker[26], A. Blue[57], U. Blumenschein[93], G.J. Bobbink[120], V.S. Bobrovnikov[122b,122a], S.S. Bocchetta[97], D. Bogavac[14], A.G. Bogdanchikov[122b,122a], C. Bohm[45a], V. Boisvert[94], P. Bokan[172,53], T. Bold[84a], A.E. Bolz[61b], M. Bomben[135], M. Bona[93], J.S. Bonilla[131], M. Boonekamp[144], C.D. Booth[94], A.G. Borbély[57], H.M. Borecka-Bielska[91], L.S. Borgna[95], A. Borisov[123], G. Borissov[90], D. Bortoletto[134], D. Boscherini[23b], M. Bosman[14], J.D. Bossio Sola[104], K. Bouaouda[35a], J. Boudreau[138], E.V. Bouhova-Thacker[90], D. Boumediene[38], A. Boveia[127], J. Boyd[36], D. Boye[33c], I.R. Boyko[80], A.J. Bozson[94], J. Bracinik[21], N. Brahimi[60d,60c], G. Brandt[182], O. Brandt[32], F. Braren[46], B. Brau[103], J.E. Brau[131], W.D. Breaden Madden[57], K. Brendlinger[46], R. Brener[160], L. Brenner[36], R. Brenner[172], S. Bressler[180], B. Brickwedde[100], D.L. Briglin[21], D. Britton[57], D. Britzger[115], I. Brock[24], R. Brock[107], G. Brooijmans[39], W.K. Brooks[146d], E. Brost[29], P.A. Bruckman de Renstrom[85], B. Brüers[46], D. Bruncko[28b], A. Bruni[23b], G. Bruni[23b], M. Bruschi[23b], N. Bruscino[73a,73b], L. Bryngemark[153], T. Buanes[17], Q. Buat[155], P. Buchholz[151], A.G. Buckley[57], I.A. Budagov[80], M.K. Bugge[133], O. Bulekov[112], B.A. Bullard[59], T.J. Burch[121], S. Burdin[91], C.D. Burgard[120], A.M. Burger[129], B. Burghgrave[8], J.T.P. Burr[46], C.D. Burton[11], J.C. Burzynski[103], V. Büscher[100], E. Buschmann[53], P.J. Bussey[57], J.M. Butler[25], C.M. Buttar[57], J.M. Butterworth[95], P. Butti[36], W. Buttinger[143], C.J. Buxo Vazquez[107], A. Buzatu[158], A.R. Buzykaev[122b,122a], G. Cabras[23b,23a], S. Cabrera Urbán[174], D. Caforio[56], H. Cai[138], V.M.M. Cairo[153], O. Cakir[4a], N. Calace[36], P. Calafiura[18], G. Calderini[135], P. Calfayan[66], G. Callea[57], L.P. Caloba[81b], A. Caltabiano[74a,74b], S. Calvente Lopez[99], D. Calvet[38], S. Calvet[38], T.P. Calvet[102], M. Calvetti[72a,72b], R. Camacho Toro[135], S. Camarda[36], D. Camarero Munoz[99], P. Camarri[74a,74b], M.T. Camerlingo[75a,75b], D. Cameron[133], C. Camincher[36], S. Campana[36], M. Campanelli[95], A. Camplani[40], V. Canale[70a,70b], A. Canesse[104], M. Cano Bret[78], J. Cantero[129], T. Cao[161], Y. Cao[173], M. Capua[41b,41a], R. Cardarelli[74a], F. Cardillo[174], G. Carducci[41b,41a], I. Carli[142], T. Carli[36], G. Carlino[70a], B.T. Carlson[138], E.M. Carlson[176,168a], L. Carminati[69a,69b], R.M.D. Carney[153], S. Caron[119], E. Carquin[146d], S. Carrá[46], G. Carratta[23b,23a], J.W.S. Carter[167], T.M. Carter[50], M.P. Casado[14,g], A.F. Casha[167], E.G. Castiglia[183], F.L. Castillo[174], L. Castillo Garcia[14], V. Castillo Gimenez[174], N.F. Castro[139a,139e], A. Catinaccio[36], J.R. Catmore[133], A. Cattai[36], V. Cavaliere[29], V. Cavasinni[72a,72b], E. Celebi[12b], F. Celli[134], K. Cerny[130], A.S. Cerqueira[81a], A. Cerri[156], L. Cerrito[74a,74b], F. Cerutti[18], A. Cervelli[23b,23a], S.A. Cetin[12b], Z. Chadi[35a], D. Chakraborty[121], J. Chan[181], W.S. Chan[120], W.Y. Chan[91], J.D. Chapman[32], B. Chargeishvili[159b], D.G. Charlton[21], T.P. Charman[93], M. Chatterjee[20], C.C. Chau[34], S. Che[127], S. Chekanov[6], S.V. Chekulaev[168a], G.A. Chelkov[80,af], B. Chen[79], C. Chen[60a], C.H. Chen[79], H. Chen[15c], H. Chen[29], J. Chen[60a], J. Chen[39], J. Chen[26], S. Chen[136], S.J. Chen[15c], X. Chen[15b], Y. Chen[60a], Y-H. Chen[46], H.C. Cheng[63a], H.J. Cheng[15a], A. Cheplakov[80], E. Cheremushkina[123], R. Cherkaoui El Moursli[35f], E. Cheu[7], K. Cheung[64], T.J.A. Chevalérias[144], L. Chevalier[144], V. Chiarella[51], G. Chiarelli[72a], G. Chiodini[68a], A.S. Chisholm[21], A. Chitan[27b], I. Chiu[163], Y.H. Chiu[176], M.V. Chizhov[80], K. Choi[11], A.R. Chomont[73a,73b], Y. Chou[103], Y.S. Chow[120], L.D. Christopher[33e], M.C. Chu[63a], X. Chu[15a,15d], J. Chudoba[140], J.J. Chwastowski[85], L. Chytka[130], D. Cieri[115], K.M. Ciesla[85], V. Cindro[92], I.A. Cioară[27b], A. Ciocio[18], F. Cirotto[70a,70b], Z.H. Citron[180,k], M. Citterio[69a], D.A. Ciubotaru[27b], B.M. Ciungu[167], A. Clark[54], P.J. Clark[50], S.E. Clawson[101], C. Clement[45a,45b], L. Clissa[23b,23a], Y. Coadou[102], M. Cobal[67a,67c], A. Coccaro[55b], J. Cochran[79],

JHEP06(2021)145

R. Coelho Lopes De Sa[103], H. Cohen[161], A.E.C. Coimbra[36], B. Cole[39], A.P. Colijn[120], J. Collot[58], P. Conde Muiño[139a,139h], S.H. Connell[33c], I.A. Connelly[57], S. Constantinescu[27b], F. Conventi[70a,al], A.M. Cooper-Sarkar[134], F. Cormier[175], K.J.R. Cormier[167], L.D. Corpe[95], M. Corradi[73a,73b], E.E. Corrigan[97], F. Corriveau[104,aa], M.J. Costa[174], F. Costanza[5], D. Costanzo[149], G. Cowan[94], J.W. Cowley[32], J. Crane[101], K. Cranmer[125], R.A. Creager[136], S. Crépé-Renaudin[58], F. Crescioli[135], M. Cristinziani[24], V. Croft[170], G. Crosetti[41b,41a], A. Cueto[5], T. Cuhadar Donszelmann[171], H. Cui[15a,15d], A.R. Cukierman[153], W.R. Cunningham[57], S. Czekierda[85], P. Czodrowski[36], M.M. Czurylo[61b], M.J. Da Cunha Sargedas De Sousa[60b], J.V. Da Fonseca Pinto[81b], C. Da Via[101], W. Dabrowski[84a], F. Dachs[36], T. Dado[47], S. Dahbi[33e], T. Dai[106], C. Dallapiccola[103], M. Dam[40], G. D'amen[29], V. D'Amico[75a,75b], J. Damp[100], J.R. Dandoy[136], M.F. Daneri[30], M. Danninger[152], V. Dao[36], G. Darbo[55b], O. Dartsi[5], A. Dattagupta[131], T. Daubney[46], S. D'Auria[69a,69b], C. David[168b], T. Davidek[142], D.R. Davis[49], I. Dawson[149], K. De[8], R. De Asmundis[70a], M. De Beurs[120], S. De Castro[23b,23a], N. De Groot[119], P. de Jong[120], H. De la Torre[107], A. De Maria[15c], D. De Pedis[73a], A. De Salvo[73a], U. De Sanctis[74a,74b], M. De Santis[74a,74b], A. De Santo[156], J.B. De Vivie De Regie[65], D.V. Dedovich[80], A.M. Deiana[42], J. Del Peso[99], Y. Delabat Diaz[46], D. Delgove[65], F. Deliot[144], C.M. Delitzsch[7], M. Della Pietra[70a,70b], D. Della Volpe[54], A. Dell'Acqua[36], L. Dell'Asta[74a,74b], M. Delmastro[5], C. Delporte[65], P.A. Delsart[58], S. Demers[183], M. Demichev[80], G. Demontigny[110], S.P. Denisov[123], L. D'Eramo[121], D. Derendarz[85], J.E. Derkaoui[35e], F. Derue[135], P. Dervan[91], K. Desch[24], K. Dette[167], C. Deutsch[24], M.R. Devesa[30], P.O. Deviveiros[36], F.A. Di Bello[73a,73b], A. Di Ciaccio[74a,74b], L. Di Ciaccio[5], C. Di Donato[70a,70b], A. Di Girolamo[36], G. Di Gregorio[72a,72b], A. Di Luca[76a,76b], B. Di Micco[75a,75b], R. Di Nardo[75a,75b], K.F. Di Petrillo[59], R. Di Sipio[167], C. Diaconu[102], F.A. Dias[120], T. Dias Do Vale[139a], M.A. Diaz[146a], F.G. Diaz Capriles[24], J. Dickinson[18], M. Didenko[166], E.B. Diehl[106], J. Dietrich[19], S. Díez Cornell[46], C. Diez Pardos[151], A. Dimitrievska[18], W. Ding[15b], J. Dingfelder[24], S.J. Dittmeier[61b], F. Dittus[36], F. Djama[102], T. Djobava[159b], J.I. Djuvsland[17], M.A.B. Do Vale[147], M. Dobre[27b], D. Dodsworth[26], C. Doglioni[97], J. Dolejsi[142], Z. Dolezal[142], M. Donadelli[81c], B. Dong[60c], J. Donini[38], A. D'onofrio[15c], M. D'Onofrio[91], J. Dopke[143], A. Doria[70a], M.T. Dova[89], A.T. Doyle[57], E. Drechsler[152], E. Dreyer[152], T. Dreyer[53], A.S. Drobac[170], D. Du[60b], T.A. du Pree[120], Y. Duan[60d], F. Dubinin[111], M. Dubovsky[28a], A. Dubreuil[54], E. Duchovni[180], G. Duckeck[114], O.A. Ducu[36,27b], D. Duda[115], A. Dudarev[36], A.C. Dudder[100], E.M. Duffield[18], M. D'uffizi[101], L. Duflot[65], M. Dührssen[36], C. Dülsen[182], M. Dumancic[180], A.E. Dumitriu[27b], M. Dunford[61a], S. Dungs[47], A. Duperrin[102], H. Duran Yildiz[4a], M. Düren[56], A. Durglishvili[159b], D. Duschinger[48], B. Dutta[46], D. Duvnjak[1], G.I. Dyckes[136], M. Dyndal[36], S. Dysch[101], B.S. Dziedzic[85], M.G. Eggleston[49], T. Eifert[8], G. Eigen[17], K. Einsweiler[18], T. Ekelof[172], H. El Jarrari[35f], V. Ellajosyula[172], M. Ellert[172], F. Ellinghaus[182], A.A. Elliot[93], N. Ellis[36], J. Elmsheuser[29], M. Elsing[36], D. Emeliyanov[143], A. Emerman[39], Y. Enari[163], M.B. Epland[49], J. Erdmann[47], A. Ereditato[20], P.A. Erland[85], M. Errenst[182], M. Escalier[65], C. Escobar[174], O. Estrada Pastor[174], E. Etzion[161], G. Evans[139a], H. Evans[66], M.O. Evans[156], A. Ezhilov[137], F. Fabbri[57], L. Fabbri[23b,23a], V. Fabiani[119], G. Facini[178], R.M. Fakhrutdinov[123], S. Falciano[73a], P.J. Falke[24], S. Falke[36], J. Faltova[142], Y. Fang[15a], Y. Fang[15a], G. Fanourakis[44], M. Fanti[69a,69b], M. Faraj[67a,67c], A. Farbin[8], A. Farilla[75a], E.M. Farina[71a,71b], T. Farooque[107], S.M. Farrington[50], P. Farthouat[36], F. Fassi[35f], P. Fassnacht[36], D. Fassouliotis[9], M. Faucci Giannelli[50], W.J. Fawcett[32], L. Fayard[65], O.L. Fedin[137,p], W. Fedorko[175], A. Fehr[20], M. Feickert[173], L. Feligioni[102], A. Fell[149], C. Feng[60b], M. Feng[49], M.J. Fenton[171], A.B. Fenyuk[123], S.W. Ferguson[43], J. Ferrando[46], A. Ferrari[172], P. Ferrari[120], R. Ferrari[71a], D.E. Ferreira de Lima[61b], A. Ferrer[174], D. Ferrere[54], C. Ferretti[106], F. Fiedler[100], A. Filipčič[92], F. Filthaut[119], K.D. Finelli[25], M.C.N. Fiolhais[139a,139c,a], L. Fiorini[174], F. Fischer[114], J. Fischer[100], W.C. Fisher[107], T. Fitschen[21], I. Fleck[151], P. Fleischmann[106],

JHEP06(2021)145

T. Flick[182], B.M. Flierl[114], L. Flores[136], L.R. Flores Castillo[63a], F.M. Follega[76a,76b], N. Fomin[17], J.H. Foo[167], G.T. Forcolin[76a,76b], B.C. Forland[66], A. Formica[144], F.A. Förster[14], A.C. Forti[101], E. Fortin[102], M.G. Foti[134], D. Fournier[65], H. Fox[90], P. Francavilla[72a,72b], S. Francescato[73a,73b], M. Franchini[23b,23a], S. Franchino[61a], D. Francis[36], L. Franco[5], L. Franconi[20], M. Franklin[59], G. Frattari[73a,73b], A.N. Fray[93], P.M. Freeman[21], B. Freund[110], W.S. Freund[81b], E.M. Freundlich[47], D.C. Frizzell[128], D. Froidevaux[36], J.A. Frost[134], M. Fujimoto[126], C. Fukunaga[164], E. Fullana Torregrosa[174], T. Fusayasu[116], J. Fuster[174], A. Gabrielli[23b,23a], A. Gabrielli[36], S. Gadatsch[54], P. Gadow[115], G. Gagliardi[55b,55a], L.G. Gagnon[110], G.E. Gallardo[134], E.J. Gallas[134], B.J. Gallop[143], R. Gamboa Goni[93], K.K. Gan[127], S. Ganguly[180], J. Gao[60a], Y. Gao[50], Y.S. Gao[31,m], F.M. Garay Walls[146a], C. García[174], J.E. García Navarro[174], J.A. García Pascual[15a], C. Garcia-Argos[52], M. Garcia-Sciveres[18], R.W. Gardner[37], N. Garelli[153], S. Gargiulo[52], C.A. Garner[167], V. Garonne[133], S.J. Gasiorowski[148], P. Gaspar[81b], A. Gaudiello[55b,55a], G. Gaudio[71a], P. Gauzzi[73a,73b], I.L. Gavrilenko[111], A. Gavrilyuk[124], C. Gay[175], G. Gaycken[46], E.N. Gazis[10], A.A. Geanta[27b], C.M. Gee[145], C.N.P. Gee[143], J. Geisen[97], M. Geisen[100], C. Gemme[55b], M.H. Genest[58], C. Geng[106], S. Gentile[73a,73b], S. George[94], T. Geralis[44], L.O. Gerlach[53], P. Gessinger-Befurt[100], G. Gessner[47], M. Ghasemi Bostanabad[176], M. Ghneimat[151], A. Ghosh[65], A. Ghosh[78], B. Giacobbe[23b], S. Giagu[73a,73b], N. Giangiacomi[167], P. Giannetti[72a], A. Giannini[70a,70b], G. Giannini[14], S.M. Gibson[94], M. Gignac[145], D.T. Gil[84b], B.J. Gilbert[39], D. Gillberg[34], G. Gilles[182], N.E.K. Gillwald[46], D.M. Gingrich[3,ak], M.P. Giordani[67a,67c], P.F. Giraud[144], G. Giugliarelli[67a,67c], D. Giugni[69a], F. Giuli[74a,74b], S. Gkaitatzis[162], I. Gkialas[9,h], E.L. Gkougkousis[14], P. Gkountoumis[10], L.K. Gladilin[113], C. Glasman[99], J. Glatzer[14], P.C.F. Glaysher[46], A. Glazov[46], G.R. Gledhill[131], I. Gnesi[41b,c], M. Goblirsch-Kolb[26], D. Godin[110], S. Goldfarb[105], T. Golling[54], D. Golubkov[123], A. Gomes[139a,139b], R. Goncalves Gama[53], R. Gonçalo[139a,139c], G. Gonella[131], L. Gonella[21], A. Gongadze[80], F. Gonnella[21], J.L. Gonski[39], S. González de la Hoz[174], S. Gonzalez Fernandez[14], R. Gonzalez Lopez[91], C. Gonzalez Renteria[18], R. Gonzalez Suarez[172], S. Gonzalez-Sevilla[54], G.R. Gonzalvo Rodriguez[174], L. Goossens[36], N.A. Gorasia[21], P.A. Gorbounov[124], H.A. Gordon[29], B. Gorini[36], E. Gorini[68a,68b], A. Gorišek[92], A.T. Goshaw[49], M.I. Gostkin[80], C.A. Gottardo[119], M. Gouighri[35b], A.G. Goussiou[148], N. Govender[33c], C. Goy[5], I. Grabowska-Bold[84a], E.C. Graham[91], J. Gramling[171], E. Gramstad[133], S. Grancagnolo[19], M. Grandi[156], V. Gratchev[137], P.M. Gravila[27f], F.G. Gravili[68a,68b], C. Gray[57], H.M. Gray[18], C. Grefe[24], K. Gregersen[97], I.M. Gregor[46], P. Grenier[153], K. Grevtsov[46], C. Grieco[14], N.A. Grieser[128], A.A. Grillo[145], K. Grimm[31,l], S. Grinstein[14,w], J.-F. Grivaz[65], S. Groh[100], E. Gross[180], J. Grosse-Knetter[53], Z.J. Grout[95], C. Grud[106], A. Grummer[118], J.C. Grundy[134], L. Guan[106], W. Guan[181], C. Gubbels[175], J. Guenther[77], A. Guerguichon[65], J.G.R. Guerrero Rojas[174], F. Guescini[115], D. Guest[77], R. Gugel[100], A. Guida[46], T. Guillemin[5], S. Guindon[36], J. Guo[60c], W. Guo[106], Y. Guo[60a], Z. Guo[102], R. Gupta[46], S. Gurbuz[12c], G. Gustavino[128], M. Guth[52], P. Gutierrez[128], C. Gutschow[95], C. Guyot[144], C. Gwenlan[134], C.B. Gwilliam[91], E.S. Haaland[133], A. Haas[125], C. Haber[18], H.K. Hadavand[8], A. Hadef[100], M. Haleem[177], J. Haley[129], J.J. Hall[149], G. Halladjian[107], G.D. Hallewell[102], K. Hamano[176], H. Hamdaoui[35f], M. Hamer[24], G.N. Hamity[50], K. Han[60a], L. Han[15c], L. Han[60a], S. Han[18], Y.F. Han[167], K. Hanagaki[82,u], M. Hance[145], D.M. Handl[114], M.D. Hank[37], R. Hankache[135], E. Hansen[97], J.B. Hansen[40], J.D. Hansen[40], M.C. Hansen[24], P.H. Hansen[40], E.C. Hanson[101], K. Hara[169], T. Harenberg[182], S. Harkusha[108], P.F. Harrison[178], N.M. Hartman[153], N.M. Hartmann[114], Y. Hasegawa[150], A. Hasib[50], S. Hassani[144], S. Haug[20], R. Hauser[107], M. Havranek[141], C.M. Hawkes[21], R.J. Hawkings[36], S. Hayashida[117], D. Hayden[107], C. Hayes[106], R.L. Hayes[175], C.P. Hays[134], J.M. Hays[93], H.S. Hayward[91], S.J. Haywood[143], F. He[60a], Y. He[165], M.P. Heath[50], V. Hedberg[97], A.L. Heggelund[133], N.D. Hehir[93], C. Heidegger[52], K.K. Heidegger[52], W.D. Heidorn[79],

JHEP06(2021)145

J. Heilman[34], S. Heim[46], T. Heim[18], B. Heinemann[46,ai], J.G. Heinlein[136], J.J. Heinrich[131], L. Heinrich[36], J. Hejbal[140], L. Helary[46], A. Held[125], S. Hellesund[133], C.M. Helling[145], S. Hellman[45a,45b], C. Helsens[36], R.C.W. Henderson[90], L. Henkelmann[32], A.M. Henriques Correia[36], H. Herde[26], Y. Hernández Jiménez[33e], H. Herr[100], M.G. Herrmann[114], T. Herrmann[48], G. Herten[52], R. Hertenberger[114], L. Hervas[36], G.G. Hesketh[95], N.P. Hessey[168a], H. Hibi[83], S. Higashino[82], E. Higón-Rodriguez[174], K. Hildebrand[37], J.C. Hill[32], K.K. Hill[29], K.H. Hiller[46], S.J. Hillier[21], M. Hils[48], I. Hinchliffe[18], F. Hinterkeuser[24], M. Hirose[132], S. Hirose[169], D. Hirschbuehl[182], B. Hiti[92], O. Hladik[140], J. Hobbs[155], R. Hobincu[27e], N. Hod[180], M.C. Hodgkinson[149], A. Hoecker[36], D. Hohn[52], D. Hohov[65], T. Holm[24], T.R. Holmes[37], M. Holzbock[115], L.B.A.H. Hommels[32], T.M. Hong[138], J.C. Honig[52], A. Hönle[115], B.H. Hooberman[173], W.H. Hopkins[6], Y. Horii[117], P. Horn[48], L.A. Horyn[37], S. Hou[158], A. Hoummada[35a], J. Howarth[57], J. Hoya[89], M. Hrabovsky[130], J. Hrivnac[65], A. Hrynevich[109], T. Hryn'ova[5], P.J. Hsu[64], S.-C. Hsu[148], Q. Hu[39], S. Hu[60c], Y.F. Hu[15a,15d,am], D.P. Huang[95], X. Huang[15c], Y. Huang[60a], Y. Huang[15a], Z. Hubacek[141], F. Hubaut[102], M. Huebner[24], F. Huegging[24], T.B. Huffman[134], M. Huhtinen[36], R. Hulsken[58], R.F.H. Hunter[34], N. Huseynov[80,ab], J. Huston[107], J. Huth[59], R. Hyneman[153], S. Hyrych[28a], G. Iacobucci[54], G. Iakovidis[29], I. Ibragimov[151], L. Iconomidou-Fayard[65], P. Iengo[36], R. Ignazzi[40], R. Iguchi[163], T. Iizawa[54], Y. Ikegami[82], M. Ikeno[82], N. Ilic[119,167,aa], F. Iltzsche[48], H. Imam[35a], G. Introzzi[71a,71b], M. Iodice[75a], K. Iordanidou[168a], V. Ippolito[73a,73b], M.F. Isacson[172], M. Ishino[163], W. Islam[129], C. Issever[19,46], S. Istin[160], J.M. Iturbe Ponce[63a], R. Iuppa[76a,76b], A. Ivina[180], J.M. Izen[43], V. Izzo[70a], P. Jacka[140], P. Jackson[1], R.M. Jacobs[46], B.P. Jaeger[152], V. Jain[2], G. Jäkel[182], K.B. Jakobi[100], K. Jakobs[52], T. Jakoubek[180], J. Jamieson[57], K.W. Janas[84a], R. Jansky[54], M. Janus[53], P.A. Janus[84a], G. Jarlskog[97], A.E. Jaspan[91], N. Javadov[80,ab], T. Javůrek[36], M. Javurkova[103], F. Jeanneau[144], L. Jeanty[131], J. Jejelava[159a], P. Jenni[52,d], N. Jeong[46], S. Jézéquel[5], J. Jia[155], Z. Jia[15c], H. Jiang[79], Y. Jiang[60a], Z. Jiang[153], S. Jiggins[52], F.A. Jimenez Morales[38], J. Jimenez Pena[115], S. Jin[15c], A. Jinaru[27b], O. Jinnouchi[165], H. Jivan[33e], P. Johansson[149], K.A. Johns[7], C.A. Johnson[66], E. Jones[178], R.W.L. Jones[90], S.D. Jones[156], T.J. Jones[91], J. Jovicevic[36], X. Ju[18], J.J. Junggeburth[115], A. Juste Rozas[14,w], A. Kaczmarska[85], M. Kado[73a,73b], H. Kagan[127], M. Kagan[153], A. Kahn[39], C. Kahra[100], T. Kaji[179], E. Kajomovitz[160], C.W. Kalderon[29], A. Kaluza[100], A. Kamenshchikov[123], M. Kaneda[163], N.J. Kang[145], S. Kang[79], Y. Kano[117], J. Kanzaki[82], L.S. Kaplan[181], D. Kar[33e], K. Karava[134], M.J. Kareem[168b], I. Karkanias[162], S.N. Karpov[80], Z.M. Karpova[80], V. Kartvelishvili[90], A.N. Karyukhin[123], E. Kasimi[162], A. Kastanas[45a,45b], C. Kato[60d], J. Katzy[46], K. Kawade[150], K. Kawagoe[88], T. Kawaguchi[117], T. Kawamoto[144], G. Kawamura[53], E.F. Kay[176], F.I. Kaya[170], S. Kazakos[14], V.F. Kazanin[122b,122a], J.M. Keaveney[33a], R. Keeler[176], J.S. Keller[34], E. Kellermann[97], D. Kelsey[156], J.J. Kempster[21], J. Kendrick[21], K.E. Kennedy[39], O. Kepka[140], S. Kersten[182], B.P. Kerševan[92], S. Ketabchi Haghighat[167], F. Khalil-Zada[13], M. Khandoga[144], A. Khanov[129], A.G. Kharlamov[122b,122a], T. Kharlamova[122b,122a], E.E. Khoda[175], T.J. Khoo[77], G. Khoriauli[177], E. Khramov[80], J. Khubua[159b], S. Kido[83], M. Kiehn[36], E. Kim[165], Y.K. Kim[37], N. Kimura[95], A. Kirchhoff[53], D. Kirchmeier[48], J. Kirk[143], A.E. Kiryunin[115], T. Kishimoto[163], D.P. Kisliuk[167], V. Kitali[46], C. Kitsaki[10], O. Kivernyk[24], T. Klapdor-Kleingrothaus[52], M. Klassen[61a], C. Klein[34], M.H. Klein[106], M. Klein[91], U. Klein[91], K. Kleinknecht[100], P. Klimek[36], A. Klimentov[29], F. Klimpel[36], T. Klingl[24], T. Klioutchnikova[36], F.F. Klitzner[114], P. Kluit[120], S. Kluth[115], E. Kneringer[77], E.B.F.G. Knoops[102], A. Knue[52], D. Kobayashi[88], M. Kobel[48], M. Kocian[153], T. Kodama[163], P. Kodys[142], D.M. Koeck[156], P.T. Koenig[24], T. Koffas[34], N.M. Köhler[36], M. Kolb[144], I. Koletsou[5], T. Komarek[130], T. Kondo[82], K. Köneke[52], A.X.Y. Kong[1], A.C. König[119], T. Kono[126], V. Konstantinides[95], N. Konstantinidis[95], B. Konya[97], R. Kopeliansky[66], S. Koperny[84a], K. Korcyl[85], K. Kordas[162], G. Koren[161], A. Korn[95],

JHEP06(2021)145

I. Korolkov[14], E.V. Korolkova[149], N. Korotkova[113], O. Kortner[115], S. Kortner[115], V.V. Kostyukhin[149,166], A. Kotsokechagia[65], A. Kotwal[49], A. Koulouris[10], A. Kourkoumeli-Charalampidi[71a,71b], C. Kourkoumelis[9], E. Kourlitis[6], V. Kouskoura[29], R. Kowalewski[176], W. Kozanecki[101], A.S. Kozhin[123], V.A. Kramarenko[113], G. Kramberger[92], D. Krasnopevtsev[60a], M.W. Krasny[135], A. Krasznahorkay[36], D. Krauss[115], J.A. Kremer[100], J. Kretzschmar[91], K. Kreul[19], P. Krieger[167], F. Krieter[114], S. Krishnamurthy[103], A. Krishnan[61b], M. Krivos[142], K. Krizka[18], K. Kroeninger[47], H. Kroha[115], J. Kroll[140], J. Kroll[136], K.S. Krowpman[107], U. Kruchonak[80], H. Krüger[24], N. Krumnack[79], M.C. Kruse[49], J.A. Krzysiak[85], A. Kubota[165], O. Kuchinskaia[166], S. Kuday[4b], D. Kuechler[46], J.T. Kuechler[46], S. Kuehn[36], T. Kuhl[46], V. Kukhtin[80], Y. Kulchitsky[108,ae], S. Kuleshov[146b], Y.P. Kulinich[173], M. Kuna[58], A. Kupco[140], T. Kupfer[47], O. Kuprash[52], H. Kurashige[83], L.L. Kurchaninov[168a], Y.A. Kurochkin[108], A. Kurova[112], M.G. Kurth[15a,15d], E.S. Kuwertz[36], M. Kuze[165], A.K. Kvam[148], J. Kvita[130], T. Kwan[104], C. Lacasta[174], F. Lacava[73a,73b], D.P.J. Lack[101], H. Lacker[19], D. Lacour[135], E. Ladygin[80], R. Lafaye[5], B. Laforge[135], T. Lagouri[146c], S. Lai[53], I.K. Lakomiec[84a], J.E. Lambert[128], S. Lammers[66], W. Lampl[7], C. Lampoudis[162], E. Lançon[29], U. Landgraf[52], M.P.J. Landon[93], V.S. Lang[52], J.C. Lange[53], R.J. Langenberg[103], A.J. Lankford[171], F. Lanni[29], K. Lantzsch[24], A. Lanza[71a], A. Lapertosa[55b,55a], J.F. Laporte[144], T. Lari[69a], F. Lasagni Manghi[23b,23a], M. Lassnig[36], V. Latonova[140], T.S. Lau[63a], A. Laudrain[100], A. Laurier[34], M. Lavorgna[70a,70b], S.D. Lawlor[94], M. Lazzaroni[69a,69b], B. Le[101], E. Le Guirriec[102], A. Lebedev[79], M. LeBlanc[7], T. LeCompte[6], F. Ledroit-Guillon[58], A.C.A. Lee[95], C.A. Lee[29], G.R. Lee[17], L. Lee[59], S.C. Lee[158], S. Lee[79], B. Lefebvre[168a], H.P. Lefebvre[94], M. Lefebvre[176], C. Leggett[18], K. Lehmann[152], N. Lehmann[20], G. Lehmann Miotto[36], W.A. Leight[46], A. Leisos[162,v], M.A.L. Leite[81c], C.E. Leitgeb[114], R. Leitner[142], K.J.C. Leney[42], T. Lenz[24], S. Leone[72a], C. Leonidopoulos[50], A. Leopold[135], C. Leroy[110], R. Les[107], C.G. Lester[32], M. Levchenko[137], J. Levêque[5], D. Levin[106], L.J. Levinson[180], D.J. Lewis[21], B. Li[15b], B. Li[106], C-Q. Li[60c,60d], F. Li[60c], H. Li[60a], H. Li[60b], J. Li[60c], K. Li[148], L. Li[60c], M. Li[15a,15d], Q.Y. Li[60a], S. Li[60d,60c,b], X. Li[46], Y. Li[46], Z. Li[60b], Z. Li[134], Z. Li[104], Z. Li[91], Z. Liang[15a], M. Liberatore[46], B. Liberti[74a], K. Lie[63c], S. Lim[29], C.Y. Lin[32], K. Lin[107], R.A. Linck[66], R.E. Lindley[7], J.H. Lindon[21], A. Linss[46], A.L. Lionti[54], E. Lipeles[136], A. Lipniacka[17], T.M. Liss[173,aj], A. Lister[175], J.D. Little[8], B. Liu[79], B.X. Liu[152], H.B. Liu[29], J.B. Liu[60a], J.K.K. Liu[37], K. Liu[60d,60c], M. Liu[60a], M.Y. Liu[60a], P. Liu[15a], X. Liu[60a], Y. Liu[46], Y. Liu[15a,15d], Y.L. Liu[106], Y.W. Liu[60a], M. Livan[71a,71b], A. Lleres[58], J. Llorente Merino[152], S.L. Lloyd[93], C.Y. Lo[63b], E.M. Lobodzinska[46], P. Loch[7], S. Loffredo[74a,74b], T. Lohse[19], K. Lohwasser[149], M. Lokajicek[140], J.D. Long[173], R.E. Long[90], I. Longarini[73a,73b], L. Longo[36], I. Lopez Paz[101], A. Lopez Solis[149], J. Lorenz[114], N. Lorenzo Martinez[5], A.M. Lory[114], A. Lösle[52], X. Lou[45a,45b], X. Lou[15a], A. Lounis[65], J. Love[6], P.A. Love[90], J.J. Lozano Bahilo[174], M. Lu[60a], Y.J. Lu[64], H.J. Lubatti[148], C. Luci[73a,73b], F.L. Lucio Alves[15c], A. Lucotte[58], F. Luehring[66], I. Luise[155], L. Luminari[73a], B. Lund-Jensen[154], N.A. Luongo[131], M.S. Lutz[161], D. Lynn[29], H. Lyons[91], R. Lysak[140], E. Lytken[97], F. Lyu[15a], V. Lyubushkin[80], T. Lyubushkina[80], H. Ma[29], L.L. Ma[60b], Y. Ma[95], D.M. Mac Donell[176], G. Maccarrone[51], C.M. Macdonald[149], J.C. MacDonald[149], J. Machado Miguens[136], R. Madar[38], W.F. Mader[48], M. Madugoda Ralalage Don[129], N. Madysa[48], J. Maeda[83], T. Maeno[29], M. Maerker[48], V. Magerl[52], N. Magini[79], J. Magro[67a,67c,r], D.J. Mahon[39], C. Maidantchik[81b], A. Maio[139a,139b,139d], K. Maj[84a], O. Majersky[28a], S. Majewski[131], Y. Makida[82], N. Makovec[65], B. Malaescu[135], Pa. Malecki[85], V.P. Maleev[137], F. Malek[58], D. Malito[41b,41a], U. Mallik[78], C. Malone[32], S. Maltezos[10], S. Malyukov[80], J. Mamuzic[174], G. Mancini[51], J.P. Mandalia[93], I. Mandić[92], L. Manhaes de Andrade Filho[81a], I.M. Maniatis[162], J. Manjarres Ramos[48], K.H. Mankinen[97], A. Mann[114], A. Manousos[77], B. Mansoulie[144], I. Manthos[162], S. Manzoni[120], A. Marantis[162], G. Marceca[30], L. Marchese[134],

JHEP06(2021)145

G. Marchiori[135], M. Marcisovsky[140], L. Marcoccia[74a,74b], C. Marcon[97], M. Marjanovic[128], Z. Marshall[18], M.U.F. Martensson[172], S. Marti-Garcia[174], C.B. Martin[127], T.A. Martin[178], V.J. Martin[50], B. Martin dit Latour[17], L. Martinelli[75a,75b], M. Martinez[14,w], P. Martinez Agullo[174], V.I. Martinez Outschoorn[103], S. Martin-Haugh[143], V.S. Martoiu[27b], A.C. Martyniuk[95], A. Marzin[36], S.R. Maschek[115], L. Masetti[100], T. Mashimo[163], R. Mashinistov[111], J. Masik[101], A.L. Maslennikov[122b,122a], L. Massa[23b,23a], P. Massarotti[70a,70b], P. Mastrandrea[72a,72b], A. Mastroberardino[41b,41a], T. Masubuchi[163], D. Matakias[29], A. Matic[114], N. Matsuzawa[163], P. Mättig[24], J. Maurer[27b], B. Maček[92], D.A. Maximov[122b,122a], R. Mazini[158], I. Maznas[162], S.M. Mazza[145], J.P. Mc Gowan[104], S.P. Mc Kee[106], T.G. McCarthy[115], W.P. McCormack[18], E.F. McDonald[105], A.E. McDougall[120], J.A. Mcfayden[18], G. Mchedlidze[159b], M.A. McKay[42], K.D. McLean[176], S.J. McMahon[143], P.C. McNamara[105], C.J. McNicol[178], R.A. McPherson[176,aa], J.E. Mdhluli[33e], Z.A. Meadows[103], S. Meehan[36], T. Megy[38], S. Mehlhase[114], A. Mehta[91], B. Meirose[43], D. Melini[160], B.R. Mellado Garcia[33e], J.D. Mellenthin[53], M. Melo[28a], F. Meloni[46], A. Melzer[24], E.D. Mendes Gouveia[139a,139e], A.M. Mendes Jacques Da Costa[21], H.Y. Meng[167], L. Meng[36], X.T. Meng[106], S. Menke[115], E. Meoni[41b,41a], S. Mergelmeyer[19], S.A.M. Merkt[138], C. Merlassino[134], P. Mermod[54], L. Merola[70a,70b], C. Meroni[69a], G. Merz[106], O. Meshkov[113,111], J.K.R. Meshreki[151], J. Metcalfe[6], A.S. Mete[6], C. Meyer[66], J-P. Meyer[144], M. Michetti[19], R.P. Middleton[143], L. Mijović[50], G. Mikenberg[180], M. Mikestikova[140], M. Mikuž[92], H. Mildner[149], A. Milic[167], C.D. Milke[42], D.W. Miller[37], L.S. Miller[34], A. Milov[180], D.A. Milstead[45a,45b], A.A. Minaenko[123], I.A. Minashvili[159b], L. Mince[57], A.I. Mincer[125], B. Mindur[84a], M. Mineev[80], Y. Minegishi[163], Y. Mino[86], L.M. Mir[14], M. Mironova[134], T. Mitani[179], J. Mitrevski[114], V.A. Mitsou[174], M. Mittal[60c], O. Miu[167], A. Miucci[20], P.S. Miyagawa[93], A. Mizukami[82], J.U. Mjörnmark[97], T. Mkrtchyan[61a], M. Mlynarikova[121], T. Moa[45a,45b], S. Mobius[53], K. Mochizuki[110], P. Moder[46], P. Mogg[114], S. Mohapatra[39], R. Moles-Valls[24], K. Mönig[46], E. Monnier[102], A. Montalbano[152], J. Montejo Berlingen[36], M. Montella[95], F. Monticelli[89], S. Monzani[69a], N. Morange[65], A.L. Moreira De Carvalho[139a], D. Moreno[22a], M. Moreno Llácer[174], C. Moreno Martinez[14], P. Morettini[55b], M. Morgenstern[160], S. Morgenstern[48], D. Mori[152], M. Morii[59], M. Morinaga[179], V. Morisbak[133], A.K. Morley[36], G. Mornacchi[36], A.P. Morris[95], L. Morvaj[36], P. Moschovakos[36], B. Moser[120], M. Mosidze[159b], T. Moskalets[144], P. Moskvitina[119], J. Moss[31,n], E.J.W. Moyse[103], S. Muanza[102], J. Mueller[138], R.S.P. Mueller[114], D. Muenstermann[90], G.A. Mullier[97], D.P. Mungo[69a,69b], J.L. Munoz Martinez[14], F.J. Munoz Sanchez[101], P. Murin[28b], W.J. Murray[178,143], A. Murrone[69a,69b], J.M. Muse[128], M. Muškinja[18], C. Mwewa[33a], A.G. Myagkov[123,af], A.A. Myers[138], G. Myers[66], J. Myers[131], M. Myska[141], B.P. Nachman[18], O. Nackenhorst[47], A.Nag Nag[48], K. Nagai[134], K. Nagano[82], Y. Nagasaka[62], J.L. Nagle[29], E. Nagy[102], A.M. Nairz[36], Y. Nakahama[117], K. Nakamura[82], T. Nakamura[163], H. Nanjo[132], F. Napolitano[61a], R.F. Naranjo Garcia[46], R. Narayan[42], I. Naryshkin[137], M. Naseri[34], T. Naumann[46], G. Navarro[22a], P.Y. Nechaeva[111], F. Nechansky[46], T.J. Neep[21], A. Negri[71a,71b], M. Negrini[23b], C. Nellist[119], C. Nelson[104], M.E. Nelson[45a,45b], S. Nemecek[140], M. Nessi[36,f], M.S. Neubauer[173], F. Neuhaus[100], M. Neumann[182], R. Newhouse[175], P.R. Newman[21], C.W. Ng[138], Y.S. Ng[19], Y.W.Y. Ng[171], B. Ngair[35f], H.D.N. Nguyen[102], T. Nguyen Manh[110], E. Nibigira[38], R.B. Nickerson[134], R. Nicolaidou[144], D.S. Nielsen[40], J. Nielsen[145], M. Niemeyer[53], N. Nikiforou[11], V. Nikolaenko[123,af], I. Nikolic-Audit[135], K. Nikolopoulos[21], P. Nilsson[29], H.R. Nindhito[54], A. Nisati[73a], N. Nishu[60c], R. Nisius[115], I. Nitsche[47], T. Nitta[179], T. Nobe[163], D.L. Noel[32], Y. Noguchi[86], I. Nomidis[135], M.A. Nomura[29], M. Nordberg[36], J. Novak[92], T. Novak[92], O. Novgorodova[48], R. Novotny[118], L. Nozka[130], K. Ntekas[171], E. Nurse[95], F.G. Oakham[34,ak], J. Ocariz[135], A. Ochi[83], I. Ochoa[139a], J.P. Ochoa-Ricoux[146a], K. O'Connor[26], S. Oda[88], S. Odaka[82], S. Oerdek[53], A. Ogrodnik[84a], A. Oh[101], C.C. Ohm[154], H. Oide[165],

JHEP06(2021)145

R. Oishi[163], M.L. Ojeda[167], H. Okawa[169], Y. Okazaki[86], M.W. O'Keefe[91], Y. Okumura[163], A. Olariu[27b], L.F. Oleiro Seabra[139a], S.A. Olivares Pino[146a], D. Oliveira Damazio[29], J.L. Oliver[1], M.J.R. Olsson[171], A. Olszewski[85], J. Olszowska[85], Ö.O. Öncel[24], D.C. O'Neil[152], A.P. O'neill[134], A. Onofre[139a,139e], P.U.E. Onyisi[11], H. Oppen[133], R.G. Oreamuno Madriz[121], M.J. Oreglia[37], G.E. Orellana[89], D. Orestano[75a,75b], N. Orlando[14], R.S. Orr[167], V. O'Shea[57], R. Ospanov[60a], G. Otero y Garzon[30], H. Otono[88], P.S. Ott[61a], G.J. Ottino[18], M. Ouchrif[35e], J. Ouellette[29], F. Ould-Saada[133], A. Ouraou[144,*], Q. Ouyang[15a], M. Owen[57], R.E. Owen[143], V.E. Ozcan[12c], N. Ozturk[8], J. Pacalt[130], H.A. Pacey[32], K. Pachal[49], A. Pacheco Pages[14], C. Padilla Aranda[14], S. Pagan Griso[18], G. Palacino[66], S. Palazzo[50], S. Palestini[36], M. Palka[84b], P. Palni[84a], C.E. Pandini[54], J.G. Panduro Vazquez[94], P. Pani[46], G. Panizzo[67a,67c], L. Paolozzi[54], C. Papadatos[110], K. Papageorgiou[9,h], S. Parajuli[42], A. Paramonov[6], C. Paraskevopoulos[10], D. Paredes Hernandez[63b], S.R. Paredes Saenz[134], B. Parida[180], T.H. Park[167], A.J. Parker[31], M.A. Parker[32], F. Parodi[55b,55a], E.W. Parrish[121], J.A. Parsons[39], U. Parzefall[52], L. Pascual Dominguez[135], V.R. Pascuzzi[18], J.M.P. Pasner[145], F. Pasquali[120], E. Pasqualucci[73a], S. Passaggio[55b], F. Pastore[94], P. Pasuwan[45a,45b], S. Pataraia[100], J.R. Pater[101], A. Pathak[181,j], J. Patton[91], T. Pauly[36], J. Pearkes[153], M. Pedersen[133], L. Pedraza Diaz[119], R. Pedro[139a], T. Peiffer[53], S.V. Peleganchuk[122b,122a], O. Penc[140], C. Peng[63b], H. Peng[60a], B.S. Peralva[81a], M.M. Perego[65], A.P. Pereira Peixoto[139a], L. Pereira Sanchez[45a,45b], D.V. Perepelitsa[29], E. Perez Codina[168a], L. Perini[69a,69b], H. Pernegger[36], S. Perrella[36], A. Perrevoort[120], K. Peters[46], R.F.Y. Peters[101], B.A. Petersen[36], T.C. Petersen[40], E. Petit[102], V. Petousis[141], C. Petridou[162], F. Petrucci[75a,75b], M. Pettee[183], N.E. Pettersson[103], K. Petukhova[142], A. Peyaud[144], R. Pezoa[146d], L. Pezzotti[71a,71b], T. Pham[105], P.W. Phillips[143], M.W. Phipps[173], G. Piacquadio[155], E. Pianori[18], A. Picazio[103], R.H. Pickles[101], R. Piegaia[30], D. Pietreanu[27b], J.E. Pilcher[37], A.D. Pilkington[101], M. Pinamonti[67a,67c], J.L. Pinfold[3], C. Pitman Donaldson[95], M. Pitt[161], L. Pizzimento[74a,74b], A. Pizzini[120], M.-A. Pleier[29], V. Plesanovs[52], V. Pleskot[142], E. Plotnikova[80], P. Podberezko[122b,122a], R. Poettgen[97], R. Poggi[54], L. Poggioli[135], I. Pogrebnyak[107], D. Pohl[24], I. Pokharel[53], G. Polesello[71a], A. Poley[152,168a], A. Policicchio[73a,73b], R. Polifka[142], A. Polini[23b], C.S. Pollard[46], V. Polychronakos[29], D. Ponomarenko[112], L. Pontecorvo[36], S. Popa[27a], G.A. Popeneciu[27d], L. Portales[5], D.M. Portillo Quintero[58], S. Pospisil[141], K. Potamianos[46], I.N. Potrap[80], C.J. Potter[32], H. Potti[11], T. Poulsen[97], J. Poveda[174], T.D. Powell[149], G. Pownall[46], M.E. Pozo Astigarraga[36], A. Prades Ibanez[174], P. Pralavorio[102], M.M. Prapa[44], S. Prell[79], D. Price[101], M. Primavera[68a], M.L. Proffitt[148], N. Proklova[112], K. Prokofiev[63c], F. Prokoshin[80], S. Protopopescu[29], J. Proudfoot[6], M. Przybycien[84a], D. Pudzha[137], A. Puri[173], P. Puzo[65], D. Pyatiizbyantseva[112], J. Qian[106], Y. Qin[101], A. Quadt[53], M. Queitsch-Maitland[36], G. Rabanal Bolanos[59], M. Racko[28a], F. Ragusa[69a,69b], G. Rahal[98], J.A. Raine[54], S. Rajagopalan[29], A. Ramirez Morales[93], K. Ran[15a,15d], D.F. Rassloff[61a], D.M. Rauch[46], F. Rauscher[114], S. Rave[100], B. Ravina[57], I. Ravinovich[180], J.H. Rawling[101], M. Raymond[36], A.L. Read[133], N.P. Readioff[149], M. Reale[68a,68b], D.M. Rebuzzi[71a,71b], G. Redlinger[29], K. Reeves[43], D. Reikher[161], A. Reiss[100], A. Rej[151], C. Rembser[36], A. Renardi[46], M. Renda[27b], M.B. Rendel[115], A.G. Rennie[57], S. Resconi[69a], E.D. Resseguie[18], S. Rettie[95], B. Reynolds[127], E. Reynolds[21], O.L. Rezanova[122b,122a], P. Reznicek[142], E. Ricci[76a,76b], R. Richter[115], S. Richter[46], E. Richter-Was[84b], M. Ridel[135], P. Rieck[115], O. Rifki[46], M. Rijssenbeek[155], A. Rimoldi[71a,71b], M. Rimoldi[46], L. Rinaldi[23b], T.T. Rinn[173], G. Ripellino[154], I. Riu[14], P. Rivadeneira[46], J.C. Rivera Vergara[176], F. Rizatdinova[129], E. Rizvi[93], C. Rizzi[36], S.H. Robertson[104,aa], M. Robin[46], D. Robinson[32], C.M. Robles Gajardo[146d], M. Robles Manzano[100], A. Robson[57], A. Rocchi[74a,74b], C. Roda[72a,72b], S. Rodriguez Bosca[174], A. Rodriguez Rodriguez[52], A.M. Rodríguez Vera[168b], S. Roe[36], J. Roggel[182], O. Røhne[133], R. Röhrig[115], R.A. Rojas[146d], B. Roland[52], C.P.A. Roland[66], J. Roloff[29], A. Romaniouk[112], M. Romano[23b,23a], N. Rompotis[91],

JHEP06(2021)145

M. Ronzani[125], L. Roos[135], S. Rosati[73a], G. Rosin[103], B.J. Rosser[136], E. Rossi[46], E. Rossi[75a,75b], E. Rossi[70a,70b], L.P. Rossi[55b], L. Rossini[46], R. Rosten[14], M. Rotaru[27b], B. Rottler[52], D. Rousseau[65], G. Rovelli[71a,71b], A. Roy[11], D. Roy[33e], A. Rozanov[102], Y. Rozen[160], X. Ruan[33e], T.A. Ruggeri[1], F. Rühr[52], A. Ruiz-Martinez[174], A. Rummler[36], Z. Rurikova[52], N.A. Rusakovich[80], H.L. Russell[104], L. Rustige[38,47], J.P. Rutherfoord[7], E.M. Rüttinger[149], M. Rybar[142], G. Rybkin[65], E.B. Rye[133], A. Ryzhov[123], J.A. Sabater Iglesias[46], P. Sabatini[174], L. Sabetta[73a,73b], S. Sacerdoti[65], H.F-W. Sadrozinski[145], R. Sadykov[80], F. Safai Tehrani[73a], B. Safarzadeh Samani[156], M. Safdari[153], P. Saha[121], S. Saha[104], M. Sahinsoy[115], A. Sahu[182], M. Saimpert[36], M. Saito[163], T. Saito[163], H. Sakamoto[163], D. Salamani[54], G. Salamanna[75a,75b], A. Salnikov[153], J. Salt[174], A. Salvador Salas[14], D. Salvatore[41b,41a], F. Salvatore[156], A. Salvucci[63a], A. Salzburger[36], J. Samarati[36], D. Sammel[52], D. Sampsonidis[162], D. Sampsonidou[60d,60c], J. Sánchez[174], A. Sanchez Pineda[67a,36,67c], H. Sandaker[133], C.O. Sander[46], I.G. Sanderswood[90], M. Sandhoff[182], C. Sandoval[22b], D.P.C. Sankey[143], M. Sannino[55b,55a], Y. Sano[117], A. Sansoni[51], C. Santoni[38], H. Santos[139a,139b], S.N. Santpur[18], A. Santra[174], K.A. Saoucha[149], A. Sapronov[80], J.G. Saraiva[139a,139d], O. Sasaki[82], K. Sato[169], F. Sauerburger[52], E. Sauvan[5], P. Savard[167,ak], R. Sawada[163], C. Sawyer[143], L. Sawyer[96], I. Sayago Galvan[174], C. Sbarra[23b], A. Sbrizzi[67a,67c], T. Scanlon[95], J. Schaarschmidt[148], P. Schacht[115], D. Schaefer[37], L. Schaefer[136], U. Schäfer[100], A.C. Schaffer[65], D. Schaile[114], R.D. Schamberger[155], E. Schanet[114], C. Scharf[19], N. Scharmberg[101], V.A. Schegelsky[137], D. Scheirich[142], F. Schenck[19], M. Schernau[171], C. Schiavi[55b,55a], L.K. Schildgen[24], Z.M. Schillaci[26], E.J. Schioppa[68a,68b], M. Schioppa[41b,41a], K.E. Schleicher[52], S. Schlenker[36], K.R. Schmidt-Sommerfeld[115], K. Schmieden[100], C. Schmitt[100], S. Schmitt[46], L. Schoeffel[144], A. Schoening[61b], P.G. Scholer[52], E. Schopf[134], M. Schott[100], J.F.P. Schouwenberg[119], J. Schovancova[36], S. Schramm[54], F. Schroeder[182], A. Schulte[100], H-C. Schultz-Coulon[61a], M. Schumacher[52], B.A. Schumm[145], Ph. Schune[144], A. Schwartzman[153], T.A. Schwarz[106], Ph. Schwemling[144], R. Schwienhorst[107], A. Sciandra[145], G. Sciolla[26], F. Scuri[72a], F. Scutti[105], L.M. Scyboz[115], C.D. Sebastiani[91], K. Sedlaczek[47], P. Seema[19], S.C. Seidel[118], A. Seiden[145], B.D. Seidlitz[29], T. Seiss[37], C. Seitz[46], J.M. Seixas[81b], G. Sekhniaidze[70a], S.J. Sekula[42], N. Semprini-Cesari[23b,23a], S. Sen[49], C. Serfon[29], L. Serin[65], L. Serkin[67a,67b], M. Sessa[60a], H. Severini[128], S. Sevova[153], F. Sforza[55b,55a], A. Sfyrla[54], E. Shabalina[53], J.D. Shahinian[136], N.W. Shaikh[45a,45b], D. Shaked Renous[180], L.Y. Shan[15a], M. Shapiro[18], A. Sharma[36], A.S. Sharma[1], P.B. Shatalov[124], K. Shaw[156], S.M. Shaw[101], M. Shehade[180], Y. Shen[128], A.D. Sherman[25], P. Sherwood[95], L. Shi[95], C.O. Shimmin[183], Y. Shimogama[179], M. Shimojima[116], J.D. Shinner[94], I.P.J. Shipsey[134], S. Shirabe[165], M. Shiyakova[80,y], J. Shlomi[180], A. Shmeleva[111], M.J. Shochet[37], J. Shojaii[105], D.R. Shope[154], S. Shrestha[127], E.M. Shrif[33e], M.J. Shroff[176], E. Shulga[180], P. Sicho[140], A.M. Sickles[173], E. Sideras Haddad[33e], O. Sidiropoulou[36], A. Sidoti[23b,23a], F. Siegert[48], Dj. Sijacki[16], M.Jr. Silva[181], M.V. Silva Oliveira[36], S.B. Silverstein[45a], S. Simion[65], R. Simoniello[100], C.J. Simpson-allsop[21], S. Simsek[12b], P. Sinervo[167], V. Sinetckii[113], S. Singh[152], S. Sinha[33e], M. Sioli[23b,23a], I. Siral[131], S.Yu. Sivoklokov[113], J. Sjölin[45a,45b], A. Skaf[53], E. Skorda[97], P. Skubic[128], M. Slawinska[85], K. Sliwa[170], V. Smakhtin[180], B.H. Smart[143], J. Smiesko[28b], N. Smirnov[112], S.Yu. Smirnov[112], Y. Smirnov[112], L.N. Smirnova[113,s], O. Smirnova[97], E.A. Smith[37], H.A. Smith[134], M. Smizanska[90], K. Smolek[141], A. Smykiewicz[85], A.A. Snesarev[111], H.L. Snoek[120], I.M. Snyder[131], S. Snyder[29], R. Sobie[176,aa], A. Soffer[161], A. Søgaard[50], F. Sohns[53], C.A. Solans Sanchez[36], E.Yu. Soldatov[112], U. Soldevila[174], A.A. Solodkov[123], A. Soloshenko[80], O.V. Solovyanov[123], V. Solovyev[137], P. Sommer[149], H. Son[170], A. Sonay[14], W. Song[143], W.Y. Song[168b], A. Sopczak[141], A.L. Sopio[95], F. Sopkova[28b], S. Sottocornola[71a,71b], R. Soualah[67a,67c], A.M. Soukharev[122b,122a], D. South[46], S. Spagnolo[68a,68b], M. Spalla[115], M. Spangenberg[178], F. Spanò[94], D. Sperlich[52], T.M. Spieker[61a], G. Spigo[36], M. Spina[156], D.P. Spiteri[57], M. Spousta[142], A. Stabile[69a,69b], B.L. Stamas[121],

JHEP06(2021)145

R. Stamen[61a], M. Stamenkovic[120], A. Stampekis[21], E. Stanecka[85], B. Stanislaus[134], M.M. Stanitzki[46], M. Stankaityte[134], B. Stapf[120], E.A. Starchenko[123], G.H. Stark[145], J. Stark[58], P. Staroba[140], P. Starovoitov[61a], S. Stärz[104], R. Staszewski[85], G. Stavropoulos[44], M. Stegler[46], P. Steinberg[29], A.L. Steinhebel[131], B. Stelzer[152,168a], H.J. Stelzer[138], O. Stelzer-Chilton[168a], H. Stenzel[56], T.J. Stevenson[156], G.A. Stewart[36], M.C. Stockton[36], G. Stoicea[27b], M. Stolarski[139a], S. Stonjek[115], A. Straessner[48], J. Strandberg[154], S. Strandberg[45a,45b], M. Strauss[128], T. Strebler[102], P. Strizenec[28b], R. Ströhmer[177], D.M. Strom[131], R. Stroynowski[42], A. Strubig[45a,45b], S.A. Stucci[29], B. Stugu[17], J. Stupak[128], N.A. Styles[46], D. Su[153], W. Su[60d,148,60c], X. Su[60a], N.B. Suarez[138], V.V. Sulin[111], M.J. Sullivan[91], D.M.S. Sultan[54], S. Sultansoy[4c], T. Sumida[86], S. Sun[106], X. Sun[101], C.J.E. Suster[157], M.R. Sutton[156], S. Suzuki[82], M. Svatos[140], M. Swiatlowski[168a], S.P. Swift[2], T. Swirski[177], A. Sydorenko[100], I. Sykora[28a], M. Sykora[142], T. Sykora[142], D. Ta[100], K. Tackmann[46,x], J. Taenzer[161], A. Taffard[171], R. Tafirout[168a], E. Tagiev[123], R.H.M. Taibah[135], R. Takashima[87], K. Takeda[83], T. Takeshita[150], E.P. Takeva[50], Y. Takubo[82], M. Talby[102], A.A. Talyshev[122b,122a], K.C. Tam[63b], N.M. Tamir[161], J. Tanaka[163], R. Tanaka[65], S. Tapia Araya[173], S. Tapprogge[100], A. Tarek Abouelfadl Mohamed[107], S. Tarem[160], K. Tariq[60b], G. Tarna[27b,e], G.F. Tartarelli[69a], P. Tas[142], M. Tasevsky[140], E. Tassi[41b,41a], G. Tateno[163], A. Tavares Delgado[139a], Y. Tayalati[35f], A.J. Taylor[50], G.N. Taylor[105], W. Taylor[168b], H. Teagle[91], A.S. Tee[90], R. Teixeira De Lima[153], P. Teixeira-Dias[94], H. Ten Kate[36], J.J. Teoh[120], K. Terashi[163], J. Terron[99], S. Terzo[14], M. Testa[51], R.J. Teuscher[167,aa], N. Themistokleous[50], T. Theveneaux-Pelzer[19], D.W. Thomas[94], J.P. Thomas[21], E.A. Thompson[46], P.D. Thompson[21], E. Thomson[136], E.J. Thorpe[93], V.O. Tikhomirov[111,ag], Yu.A. Tikhonov[122b,122a], S. Timoshenko[112], P. Tipton[183], S. Tisserant[102], K. Todome[23b,23a], S. Todorova-Nova[142], S. Todt[48], J. Tojo[88], S. Tokár[28a], K. Tokushuku[82], E. Tolley[127], R. Tombs[32], K.G. Tomiwa[33e], M. Tomoto[82,117], L. Tompkins[153], P. Tornambe[103], E. Torrence[131], H. Torres[48], E. Torró Pastor[174], M. Toscani[30], C. Tosciri[134], J. Toth[102,z], D.R. Tovey[149], A. Traeet[17], C.J. Treado[125], T. Trefzger[177], F. Tresoldi[156], A. Tricoli[29], I.M. Trigger[168a], S. Trincaz-Duvoid[135], D.A. Trischuk[175], W. Trischuk[167], B. Trocmé[58], A. Trofymov[65], C. Troncon[69a], F. Trovato[156], L. Truong[33c], M. Trzebinski[85], A. Trzupek[85], F. Tsai[46], P.V. Tsiareshka[108,ae], A. Tsirigotis[162,v], V. Tsiskaridze[155], E.G. Tskhadadze[159a], M. Tsopoulou[162], I.I. Tsukerman[124], V. Tsulaia[18], S. Tsuno[82], D. Tsybychev[155], Y. Tu[63b], A. Tudorache[27b], V. Tudorache[27b], A.N. Tuna[36], S. Turchikhin[80], D. Turgeman[180], I. Turk Cakir[4b,t], R.J. Turner[21], R. Turra[69a], P.M. Tuts[39], S. Tzamarias[162], E. Tzovara[100], K. Uchida[163], F. Ukegawa[169], G. Unal[36], M. Unal[11], A. Undrus[29], G. Unel[171], F.C. Ungaro[105], Y. Unno[82], K. Uno[163], J. Urban[28b], P. Urquijo[105], G. Usai[8], Z. Uysal[12d], V. Vacek[141], B. Vachon[104], K.O.H. Vadla[133], T. Vafeiadis[36], A. Vaidya[95], C. Valderanis[114], E. Valdes Santurio[45a,45b], M. Valente[168a], S. Valentinetti[23b,23a], A. Valero[174], L. Valéry[46], R.A. Vallance[21], A. Vallier[36], J.A. Valls Ferrer[174], T.R. Van Daalen[14], P. Van Gemmeren[6], S. Van Stroud[95], I. Van Vulpen[120], M. Vanadia[74a,74b], W. Vandelli[36], M. Vandenbroucke[144], E.R. Vandewall[129], D. Vannicola[73a,73b], R. Vari[73a], E.W. Varnes[7], C. Varni[55b,55a], T. Varol[158], D. Varouchas[65], K.E. Varvell[157], M.E. Vasile[27b], G.A. Vasquez[176], F. Vazeille[38], D. Vazquez Furelos[14], T. Vazquez Schroeder[36], J. Veatch[53], V. Vecchio[101], M.J. Veen[120], L.M. Veloce[167], F. Veloso[139a,139c], S. Veneziano[73a], A. Ventura[68a,68b], A. Verbytskyi[115], V. Vercesi[71a], M. Verducci[72a,72b], C.M. Vergel Infante[79], C. Vergis[24], W. Verkerke[120], A.T. Vermeulen[120], J.C. Vermeulen[120], C. Vernieri[153], P.J. Verschuuren[94], M.C. Vetterli[152,ak], N. Viaux Maira[146d], T. Vickey[149], O.E. Vickey Boeriu[149], G.H.A. Viehhauser[134], L. Vigani[61b], M. Villa[23b,23a], M. Villaplana Perez[174], E.M. Villhauer[50], E. Vilucchi[51], M.G. Vincter[34], G.S. Virdee[21], A. Vishwakarma[50], C. Vittori[23b,23a], I. Vivarelli[156], M. Vogel[182], P. Vokac[141], J. Von Ahnen[46], S.E. von Buddenbrock[33e], E. Von Toerne[24], V. Vorobel[142], K. Vorobev[112],

JHEP06(2021)145

M. Vos[174], J.H. Vossebeld[91], M. Vozak[101], N. Vranjes[16], M. Vranjes Milosavljevic[16], V. Vrba[141,*], M. Vreeswijk[120], N.K. Vu[102], R. Vuillermet[36], I. Vukotic[37], S. Wada[169], P. Wagner[24], W. Wagner[182], J. Wagner-Kuhr[114], S. Wahdan[182], H. Wahlberg[89], R. Wakasa[169], V.M. Walbrecht[115], J. Walder[143], R. Walker[114], S.D. Walker[94], W. Walkowiak[151], V. Wallangen[45a,45b], A.M. Wang[59], A.Z. Wang[181], C. Wang[60a], C. Wang[60c], H. Wang[18], H. Wang[3], J. Wang[63a], P. Wang[42], Q. Wang[128], R.-J. Wang[100], R. Wang[60a], R. Wang[6], S.M. Wang[158], W.T. Wang[60a], W. Wang[15c], W.X. Wang[60a], Y. Wang[60a], Z. Wang[106], C. Wanotayaroj[46], A. Warburton[104], C.P. Ward[32], R.J. Ward[21], N. Warrack[57], A.T. Watson[21], M.F. Watson[21], G. Watts[148], B.M. Waugh[95], A.F. Webb[11], C. Weber[29], M.S. Weber[20], S.A. Weber[34], S.M. Weber[61a], Y. Wei[134], A.R. Weidberg[134], J. Weingarten[47], M. Weirich[100], C. Weiser[52], P.S. Wells[36], T. Wenaus[29], B. Wendland[47], T. Wengler[36], S. Wenig[36], N. Wermes[24], M. Wessels[61a], T.D. Weston[20], K. Whalen[131], A.M. Wharton[90], A.S. White[106], A. White[8], M.J. White[1], D. Whiteson[171], B.W. Whitmore[90], W. Wiedenmann[181], C. Wiel[48], M. Wielers[143], N. Wieseotte[100], C. Wiglesworth[40], L.A.M. Wiik-Fuchs[52], H.G. Wilkens[36], L.J. Wilkins[94], D.M. Williams[39], H.H. Williams[136], S. Williams[32], S. Willocq[103], P.J. Windischhofer[134], I. Wingerter-Seez[5], E. Winkels[156], F. Winklmeier[131], B.T. Winter[52], M. Wittgen[153], M. Wobisch[96], A. Wolf[100], R. Wölker[134], J. Wollrath[52], M.W. Wolter[85], H. Wolters[139a,139c], V.W.S. Wong[175], A.F. Wongel[46], N.L. Woods[145], S.D. Worm[46], B.K. Wosiek[85], K.W. Woźniak[85], K. Wraight[57], S.L. Wu[181], X. Wu[54], Y. Wu[60a], J. Wuerzinger[134], T.R. Wyatt[101], B.M. Wynne[50], S. Xella[40], J. Xiang[63c], X. Xiao[106], X. Xie[60a], I. Xiotidis[156], D. Xu[15a], H. Xu[60a], H. Xu[60a], L. Xu[29], R. Xu[136], T. Xu[144], W. Xu[106], Y. Xu[15b], Z. Xu[60b], Z. Xu[153], B. Yabsley[157], S. Yacoob[33a], D.P. Yallup[95], N. Yamaguchi[88], Y. Yamaguchi[165], A. Yamamoto[82], M. Yamatani[163], T. Yamazaki[163], Y. Yamazaki[83], J. Yan[60c], Z. Yan[25], H.J. Yang[60c,60d], H.T. Yang[18], S. Yang[60a], T. Yang[63c], X. Yang[60a], X. Yang[60b,58], Y. Yang[163], Z. Yang[106,60a], W-M. Yao[18], Y.C. Yap[46], H. Ye[15c], J. Ye[42], S. Ye[29], I. Yeletskikh[80], M.R. Yexley[90], E. Yigitbasi[25], P. Yin[39], K. Yorita[179], K. Yoshihara[79], C.J.S. Young[36], C. Young[153], J. Yu[79], R. Yuan[60b,i], X. Yue[61a], M. Zaazoua[35f], B. Zabinski[85], G. Zacharis[10], E. Zaffaroni[54], J. Zahreddine[135], A.M. Zaitsev[123,af], T. Zakareishvili[159b], N. Zakharchuk[34], S. Zambito[36], D. Zanzi[36], S.V. Zeißner[47], C. Zeitnitz[182], G. Zemaityte[134], J.C. Zeng[173], O. Zenin[123], T. Ženiš[28a], D. Zerwas[65], M. Zgubič[134], B. Zhang[15c], D.F. Zhang[15b], G. Zhang[15b], J. Zhang[6], K. Zhang[15a], L. Zhang[15c], L. Zhang[60a], M. Zhang[173], R. Zhang[181], S. Zhang[106], X. Zhang[60c], X. Zhang[60b], Y. Zhang[15a,15d], Z. Zhang[63a], Z. Zhang[65], P. Zhao[49], Y. Zhao[145], Z. Zhao[60a], A. Zhemchugov[80], Z. Zheng[106], D. Zhong[173], B. Zhou[106], C. Zhou[181], H. Zhou[7], M. Zhou[155], N. Zhou[60c], Y. Zhou[7], C.G. Zhu[60b], C. Zhu[15a,15d], H.L. Zhu[60a], H. Zhu[15a], J. Zhu[106], Y. Zhu[60a], X. Zhuang[15a], K. Zhukov[111], V. Zhulanov[122b,122a], D. Zieminska[66], N.I. Zimine[80], S. Zimmermann[52,*], Z. Zinonos[115], M. Ziolkowski[151], L. Živković[16], G. Zobernig[181], A. Zoccoli[23b,23a], K. Zoch[53], T.G. Zorbas[149], R. Zou[37], L. Zwalinski[36]

[1] *Department of Physics, University of Adelaide, Adelaide, Australia*
[2] *Physics Department, SUNY Albany, Albany NY, U.S.A.*
[3] *Department of Physics, University of Alberta, Edmonton AB, Canada*
[4] [(a)] *Department of Physics, Ankara University, Ankara;* [(b)] *Istanbul Aydin University, Application and Research Center for Advanced Studies, Istanbul;* [(c)] *Division of Physics, TOBB University of Economics and Technology, Ankara, Turkey*
[5] *LAPP, Université Grenoble Alpes, Université Savoie Mont Blanc, CNRS/IN2P3, Annecy, France*
[6] *High Energy Physics Division, Argonne National Laboratory, Argonne IL, U.S.A.*
[7] *Department of Physics, University of Arizona, Tucson AZ, U.S.A.*
[8] *Department of Physics, University of Texas at Arlington, Arlington TX, U.S.A.*
[9] *Physics Department, National and Kapodistrian University of Athens, Athens, Greece*
[10] *Physics Department, National Technical University of Athens, Zografou, Greece*

JHEP06(2021)145

[11] Department of Physics, University of Texas at Austin, Austin TX, U.S.A.
[12] [(a)] Bahcesehir University, Faculty of Engineering and Natural Sciences, Istanbul; [(b)] Istanbul Bilgi University, Faculty of Engineering and Natural Sciences, Istanbul; [(c)] Department of Physics, Bogazici University, Istanbul; [(d)] Department of Physics Engineering, Gaziantep University, Gaziantep, Turkey
[13] Institute of Physics, Azerbaijan Academy of Sciences, Baku, Azerbaijan
[14] Institut de Física d'Altes Energies (IFAE), Barcelona Institute of Science and Technology, Barcelona, Spain
[15] [(a)] Institute of High Energy Physics, Chinese Academy of Sciences, Beijing; [(b)] Physics Department, Tsinghua University, Beijing; [(c)] Department of Physics, Nanjing University, Nanjing; [(d)] University of Chinese Academy of Science (UCAS), Beijing, China
[16] Institute of Physics, University of Belgrade, Belgrade, Serbia
[17] Department for Physics and Technology, University of Bergen, Bergen, Norway
[18] Physics Division, Lawrence Berkeley National Laboratory and University of California, Berkeley CA, U.S.A.
[19] Institut für Physik, Humboldt Universität zu Berlin, Berlin, Germany
[20] Albert Einstein Center for Fundamental Physics and Laboratory for High Energy Physics, University of Bern, Bern, Switzerland
[21] School of Physics and Astronomy, University of Birmingham, Birmingham, U.K.
[22] [(a)] Facultad de Ciencias y Centro de Investigaciónes, Universidad Antonio Nariño, Bogotá; [(b)] Departamento de Física, Universidad Nacional de Colombia, Bogotá, Colombia, Colombia
[23] [(a)] INFN Bologna and Universita' di Bologna, Dipartimento di Fisica; [(b)] INFN Sezione di Bologna, Italy
[24] Physikalisches Institut, Universität Bonn, Bonn, Germany
[25] Department of Physics, Boston University, Boston MA, U.S.A.
[26] Department of Physics, Brandeis University, Waltham MA, U.S.A.
[27] [(a)] Transilvania University of Brasov, Brasov; [(b)] Horia Hulubei National Institute of Physics and Nuclear Engineering, Bucharest; [(c)] Department of Physics, Alexandru Ioan Cuza University of Iasi, Iasi; [(d)] National Institute for Research and Development of Isotopic and Molecular Technologies, Physics Department, Cluj-Napoca; [(e)] University Politehnica Bucharest, Bucharest; [(f)] West University in Timisoara, Timisoara, Romania
[28] [(a)] Faculty of Mathematics, Physics and Informatics, Comenius University, Bratislava; [(b)] Department of Subnuclear Physics, Institute of Experimental Physics of the Slovak Academy of Sciences, Kosice, Slovak Republic
[29] Physics Department, Brookhaven National Laboratory, Upton NY, U.S.A.
[30] Departamento de Física, Universidad de Buenos Aires, Buenos Aires, Argentina
[31] California State University, CA, U.S.A.
[32] Cavendish Laboratory, University of Cambridge, Cambridge, U.K.
[33] [(a)] Department of Physics, University of Cape Town, Cape Town; [(b)] iThemba Labs, Western Cape; [(c)] Department of Mechanical Engineering Science, University of Johannesburg, Johannesburg; [(d)] University of South Africa, Department of Physics, Pretoria; [(e)] School of Physics, University of the Witwatersrand, Johannesburg, South Africa
[34] Department of Physics, Carleton University, Ottawa ON, Canada
[35] [(a)] Faculté des Sciences Ain Chock, Réseau Universitaire de Physique des Hautes Energies — Université Hassan II, Casablanca; [(b)] Faculté des Sciences, Université Ibn-Tofail, Kénitra; [(c)] Faculté des Sciences Semlalia, Université Cadi Ayyad, LPHEA-Marrakech; [(d)] Moroccan Foundation for Advanced Science Innovation and Research (MAScIR), Rabat; [(e)] LPMR, Faculté des Sciences, Université Mohamed Premier, Oujda; [(f)] Faculté des sciences, Université Mohammed V, Rabat, Morocco
[36] CERN, Geneva, Switzerland
[37] Enrico Fermi Institute, University of Chicago, Chicago IL, U.S.A.
[38] LPC, Université Clermont Auvergne, CNRS/IN2P3, Clermont-Ferrand, France

JHEP06(2021)145

[39] Nevis Laboratory, Columbia University, Irvington NY, U.S.A.
[40] Niels Bohr Institute, University of Copenhagen, Copenhagen, Denmark
[41] [(a)] Dipartimento di Fisica, Università della Calabria, Rende; [(b)] INFN Gruppo Collegato di Cosenza, Laboratori Nazionali di Frascati, Italy
[42] Physics Department, Southern Methodist University, Dallas TX, U.S.A.
[43] Physics Department, University of Texas at Dallas, Richardson TX, U.S.A.
[44] National Centre for Scientific Research "Demokritos", Agia Paraskevi, Greece
[45] [(a)] Department of Physics, Stockholm University; [(b)] Oskar Klein Centre, Stockholm, Sweden
[46] Deutsches Elektronen-Synchrotron DESY, Hamburg and Zeuthen, Germany
[47] Lehrstuhl für Experimentelle Physik IV, Technische Universität Dortmund, Dortmund, Germany
[48] Institut für Kern und Teilchenphysik, Technische Universität Dresden, Dresden, Germany
[49] Department of Physics, Duke University, Durham NC, U.S.A.
[50] SUPA — School of Physics and Astronomy, University of Edinburgh, Edinburgh, U.K.
[51] INFN e Laboratori Nazionali di Frascati, Frascati, Italy
[52] Physikalisches Institut, Albert-Ludwigs-Universität Freiburg, Freiburg, Germany
[53] II. Physikalisches Institut, Georg-August-Universität Göttingen, Göttingen, Germany
[54] Département de Physique Nucléaire et Corpusculaire, Université de Genève, Genève, Switzerland
[55] [(a)] Dipartimento di Fisica, Università di Genova, Genova; [(b)] INFN Sezione di Genova, Italy
[56] II. Physikalisches Institut, Justus-Liebig-Universität Giessen, Giessen, Germany
[57] SUPA — School of Physics and Astronomy, University of Glasgow, Glasgow, U.K.
[58] LPSC, Université Grenoble Alpes, CNRS/IN2P3, Grenoble INP, Grenoble, France
[59] Laboratory for Particle Physics and Cosmology, Harvard University, Cambridge MA, U.S.A.
[60] [(a)] Department of Modern Physics and State Key Laboratory of Particle Detection and Electronics, University of Science and Technology of China, Hefei; [(b)] Institute of Frontier and Interdisciplinary Science and Key Laboratory of Particle Physics and Particle Irradiation (MOE), Shandong University, Qingdao; [(c)] School of Physics and Astronomy, Shanghai Jiao Tong University, Key Laboratory for Particle Astrophysics and Cosmology (MOE), SKLPPC, Shanghai; [(d)] Tsung-Dao Lee Institute, Shanghai, China
[61] [(a)] Kirchhoff-Institut für Physik, Ruprecht-Karls-Universität Heidelberg, Heidelberg; [(b)] Physikalisches Institut, Ruprecht-Karls-Universität Heidelberg, Heidelberg, Germany
[62] Faculty of Applied Information Science, Hiroshima Institute of Technology, Hiroshima, Japan
[63] [(a)] Department of Physics, Chinese University of Hong Kong, Shatin, N.T., Hong Kong; [(b)] Department of Physics, University of Hong Kong, Hong Kong; [(c)] Department of Physics and Institute for Advanced Study, Hong Kong University of Science and Technology, Clear Water Bay, Kowloon, Hong Kong, China
[64] Department of Physics, National Tsing Hua University, Hsinchu, Taiwan
[65] IJCLab, Université Paris-Saclay, CNRS/IN2P3, 91405, Orsay, France
[66] Department of Physics, Indiana University, Bloomington IN, U.S.A.
[67] [(a)] INFN Gruppo Collegato di Udine, Sezione di Trieste, Udine; [(b)] ICTP, Trieste; [(c)] Dipartimento Politecnico di Ingegneria e Architettura, Università di Udine, Udine, Italy
[68] [(a)] INFN Sezione di Lecce; [(b)] Dipartimento di Matematica e Fisica, Università del Salento, Lecce, Italy
[69] [(a)] INFN Sezione di Milano; [(b)] Dipartimento di Fisica, Università di Milano, Milano, Italy
[70] [(a)] INFN Sezione di Napoli; [(b)] Dipartimento di Fisica, Università di Napoli, Napoli, Italy
[71] [(a)] INFN Sezione di Pavia; [(b)] Dipartimento di Fisica, Università di Pavia, Pavia, Italy
[72] [(a)] INFN Sezione di Pisa; [(b)] Dipartimento di Fisica E. Fermi, Università di Pisa, Pisa, Italy
[73] [(a)] INFN Sezione di Roma; [(b)] Dipartimento di Fisica, Sapienza Università di Roma, Roma, Italy
[74] [(a)] INFN Sezione di Roma Tor Vergata; [(b)] Dipartimento di Fisica, Università di Roma Tor Vergata, Roma, Italy
[75] [(a)] INFN Sezione di Roma Tre; [(b)] Dipartimento di Matematica e Fisica, Università Roma Tre, Roma, Italy
[76] [(a)] INFN-TIFPA; [(b)] Università degli Studi di Trento, Trento, Italy

JHEP06(2021)145

[77] Institut für Astro und Teilchenphysik, Leopold-Franzens-Universität, Innsbruck, Austria
[78] University of Iowa, Iowa City IA, U.S.A.
[79] Department of Physics and Astronomy, Iowa State University, Ames IA, U.S.A.
[80] Joint Institute for Nuclear Research, Dubna, Russia
[81] [(a)] Departamento de Engenharia Elétrica, Universidade Federal de Juiz de Fora (UFJF), Juiz de Fora; [(b)] Universidade Federal do Rio De Janeiro COPPE/EE/IF, Rio de Janeiro; [(c)] Instituto de Física, Universidade de São Paulo, São Paulo, Brazil
[82] KEK, High Energy Accelerator Research Organization, Tsukuba, Japan
[83] Graduate School of Science, Kobe University, Kobe, Japan
[84] [(a)] AGH University of Science and Technology, Faculty of Physics and Applied Computer Science, Krakow; [(b)] Marian Smoluchowski Institute of Physics, Jagiellonian University, Krakow, Poland
[85] Institute of Nuclear Physics Polish Academy of Sciences, Krakow, Poland
[86] Faculty of Science, Kyoto University, Kyoto, Japan
[87] Kyoto University of Education, Kyoto, Japan
[88] Research Center for Advanced Particle Physics and Department of Physics, Kyushu University, Fukuoka , Japan
[89] Instituto de Física La Plata, Universidad Nacional de La Plata and CONICET, La Plata, Argentina
[90] Physics Department, Lancaster University, Lancaster, U.K.
[91] Oliver Lodge Laboratory, University of Liverpool, Liverpool, U.K.
[92] Department of Experimental Particle Physics, Jožef Stefan Institute and Department of Physics, University of Ljubljana, Ljubljana, Slovenia
[93] School of Physics and Astronomy, Queen Mary University of London, London, U.K.
[94] Department of Physics, Royal Holloway University of London, Egham, U.K.
[95] Department of Physics and Astronomy, University College London, London, U.K.
[96] Louisiana Tech University, Ruston LA, U.S.A.
[97] Fysiska institutionen, Lunds universitet, Lund, Sweden
[98] Centre de Calcul de l'Institut National de Physique Nucléaire et de Physique des Particules (IN2P3), Villeurbanne, France
[99] Departamento de Física Teorica C-15 and CIAFF, Universidad Autónoma de Madrid, Madrid, Spain
[100] Institut für Physik, Universität Mainz, Mainz, Germany
[101] School of Physics and Astronomy, University of Manchester, Manchester, U.K.
[102] CPPM, Aix-Marseille Université, CNRS/IN2P3, Marseille, France
[103] Department of Physics, University of Massachusetts, Amherst MA, U.S.A.
[104] Department of Physics, McGill University, Montreal QC, Canada
[105] School of Physics, University of Melbourne, Victoria, Australia
[106] Department of Physics, University of Michigan, Ann Arbor MI, U.S.A.
[107] Department of Physics and Astronomy, Michigan State University, East Lansing MI, U.S.A.
[108] B.I. Stepanov Institute of Physics, National Academy of Sciences of Belarus, Minsk, Belarus
[109] Research Institute for Nuclear Problems of Byelorussian State University, Minsk, Belarus
[110] Group of Particle Physics, University of Montreal, Montreal QC, Canada
[111] P.N. Lebedev Physical Institute of the Russian Academy of Sciences, Moscow, Russia
[112] National Research Nuclear University MEPhI, Moscow, Russia
[113] D.V. Skobeltsyn Institute of Nuclear Physics, M.V. Lomonosov Moscow State University, Moscow, Russia
[114] Fakultät für Physik, Ludwig-Maximilians-Universität München, München, Germany
[115] Max-Planck-Institut für Physik (Werner-Heisenberg-Institut), München, Germany
[116] Nagasaki Institute of Applied Science, Nagasaki, Japan
[117] Graduate School of Science and Kobayashi-Maskawa Institute, Nagoya University, Nagoya, Japan
[118] Department of Physics and Astronomy, University of New Mexico, Albuquerque NM, U.S.A.
[119] Institute for Mathematics, Astrophysics and Particle Physics, Radboud University/Nikhef, Nijmegen, Netherlands

JHEP06(2021)145

[120] *Nikhef National Institute for Subatomic Physics and University of Amsterdam, Amsterdam, Netherlands*
[121] *Department of Physics, Northern Illinois University, DeKalb IL, U.S.A.*
[122] [(a)] *Budker Institute of Nuclear Physics and NSU, SB RAS, Novosibirsk;* [(b)] *Novosibirsk State University Novosibirsk, Russia*
[123] *Institute for High Energy Physics of the National Research Centre Kurchatov Institute, Protvino, Russia*
[124] *Institute for Theoretical and Experimental Physics named by A.I. Alikhanov of National Research Centre "Kurchatov Institute", Moscow, Russia*
[125] *Department of Physics, New York University, New York NY, U.S.A.*
[126] *Ochanomizu University, Otsuka, Bunkyo-ku, Tokyo, Japan*
[127] *Ohio State University, Columbus OH, U.S.A.*
[128] *Homer L. Dodge Department of Physics and Astronomy, University of Oklahoma, Norman OK, U.S.A.*
[129] *Department of Physics, Oklahoma State University, Stillwater OK, U.S.A.*
[130] *Palacký University, RCPTM, Joint Laboratory of Optics, Olomouc, Czech Republic*
[131] *Institute for Fundamental Science, University of Oregon, Eugene, OR, U.S.A.*
[132] *Graduate School of Science, Osaka University, Osaka, Japan*
[133] *Department of Physics, University of Oslo, Oslo, Norway*
[134] *Department of Physics, Oxford University, Oxford, U.K.*
[135] *LPNHE, Sorbonne Université, Université de Paris, CNRS/IN2P3, Paris, France*
[136] *Department of Physics, University of Pennsylvania, Philadelphia PA, U.S.A.*
[137] *Konstantinov Nuclear Physics Institute of National Research Centre "Kurchatov Institute", PNPI, St. Petersburg, Russia*
[138] *Department of Physics and Astronomy, University of Pittsburgh, Pittsburgh PA, U.S.A.*
[139] [(a)] *Laboratório de Instrumentação e Física Experimental de Partículas — LIP, Lisboa;* [(b)] *Departamento de Física, Faculdade de Ciências, Universidade de Lisboa, Lisboa;* [(c)] *Departamento de Física, Universidade de Coimbra, Coimbra;* [(d)] *Centro de Física Nuclear da Universidade de Lisboa, Lisboa;* [(e)] *Departamento de Física, Universidade do Minho, Braga;* [(f)] *Departamento de Física Teórica y del Cosmos, Universidad de Granada, Granada (Spain);* [(g)] *Departamento de Física and CEFITEC of Faculdade de Ciências e Tecnologia, Universidade Nova de Lisboa, Caparica;* [(h)] *Instituto Superior Técnico, Universidade de Lisboa, Lisboa, Portugal*
[140] *Institute of Physics of the Czech Academy of Sciences, Prague, Czech Republic*
[141] *Czech Technical University in Prague, Prague, Czech Republic*
[142] *Charles University, Faculty of Mathematics and Physics, Prague, Czech Republic*
[143] *Particle Physics Department, Rutherford Appleton Laboratory, Didcot, U.K.*
[144] *IRFU, CEA, Université Paris-Saclay, Gif-sur-Yvette, France*
[145] *Santa Cruz Institute for Particle Physics, University of California Santa Cruz, Santa Cruz CA, U.S.A.*
[146] [(a)] *Departamento de Física, Pontificia Universidad Católica de Chile, Santiago;* [(b)] *Universidad Andres Bello, Department of Physics, Santiago;* [(c)] *Instituto de Alta Investigación, Universidad de Tarapacá;* [(d)] *Departamento de Física, Universidad Técnica Federico Santa María, Valparaíso, Chile*
[147] *Universidade Federal de São João del Rei (UFSJ), São João del Rei, Brazil*
[148] *Department of Physics, University of Washington, Seattle WA, U.S.A.*
[149] *Department of Physics and Astronomy, University of Sheffield, Sheffield, U.K.*
[150] *Department of Physics, Shinshu University, Nagano, Japan*
[151] *Department Physik, Universität Siegen, Siegen, Germany*
[152] *Department of Physics, Simon Fraser University, Burnaby BC, Canada*
[153] *SLAC National Accelerator Laboratory, Stanford CA, U.S.A.*
[154] *Physics Department, Royal Institute of Technology, Stockholm, Sweden*
[155] *Departments of Physics and Astronomy, Stony Brook University, Stony Brook NY, U.S.A.*
[156] *Department of Physics and Astronomy, University of Sussex, Brighton, U.K.*

JHEP06(2021)145

[157] School of Physics, University of Sydney, Sydney, Australia
[158] Institute of Physics, Academia Sinica, Taipei, Taiwan
[159] [(a)] E. Andronikashvili Institute of Physics, Iv. Javakhishvili Tbilisi State University, Tbilisi; [(b)] High Energy Physics Institute, Tbilisi State University, Tbilisi, Georgia
[160] Department of Physics, Technion, Israel Institute of Technology, Haifa, Israel
[161] Raymond and Beverly Sackler School of Physics and Astronomy, Tel Aviv University, Tel Aviv, Israel
[162] Department of Physics, Aristotle University of Thessaloniki, Thessaloniki, Greece
[163] International Center for Elementary Particle Physics and Department of Physics, University of Tokyo, Tokyo, Japan
[164] Graduate School of Science and Technology, Tokyo Metropolitan University, Tokyo, Japan
[165] Department of Physics, Tokyo Institute of Technology, Tokyo, Japan
[166] Tomsk State University, Tomsk, Russia
[167] Department of Physics, University of Toronto, Toronto ON, Canada
[168] [(a)] TRIUMF, Vancouver BC; [(b)] Department of Physics and Astronomy, York University, Toronto ON, Canada
[169] Division of Physics and Tomonaga Center for the History of the Universe, Faculty of Pure and Applied Sciences, University of Tsukuba, Tsukuba, Japan
[170] Department of Physics and Astronomy, Tufts University, Medford MA, U.S.A.
[171] Department of Physics and Astronomy, University of California Irvine, Irvine CA, U.S.A.
[172] Department of Physics and Astronomy, University of Uppsala, Uppsala, Sweden
[173] Department of Physics, University of Illinois, Urbana IL, U.S.A.
[174] Instituto de Física Corpuscular (IFIC), Centro Mixto Universidad de Valencia — CSIC, Valencia, Spain
[175] Department of Physics, University of British Columbia, Vancouver BC, Canada
[176] Department of Physics and Astronomy, University of Victoria, Victoria BC, Canada
[177] Fakultät für Physik und Astronomie, Julius-Maximilians-Universität Würzburg, Würzburg, Germany
[178] Department of Physics, University of Warwick, Coventry, U.K.
[179] Waseda University, Tokyo, Japan
[180] Department of Particle Physics and Astrophysics, Weizmann Institute of Science, Rehovot, Israel
[181] Department of Physics, University of Wisconsin, Madison WI, U.S.A.
[182] Fakultät für Mathematik und Naturwissenschaften, Fachgruppe Physik, Bergische Universität Wuppertal, Wuppertal, Germany
[183] Department of Physics, Yale University, New Haven CT, U.S.A.

[a] Also at Borough of Manhattan Community College, City University of New York, New York NY, U.S.A.
[b] Also at Center for High Energy Physics, Peking University, China
[c] Also at Centro Studi e Ricerche Enrico Fermi, Italy
[d] Also at CERN, Geneva, Switzerland
[e] Also at CPPM, Aix-Marseille Université, CNRS/IN2P3, Marseille, France
[f] Also at Département de Physique Nucléaire et Corpusculaire, Université de Genève, Genève, Switzerland
[g] Also at Departament de Fisica de la Universitat Autonoma de Barcelona, Barcelona, Spain
[h] Also at Department of Financial and Management Engineering, University of the Aegean, Chios, Greece
[i] Also at Department of Physics and Astronomy, Michigan State University, East Lansing MI, U.S.A.
[j] Also at Department of Physics and Astronomy, University of Louisville, Louisville, KY, U.S.A.
[k] Also at Department of Physics, Ben Gurion University of the Negev, Beer Sheva, Israel
[l] Also at Department of Physics, California State University, East Bay, U.S.A.
[m] Also at Department of Physics, California State University, Fresno, U.S.A.
[n] Also at Department of Physics, California State University, Sacramento, U.S.A.

JHEP06(2021)145

[o] Also at Department of Physics, King's College London, London, U.K.
[p] Also at Department of Physics, St. Petersburg State Polytechnical University, St. Petersburg, Russia
[q] Also at Department of Physics, University of Fribourg, Fribourg, Switzerland
[r] Also at Dipartimento di Matematica, Informatica e Fisica, Università di Udine, Udine, Italy
[s] Also at Faculty of Physics, M.V. Lomonosov Moscow State University, Moscow, Russia
[t] Also at Giresun University, Faculty of Engineering, Giresun, Turkey
[u] Also at Graduate School of Science, Osaka University, Osaka, Japan
[v] Also at Hellenic Open University, Patras, Greece
[w] Also at Institucio Catalana de Recerca i Estudis Avancats, ICREA, Barcelona, Spain
[x] Also at Institut für Experimentalphysik, Universität Hamburg, Hamburg, Germany
[y] Also at Institute for Nuclear Research and Nuclear Energy (INRNE) of the Bulgarian Academy of Sciences, Sofia, Bulgaria
[z] Also at Institute for Particle and Nuclear Physics, Wigner Research Centre for Physics, Budapest, Hungary
[aa] Also at Institute of Particle Physics (IPP), Canada
[ab] Also at Institute of Physics, Azerbaijan Academy of Sciences, Baku, Azerbaijan
[ac] Also at Instituto de Fisica Teorica, IFT-UAM/CSIC, Madrid, Spain
[ad] Also at Istanbul University, Department of Physics, Istanbul, Turkey
[ae] Also at Joint Institute for Nuclear Research, Dubna, Russia
[af] Also at Moscow Institute of Physics and Technology State University, Dolgoprudny, Russia
[ag] Also at National Research Nuclear University MEPhI, Moscow, Russia
[ah] Also at Physics Department, An-Najah National University, Nablus, Palestine
[ai] Also at Physikalisches Institut, Albert-Ludwigs-Universität Freiburg, Freiburg, Germany
[aj] Also at The City College of New York, New York NY, U.S.A.
[ak] Also at TRIUMF, Vancouver BC, Canada
[al] Also at Universita di Napoli Parthenope, Napoli, Italy
[am] Also at University of Chinese Academy of Sciences (UCAS), Beijing, China
[*] Deceased

JHEP06(2021)145